DYNAMIC TEST RANGE I-FOLLOW-ON

NARRATIVE REPORT

L.K.B. RESOURCES, INC.
ONE AERIAL WAY
SYOSSET, NEW YORK 11791

JANUARY 1981

WORK PERFORMED UNDER
BENDIX FIELD ENGINEERING CORPORATION GRAND JUNCTION OPERATIONS
SUBCONTRACT NO. 78-213-L AND BENDIX CONTRACT EY-76-C-13-1664

PREPARED FOR THE
U.S. ENERGY RESEARCH AND DEVELOPMENT ADMINISTRATION
GRAND JUNCTION OFFICE
GRAND JUNCTION, COLORADO 81501

(LEGAL NOTICE)

ABSTRACT

The Lake Mead Dynamic Test Range was developed for the purpose of evaluating various range users radiometric equipment, data acquisition techniques and reduction methods. Further, the range is to serve as a calibration standard to assist in the normalization of survey data acquired by any of the several NURE program aerial survey subcontractors.

The current project was designed to gather the geologic, magnetic and radiometric data necessary to accomplish the above tasks. A detailed geologic ground study and airborne radiometric survey of Lake Mead Dynamic Test Range I was undertaken by LKB Resources during the period from February to June 1979. This report summarizes the results of this effort in terms of a geologic description of the regional area and a more detailed analysis of the local lithologies present. The airborne survey methods are summarized and the survey results are presented graphically in map form as stacked profiles at a scale of 1:6,000.

CONTENTS

CONTENTS - continued

CONTENTS - continued

ILLUSTRATIONS

GEOLOGY OF THE

DYNAMIC TEST RANGE - 1
LAKE MEAD, ARIZONA

in its regional context

1.0 REGIONAL

1.1 GENERAL

The Dynamic Test Range - 1 (hereafter DTR-1) is a locality selected to serve as a calibration standard for airborne gamma-ray detection systems being used in the National Uranium Resource Evaluation program currently under way. The locality appears to have been selected primarily on the grounds of ease of access.

The present study represents an effort to characterize DTR-1 and the adjacent region in terms of local and regional geology; this description will then represent a data base from which inferences drawn as to concentrations of U, Th, and K in the surficial materials of DTR-1 can be related both to surficial rock/soil type and to probable provenance.

The following tasks have been performed jointly by International Exploration and the Geology Department, University of Pennsylvania, as a portion of the overall study conducted by LKB Resources, Inc. on behalf of Bendix Field Engineering Corp.

1. Geologic mapping of the U.S. Department of Energy Dynamic Test Range at Lake Mead, Arizona.

   a. A regional geologic map of the Detrital Valley environs produced at a scale of 1:125,000 to cover the area bounded by longitudes 114°'W, 115°00'W and latitudes 35°30'N, 36°13'N. The mapping consists of compilation of existing maps and photo-mapping with some ground reconnaissance traverses.

   b. A detailed geologic map of the immediate DTR-1 environs produced at a scale of 1:6,000 to be used as a base for the aerial and geochemical survey mapping. The detail map identifies the lithologies present, surficial material cover, major drainage channels and cultural features as identified from photo interpretation and numerous ground traverses.

2. The analysis of 78 samples for petrologic description. The description includes:*

   Moisture
   pH
   Organic Concentration
   Carbonates
   Particle size analysis
   Mineralogy

   The petrologic analysis is tabulated in accordance with the above parameters and adequately identified by means of unique sample numbers.

3. A report on the geologic setting of the Dynamic Test Range, which includes and interpretation of surface cover/soil provenance and present weathering characteristics of the range utilizing 1 and 2 above.

4. A total of 228 additional samples were acquired and delivered to Bendix/DOE for Geochemical analyses. The results of these analyses are included as an appendix to the report.

The above tasks include all the necessary field work, photo geologic studies, literature searches and final report.

Geologic mapping is presented a) at a scale of 1:125,000 to place DTR-1 in its regional geologic context and b) at a scale of 1:6,000 to provide detail within DTR-1 itself (see fig. 1, p. 3).

Petrologic analysis of the 78 samples has yielded an abundance of information that will assist in characterizing, in geochemical and petrographic terms, the nature of surficial materials on the site.

1.2 GEOLOGIC MAPPING

1.21 REGIONAL

The abundance and quality of regional geologic information varies within the larger map area. Figure 2 shows the distribution over the region of geologic maps available at various scales; the Bibliography at the end of this report (section 9) lists the sources of figure 2 as well as many other published (and a few unpublished) studies of the geology of the region around DTR-1.

Several distinct programs and/or topical orientations have provided incentive for many of the comprehensive mapping efforts that fall within the larger map area:

*The initial contract also specified field measurement of soil density. In consultation with personnel of Bendix Field Engineering Corp. it was agreed that such measurements exceed the scope of the present study and would add nothing to our understanding of the surficial geology of DTR-1.

1.211: A long-standing interest in the history of the Colorado River in the Canyon Country has resulted in a rich literature of exploration; in recent years geologists have focused on reconstructing the late-Tertiary history of development of the Grand Canyon as a topographic feature (e.g. Blackwelder, 1934; Blair et al, 1977; Damon et al, 1978; Hunt, 1969; Longwell, 1946; Lovejoy, 1969; Lucchitta, 1972; Lucchitta and McKee, 1975; McKee and McKee, 1972; McKee et al, 1967; Metzger, 1968; Ransome, 1923; Smith, 1970; Young, 1970; Young and Brennan, 1974; Young and McKee, 1978).

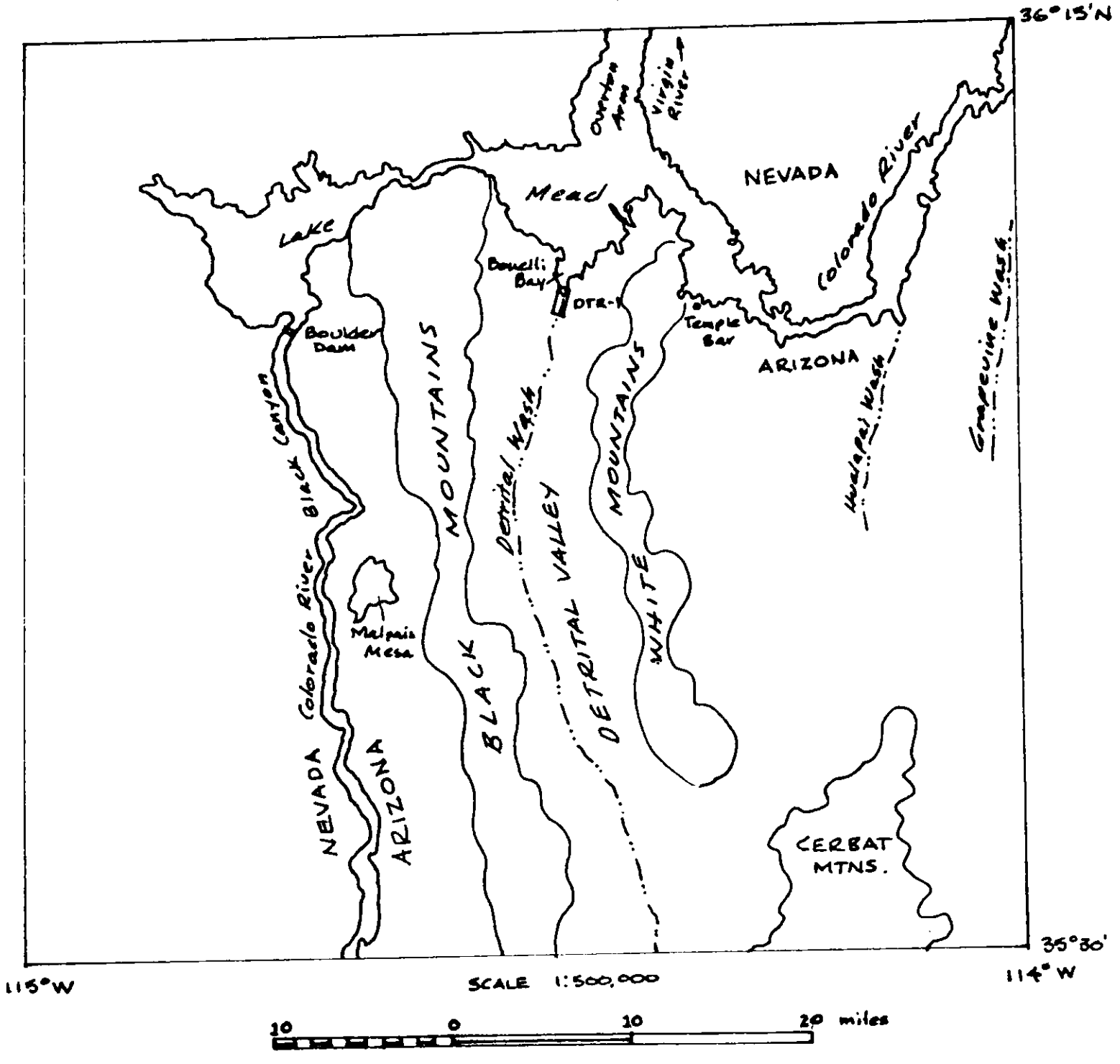

Figure 1: Index Map of Detrital Valley and surrounding region.

EXPLANATION OF FIGURE 2

On the pages that follow, a series of drawings indicates the extent of coverage of the area of Plate 1 by the published and unpublished sources consulted. Each source is assigned a code number on the drawings; those numbers refer to the sources in the list below:

CATEGORY A: Maps, part or all of which fall within the area of Plate 1:

1. Anderson, 1969, @ 1;60,700
2. Anderson, 1973, @ 1:62,500
3. Anderson, 1977, @ 1:62,500
4. Anderson, 1978, @ 1:62,500
5. Anderson and Laney, 1975, fig. 1, @ 1:575,000
6. Anderson and Laney, 1975, fig. 2, @ 1:1,100,000
7. Blair, 1978, @ 1:500,000
8. Bowyer et al, 1958, @1:200,000
9. Bentley, 1971, @ 1:62,500
10. Gillespie and Bentley, 1971, @ 1:125,000
11. Hunt, 1942: Plate 45 @ 1:2400; Plate 46 @ 1:3560
12. Laney, 1973, @ 1:62,500
13. Longwell, 1928, @ 1:250,000
14. Longwell, 1936, @ 1:120,000
15. Longwell, 1951, @ 1:150,000
16. Longwell, 1963, @ 1:125,000
17. Longwell et al, 1965, @ 1:250,000
18. McKelvey et al, 1949, Plate 39 @ 1:25,000
19. McKelvey et al, 1949, Plate 41 @ 1:500
20. McKelvey et al, 1949, Plate 42 @ 1:25,000
21. Schrader, 1909, @ 1:250,000
22. Volborth, 1962, @ 1:48,500
23. Volborth, 1973, @ 1:125,000
24. Giegengack and Brueckner, this report, @ 1:6000

CATEGORY B: Maps that cover the entire area:

25. Anderson et al, 1972, @ 1:900,000
26. Hewett et al, 1936, 3 maps @ 1:1,500,000

CATEGORY C: Maps of Arizona:

27. Wilson and Moore, 1969, @ 1:500,000

CATEGORY D: Maps of all or a large part of the state of Nevada:

28. Armstrong, 1968, @ 1:2,000,000
29. Bowyer et al, 1958, @ 1:200,000 (same area as source #17)
30. Stewart and Carlson, 1977, @ 1:1,000,000

CATEGORY E: Specialized maps:

31. Longwell, 1936, @ 1:120,000
32. Mead and Carder, 1941, @ 1:1,000,000
33. U.S. Geological Survey, 1971 (Aeromagnetic map of entire area)
34. Young, 1978, 2 field-trip-guidebook maps @ 1:267,000

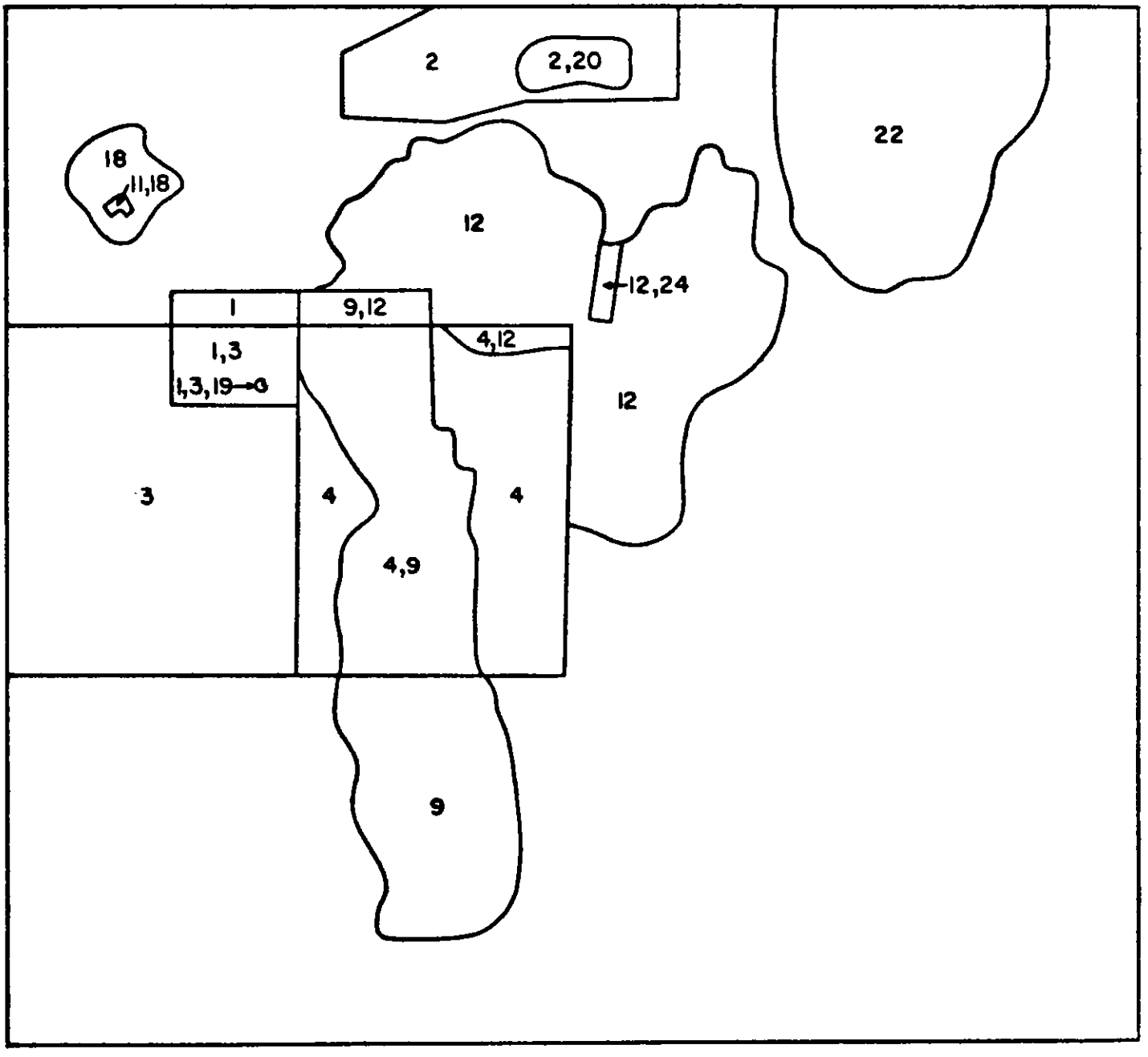

fig. 2a: Sources of map information;
Scales between 1:500 and 1:62,500

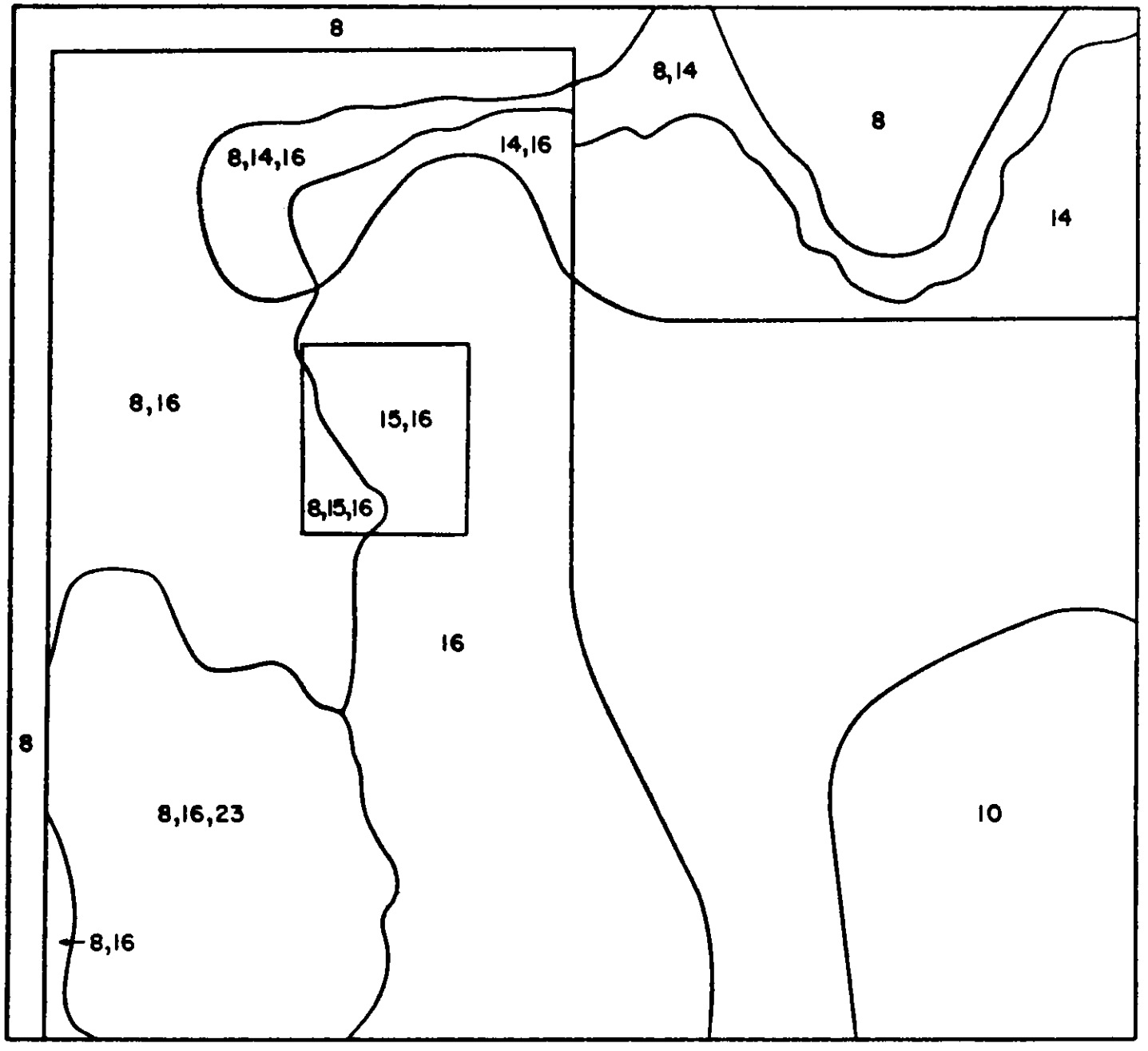

fig. 2b: Sources of map information;
Scales between 1:100,000 and 1:200,000

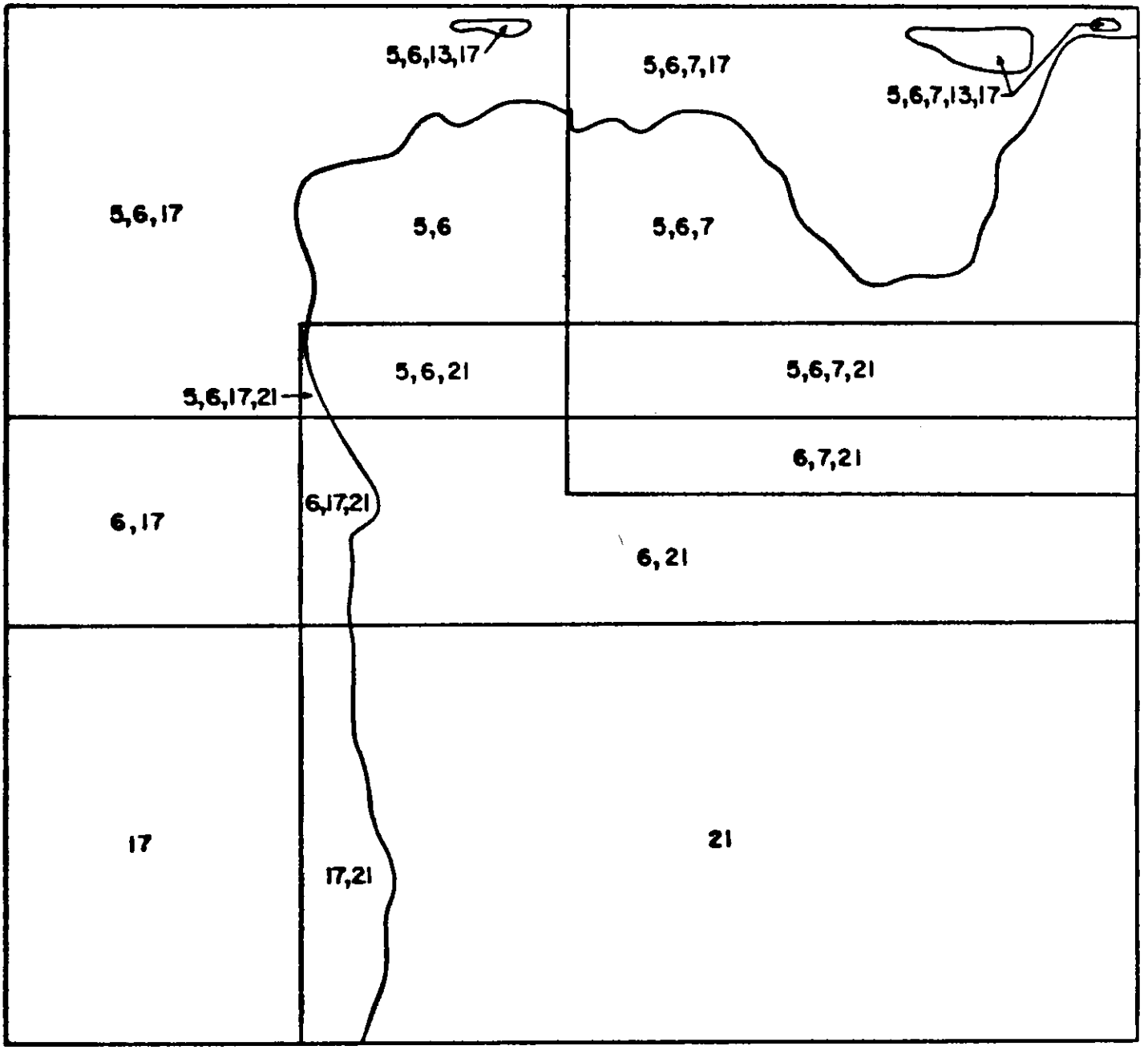

fig. 2c: Sources of map information;
Scales 1:200,000 and smaller

1.212: Construction of the Boulder Dam in Black Canyon of the Colorado River required first some detailed local and regional geologic studies (e.g. Hewett et al, 1936; Longwell, 1936; Nickell, 1942; Ransome, 1923,1931) that have been followed up by careful monitoring of the rate of accumulation of sediment in the reservoir (Smith et al, 1960), subtle changes in tne elevations of points on the triangulation network surveyed prior to impoundment of the reservoir (Raphael, 1954; Westergaard and Adkins, 1934),and the well-documented increase in the frequency of minor earthquakes, presumably related to increased pore-water pressure in rocks beneath the reservoir floor and to elastic response of the lithosphere to the load imposed by the mass of water (e.g. Anderson, 1973; Carder, 1945; Carder and Small, 1948; Jones, 1944; Lee and Matamoros, 1975; Mead and Carder, 1941; Rogers and Lee, 1976; Rogers and Gallanthine, 1978).

1.213: In response to the chronic water shortage in the southwestern United States, a condition that provided early rationale for the construction of the Boulder Dam, many studies (e.g. Gillespie and Bentley, 1971; Twenter, 1962) have been undertaken of the ground-water potential of the deeply filled structural troughs that underlie the major north-south-trending valleys of this part of the Basin-and-Range Province; in recent years several such studies have been commissioned by the National Park Service (Laney, 1973; Bentley, 1969, 1970) to provide background information for their current efforts to maintain and develop facilities within Lake Mead National Recreation Area and other public-use facilities farther downstream.

1.214: Both the U.S. Atomic Energy Commission and the U.S. Geological Survey have sponsored studies of the Nevada Test Site (e.g. Eckel, 1968; Diment et al, 1961; Ekren et al, 1968; Gibbs and Roller, 1966), just outside the limits of the regional map of Plate 1 (see fig. 1). To the extent that this material places the Test Site in a regional stratigraphic and tectonic framework, it has relevance to the region surrounding DTR-1.

1.215: Structural and tectonic geologists have long been interested in the significance of the abrupt termination of the structural patterns of the western part of the Colorado Plateau where it adjoins the Basin-and-Range Province. This transition lies along the eastern limit of the regional map presented here; discussions of the significance of that change in structural style (e.g. Lunar and Planetary Science Institute, 1977; Hamblin, 1963, 1975; Lucchitta, 1966, 1974; McKee and Anderson, 1971; Suneson and Lucchitta, 1978; Young, 1966a, b, 1978; Young and Brennan, 1974) provide much basic information about the eastern margin of the Basin-and-Range Province.

1.216: Two 15' quadrangles within the larger map area have recently been mapped in detail by U.S. Geological Survey personnel (Anderson, 1977, 1978): others nearby are being mapped but are not yet available (Dickey, Carr, and Bull, in press).

1.217: At least one earlier reconnaissance study (Geodata International, Inc., 1976) of the local and regional geology of DTR-1 is available.

1.22 LOCAL MAPPING

The area of DTR-1 and its immediate surroundings was mapped in detail on an air-photo base at a scale of 1:6000 in January 1979. This information is presented as Plate 2; the stratigraphic and structural details of that map will be discussed in section 5 of this report.

1.3 PETROLOGIC ANALYSIS

Many samples of surficial soil and/or sediment have been collected from within DTR-1 since it was first designated; of these, 78 have been delivered to the University of Pennsylvania for petrologic analysis to complement the analyses of various radioactive nuclides that have been undertaken by various other laboratories. The localities of samples collected under this study are plotted on Plate 2. Analytical procedures used by personnel of the Geology Department of the University of Pennsylvania are discussed in section 7 of this report; results of all analyses are presented in tabular form in the appendices (section 10).

1.4 ACKNOWLEDGMENTS

We are indebted to George Ulrich of the U.S. Geological Survey in Flagstaff, Arizona, who assisted us in logistic preparations for our field work and directed us to several sources of useful regional information; to Ivo Lucchitta, also of the U.S. Geological Survey in Flagstaff, who gave us the benefit of his personal field experience in the region; to Robert Laney, of the Water-Resources Division of the U.S. Geological Survey in Phoenix, whose excellent 1973 map represents information most directly pertinent to DTR-1, and who told us a great deal more over the telephone, and to personnel of the Lake Mead National Recreation Area library in Boulder City, Nevada, who loaned us what could circulate and photocopied for us information that could not leave the library.

2.0 GENERAL DESCRIPTION OF THE AREA

The Dynamic Test Range - 1 lies just south of Lake Mead, where Detrital Wash enters Bonelli Bay at an altitude of ± 1200 feet above sea level (the surface elevation of Lake Mead varies as a function of season). The area of intensive, detailed study extends 6 miles up Detrital Wash in a strip about 2 miles wide (see fig. 1). DTR-1 is centrally located within the larger, regional map that covers the area from long 114° W to long 115° W and from lat 35°30' N to lat 36°15' N.

The area lies almost entirely within the Basin-and-Range Province, a region characterized by north-south-oriented, fault-bounded mountain ranges alternating with deeply filled parallel structural valleys, many of which lack outlets in the present climatic regime. The Colorado River is the only through-flowing trunk stream in this part of the Basin-and-Range Province; it receives drainage from a network of north-south-oriented tribu-

taries, most of them intermittent, that have developed in the course of alternating periods of filling and excavation of still-active structural depressions.

The extreme eastern edge of the larger map area borders on the western part of the Colorado Plateau, a high-altitude region of flat-lying, relatively undisturbed Paleozoic and Mesozoic sediments. Drainage from this part of the Colorado Plateau is to the west to Grapevine Wash, the easternmost of the north-flowing tributaries to the Colorado River in this part of the Basin-and-Range Province.

The region lies in the rain shadow of the Sierra Nevada and other mountain masses to the west. Data from nearby Las Vegas during the years 1931-1953 (see Geodata International, inc., 1976, p. 6-7) show an average of 4.62" of rainfall per year, concentrated as winter events, presumably related to regional storm systems, and as late-summer events, presumably the result of local convective thunderstorms. Most of the smaller streams, therefore, are intermittent, as is Detrital Wash itself, despite the range of altitudes within its watershed (1200' to 5000') and the areal extent of the long, narrow watershed, which rises beyond the southern margin of the larger map area.

3.0 REGIONAL GEOLOGY

3.1 GENERAL STATEMENT

A study of the regional geology of the larger map area was undertaken to place DTR-1 in its regional stratigraphic/tectonic context. This study was conducted almost exclusively by perusal of existing published and unpublished studies, complemented by several reconnaissance traverses across the entire region, by more detailed ground reconnaissance adjacent to DTR-1, and, of course, by the extremely detailed field mapping undertaken at DTR-1 itself. Sources consulted for the regional study appear in the Bibliography (section 9). Only a few of the sources that appear there include maps of appropriate scale and quality to have been used in compilation of the map of Plate 1; areas covered by maps consulted for that compilation are plotted in fig. 2 and described in the accompanying explanation. Scales of the maps used range from 1:400 to 1:2,000,000. Much of the area of Plate 1 is covered by more than one map; hence the compilation of Plate 1 required many editorial choices in cases of conflicting map patterns or, more often, use of different stratigraphic units by different geologists contemplating the same or similar bodies of rock. The small sketch entitled Sources of Geologic Information that appears in the margin of Plate 1 identifies those sources (numbered as in the explanation of fig. 2) that most influenced the editorial decisions made for each portion of the map of Plate 1.

3.2 DESCRIPTION OF ROCK UNITS

3.21 GENERAL STATEMENT

The process of compiling a map based on 34 separate sources at widely varying scales has required that certain decisions be made about the stratigraphic units that are used. In many cases this has involved implied correlation of rock units that may not have been anticipated by any of the workers who mapped those units in the field; in other cases it has required inclusion into a single unit of stratigraphic entities mapped in the field as distinct members; in still other cases we have been able to impose on the work of an early geologist a redefinition of units studied in more detail by a field person of a later generation. Thus, the units on the map of Plate 1 are somewhat arbitrary; in the descriptions of units that follow we have relied, in most cases, on the most recent appropriate published or unpublished source.

In Fig. 3 we present in tabular form the stratigraphic column that also appears in the margin of Plate 1. In the stratigraphic-unit descriptions that follow we identify those sources from which our descriptions are principally derived. The stratigraphic units used on the detailed map of DTR-1 are described fully in section 5.

3.22 PRECAMBRIAN UNITS

3.221 GENERAL STATEMENT

This category includes rocks that have been assigned to Precambrian time by those who mapped them despite the dearth of directly measured isotope ages. In general, Precambrian rocks within the map area consist of relatively high-grade metamorphic rocks intruded by igneous bodies whose great age is inferred either by a metamorphic overprint, a petrographic dissimilarity to demonstrably younger igneous rocks, or by demonstrable stratigraphic evidence of pre-Paleozoic age.

3.222: p€r (Gillespie and Bentley, 1971)
Precambrian igneous and metamorphic rocks (undivided)
Granite, gneiss, and schist; includes some rocks of late Mesozoic to early Cenozoic age.

3.223: p€m (Anderson, 1977, 1978)
Precambrian variegated metamorphic rocks
Biotite-almandine gneiss and schist, granite pegmatite, garnetiferous granite pegmatite, and sparse amphibolite; some rocks contain sillimanite or hornblende. May occur as highly complex to chaotic, structurally disturbed assemblages that contain abundant evidence of faulting and shearing; may appear to be highly disturbed fault blocks interspersed with biotite-almandine gneiss.

3.224: p€h (Anderson, 1978)
Precambrian hornblende-biotite gneiss
Mostly medium-gray evenly foliated or banded gneiss containing conspicuous hornblende and little or no garnet. Contains pods, lenses, and layers of granite pegmatite and amphibolite in highly variable amounts.

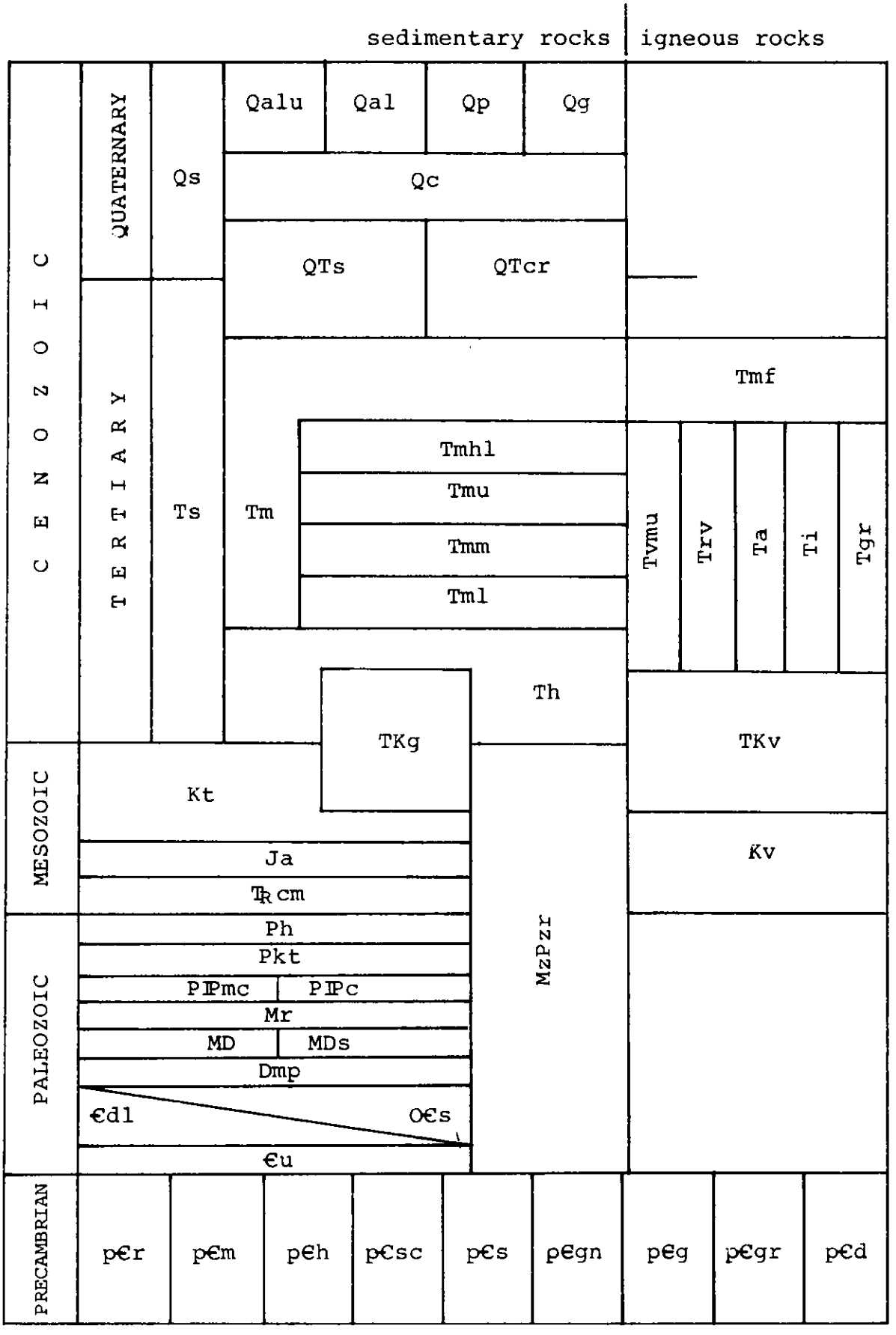

Figure 3: Schematic Stratigraphic Column for Regional Map

3.225: p€s (Anderson, 1978)
Precambrian schistose and phyllitic rocks
Greenish-brown, greenish, gray, and gray banded to highly foliated biotite or biotite-hornblende schist, augen schist, and phyllonite.

3.226: p€sc (Wilson and Moore, 1969)
Precambrian metamorphosed sedimentary and volcanic rocks
Mainly phyllite, slate, mica schist, chlorite schist, and amphibolite, derived from interbedded shale, sandstone, and rhyolitic to basaltic flows and tuffs; locally includes intrusive rhyolite, diorite, gabbro, and pyroxenite.

3.227: p€gn (Wilson and Moore, 1969; Volborth, 1973)
Precambrian gneiss
Includes some areas of undivided schist and granite

3.228: p€g (Longwell et al, 1965; Volborth, 1973)
p€gr (Wilson and Moore, 1969)
Precambrian granite
Granite, quartz monzonite, granodiorite, and quartz diorite. Locally includes areas of granitic rocks, and other igneous rocks, of post-Paleozoic age.

3.229: p€d (Volborth, 1973)
Precambrian diorite

3.23 PALEOZOIC AND MESOZOIC UNITS

3.231 GENERAL STATEMENT

Sedimentary rocks of Paleozoic and Mesozoic age crop out along the eastern edge of the larger map area, along the zone of structural transition from the Basin-and-Range Province to the Colorado Plateau, and in the mountains northwest of Lake Mead, where rocks of this age, still identifiable as the same lithostratigraphic units that lie undisturbed on the Colorado Plateau and are dramatically exposed in the walls of the Grand Canyon, occur as a contorted complex of fault-bounded blocks. Elsewhere, these rocks have been removed by late-Tertiary erosion, exposing underlying basement rocks, as in many of the fault-block mountain masses of the Basin-and-Range Province, or have been deeply buried by younger fill in the intervening structural basins.

Volcanic rocks assigned to end-Mesozoic time (Wilson and Moore, 1969; Gillespie and Bentley, 1971) may, in fact, be of Tertiary age.

3.232: MzPzr: (Anderson, 1977)
Mesozoic or Paleozoic sedimentary rocks
Unfossiliferous gray cherty carbonate, sandstone, and minor carbonate conglomerate that contains angular pebbles and cobbles of granite and limestone in small area of eastern River Mountains. Rocks are highly fractured and altered and their age is uncertain.

3.233: €u (Longwell et al, 1965)
Cambrian sedimentary rocks, undivided
Includes Tapeats Sandstone, Wood Canyon Formation, Pioche Shale, Lyndon Limestone, Chisholm Shale, and Carrara Formation.

3.234: €dl (Longwell et al, 1965)
Cambrian dolomite and limestone, undivided

3.235: O€s (Wilson and Moore, 1969)
Ordovician and Cambrian sedimentary rocks, undivided
Includes Tonto Group (Middle and Lower Cambrian) and Cambrian limestone and dolomite in NW Arizona; may be wholly or in part equivalent to €dl (see 3.234).

3.236: Dmp (Longwell et al, 1965)
Muddy Peak Limestone

3.237: MD (Longwell et al, 1965)
Mississippian and Devonian Rogers Spring Limestone and Muddy Peak Limestone, undivided

MDs (Wilson and Moore, 1969)
Mississippian and Devonian sedimentary rocks, undivided
Includes Redwall Limestone (Mississippian) and Temple Butte Limestone (Upper? Devonian).

3.238: Mr (Longwell et al, 1965)
Mississippian Rogers Spring Limestone

3.239: PIPMc (Longwell et al, 1965)
Permian and Pennsylvanian Callville Limestone

PIPc (Wilson and Moore, 1969)
Permian Pakoon Limestone and Pennsylvanian Callville Limestone

3.2310: Pkt (Longwell et al, 1965)
Permian Kaibab, Toroweap, and Coconino Formations, and red beds, undivided

3.2311: Ph (Wilson and Moore, 1969)
Permian Hermit Shale

3.2312: TRcm (Longwell et al, 1965)
Triassic Chinle and Moenkopi Formations, undivided

3.2313: Ja (Longwell et al, 1965)
Jurassic Aztec Sandstone

3.2314: Kt (Longwell et al, 1965)
Cretaceous Thumb Formation
May be correlative with lower part of Gale Hills Formation (see section 3.2422)

3.2315: Kv (Wilson and Moore, 1969)
Cretaceous volcanic rocks
Rhyolitic to andesitic flows and tuffs (may be wholly or in part equivalent to various Tertiary volcanic units described below)

3.2316: (TKg and TKv are described below, under Tertiary Units, sections 3.2422 and 3.2423)

3.24 CENOZOIC UNITS

3.241 GENERAL STATEMENT

The Cenozoic section over the larger map area is complex and subject to conflicting interpretations. Rocks of Cenozoic age consist of basin-filling materials of both sedimentary and volcanic origin.

Since the sedimentary rocks reflect compositions of parent materials, which vary in lithology throughout the larger map area; since they were deposited in discrete, typically unconnected basins under varying environments of deposition; and since included fossils are typically sparse and non-diagnostic, it has been difficult for those who described and mapped these units to establish firm time equivalence from basin to basin.

Similarly, compositions of the Cenozoic volcanic rocks vary profoundly and abruptly, both laterally and vertically; with the exception of the growing body of isotopic ages now available, few stratigraphic tools are available to allow these rocks to be correlated from basin to basin.

In addition to lying as thick fills on the floors of structural basins, these rocks are exposed on the flanks of the north-south-trending mountain ranges, where dissection of the rising masses has often resulted in isolation of individual rock bodies from the main mass of the formation. Furthermore, the section both in the basins and on the flanks of the mountain ranges typically has been much affected by late-Tertiary movement along faults, many of which appear to be high-angle reverse faults or thrust faults of minor displacement (north of Lake Mead large-magnitude late-Tertiary strike-slip faulting has been described; see Anderson, 1973), despite the dominant pattern of movement along extensional normal faults.

3.242 TERTIARY UNITS

3.2421 GENERAL STATEMENT

The great complexity of the Tertiary volcanic sequence has required that we group together several discrete volcanic units that, despite some disagreement as to their actual spatial and temporal relationships, have been recognized as distinct formations in the field. Because the DTR-1 is underlain by a late-Tertiary sedimentary section assigned by Laney (1973) to the Muddy Creek Formation, however, we have retained the full complexity of stratigraphic nomenclature assigned to sedimentary

rocks of Tertiary age.

3.2422: TKg (Longwell et al, 1965)
Tertiary Gale Hills Formation

3.2423: TKv (Gillespie and Bentley, 1971)
Cretaceous (?) and Tertiary (older) volcanic rocks
Andesite and latite flows and tuff; includes Gold Road Latite. May be wholly or in part correlative with units described below.

3.2424: Th (Longwell et al, 1965)
Tertiary Horse Spring Formation

3.2425: Tm (Anderson, 1977, 1978; Anderson and Laney, 1975; Blair, 1978; Bentley, 1971; Laney, 1973; Longwell, 1936, 1951, 1963; Longwell et al, 1965; McKelvey et al, 1949; Volborth, 1973; Wilson and Moore, 1969)
Tertiary Muddy Creek Formation; sedimentary (and volcanic) rocks, undivided
Basin-fill-type, mostly clastic strata; mostly coarse boulder and cobble conglomerate containing sand and silt as matrix; locally well-developed shale and siltstone strata. Evaporite strata and lenses, principally gypsum, common; in detrital wash a substantial thickness of bedded halite has been described from the subsurface (see Laney, 1973; U.S. Geological Survey, 1972). May include beds of air-fall tuff and/or lava not assigned to other units; locally (see McKelvey et al, 1949) contains beds of manganiferous silty gypsum of commercial value. Where possible, it has been subdivided in the field; refer to descriptions of individual members in following sections (3.2436-3.2429; 3.24215).

3.2426: Tml (Anderson, 1978; Laney, 1973; Longwell, 1951)
Tertiary Lower Muddy Creek Formation
Coarse, poorly bedded angular pebble- cobble- and boulder-conglomerates grading to weakly lithified thin-bedded sandstone, silty sandstone, siltstone, and minor thin beds of of gypsum and carbonate. Underlies megabreccia mass of Longwell (1951, 1963); see Tmm, section 3.2427.

3.2427: Tmm (Anderson, 1978; Longwell, 1951, 1963)
Tertiary Middle Muddy Creek Formation (Megabreccia)
The main mass between the Black Mountains and the Colorado River at lat 35°56' N is composed of Precambrian landslide debris stripped from Black Mountains to the east. Mass separates Tml (section 3.2426) from overlying Tmu (section 3.2428) and is distinctly tabular with major slip planes parallel to gently dipping finely comminuted lower contact zone. Shattered blocks (mosaic breccia) as large as several hundred feet across are common; large local areas of breccia are almost monolithologic; includes as much as 40' in thickness of coarse fluvial clastic rock indicating at least two landslip pulses.

3.2428: Tmu (Anderson, 1978; Laney 1973)
Tertiary Upper Muddy Creek Formation

Mostly poorly sorted, poorly stratified, coarse fanglomerate, moderately lithified except near some faults where it is strongly lithified. Overlies megabreccia mass (section 3.2427) of Longwell (1951, 1963).

3.2429: Tmhl (Laney, 1973; Anderson and Laney, 1975; Blair, 1978)

Tertiary Upper Muddy Creek Hualapai Limestone Facies

Gray to white, porous, contorted, thin to very thin limestone beds; locally contains individual nodules and/or discontinuous beds of chert.

3.24210: Tvmu (Anderson, 1977, 1978; Gillespie and Bentley, 1971; Laney, 1973; Longwell, 1963; Longwell et al, 1965, Volborth, 1973; Wilson and Moore, 1969)

Tertiary Volcanic Rocks (Mostly Miocene?), Undivided

Includes a broad variety of intimately interfingered middle Tertiary volcanic rocks, of composition ranging from basaltic to rhyolitic, including flows, air-fall tuffs, and volcanic breccias. Includes Patsy Mine, Golden Door, and Mount Davis Formations of Longwell (1963); Patsy Mine, Bridge Spring, and Mount Davis Formations of Anderson (1977, 1978); undivided Tertiary volcanic rocks of Laney (1973), Longwell et al (1965), and Wilson and Moore, and Younger Volcanic Rocks of Gillespie and Bentley (1971).

3.24211: Trv (Anderson, 1977)

Tertiary Volcanic and Intrusive Rock

Complexly altered, brecciated, and sheared transition zone that separates predominantly intrusive rocks from predominantly volcanic rocks. Intensely sheared and brecciated rock and general structural chaos, especially near transitional contacts, suggest much post-intrusive displacement on a complex fracture system not mapped.

3.24212: Ta (Anderson, 1977)

Tertiary Andesite

Numerous flows of porphyritic andesite that are medium gray, grayish purple, and pale red in their stoney interiors, and have red or yellowish-brown vesiculated to scoriaceous rinds. May be age equivalent of lavas mapped as Mount Davis Volcanic Rocks (Tvmu, section 3.24210).

3.24213: Ti (Anderson, 1977, 1978; Laney, 1973; Longwell, 1963; Longwell et al, 1965)

Tertiary Intrusive (Plutonic) Rocks

Boulder City Pluton: part of a large composite epizonal batholith; may include other plutonic rocks. Mostly light-gray, fine- to medium-grained, faintly to distinctly porphyritic, nonfoliated pyroxene-bearing quartz monzonite containing biotite and hornblende as important mafic constituents; locally dikes constitute as much as 50% of mass; mafic mineral assemblages are complex. Wilson Ridge Pluton: sparse very light-gray leucocratic biotite granite through anundant gray faintly foliated hornblende-biotite granodiorite to sparse dark gray pyroxene-biotite diorite; contacts with older rocks are sharp and both

concordant and discordant. Unit locally includes undifferentiated dikes ranging in composition from basaltic to rhyolitic; most are probably equivalent to extrusive rocks of Tmf (section 3.24215) or Mount Davis Volcanic Rocks (see Tvmu, section 3.24210).

3.24214: Tgr (Volborth, 1973)
Tertiary Granite (Intrusive)

3.24215: Tmf (Anderson, 1977, 1978; Laney, 1973; Longwell, 1963)
Tertiary Fortification Basalt
Lavas intercalated with and overlying the sedimentary rocks of the Muddy Creek Formation. Mostly thin flows of dark gray to black olivine basalt having typical oxidized and brecciated contact zones. Thin flows are commonly glassy and vesiculated throughout. Olivine is sparse in some flows; olivine and augite occur in subequal amounts in others. Zoned basalt and camptonite dikes may represent feeder dikes for some flows immediately west of Black Mountains. K-Ar age of 4.9 m.y. obtained from sample at BM 2257, just west of Black Mountains along highway U.S. 93; K-Ar age of 5.8 m.y. obtained from flow on Malpais Mesa, between Black Mountains and Colorado River.

3.24216: Ts (Gillespie and Bentley, 1971)
(Tertiary) Older Alluvium
Moderately consolidated fragments of granite, schist, gneiss, and volcanic rocks and poorly consolidated tuff and agglomerate. Occurs as dissected alluvial fans and valley-fill deposits of fluvial and lacustrine origin; may include some beds of marine origin. May be wholly or in part equivalent to Muddy Creek Formation (sections 3.2425-3.2429 and 3.24215).

3.24217: (QTs and QTcr are described below, under Quaternary Units, sections 3.2432 and 3.2433)

3.243 QUATERNARY UNITS

3.2431 GENERAL STATEMENT

The Quaternary rocks described here are the youngest of the sedimentary rock units that have been deposited on basin fills and in channels and on slopes of block-mountain ranges. Since the youngest known volcanic unit, the Fortification Basalt (section 3.24215) has been dated at 4.9-5.8 m.y. (Anderson et al, 1972), no volcanic rocks have been assigned to Quaternary time, although portions of QTs (section 3.2432), QTcr (section 3.2433) and Qalu (section 3.2435) may in fact be time equivalent to Tmf.

3.2432: QTs (Gillespie and Bentley, 1971)
(Quaternary and Tertiary) Intermediate Alluvium
Weakly to moderately consolidated fragments of granite, schist, gneiss, and volcanic rocks. Occurs as dissected alluvial fans and valley-fill deposits of fluvial and lacustrine (?) origin. Locally may include older and younger alluvium.

3.2433: QTcr (Laney, 1973)
Quaternary and Tertiary Colorado River Deposits
Individual beds and surface veneer of moderately to well sorted sand to cobble-size rounded exotic material.

3.2434: Qc (Laney, 1973; Longwell, 1963)
Quaternary Chemehuevi Formation
Light reddish-brown weakly cemented silt that contains sand and gravel beds; the gravel beds consist of subangular fragments of gneiss, schist, andesite, and basalt, and as much as 5% of rounded pebbles and cobbles of chert, quartzite, and granite.

3.2435: Qalu (Wilson and Moore, 1969)
Quaternary Alluvium, Undivided
Mainly alluvial gravel, sand, and silt in flood plains, terraces, fans, and pediment cappings, but locally includes dune sand, lake deposits, and landslide masses.

3.2436: Qal (all sources)
Quaternary Alluvium
Sheet form, unbedded unlithified detritus; unlithified pell-mell detritus that forms beds for modern intermittent washes; colluvium near bedrock slopes; areas of bedrock partially mantled by colluvium and talus; coarse stream gravel and conglomerate, etc.

3.2437: Qs (Gillespie and Bentley, 1971; Wilson and Moore, 1969)
Quaternary Sediment
Piedmont deposits consisting of poorly consolidated fragments of granite, schist, gneiss, and volcanic rocks.

3.2438: Qp (Anderson, 1977; Gillespie and Bentley, 1971)
Quaternary Playa Deposits
Playa deposits consisting of unlithified clay and silt.

3.2439: Qg (Laney, 1973)
Quaternary Terrace Gravel
Light-grayish-brown weakly cemented coarse-grained gravel of local origin.

3.3 RECAPITULATION

The foregoing descriptions are of rock units included on the larger, regional map of Plate 1. Full descriptions of the rock units mapped on DTR-1 appear in section 5.

4.0 REGIONAL GEOLOGIC STRUCTURE

The structural pattern of rocks exposed in the Basin-and-Range Province offers a dramatic contrast to the structure of rocks exposed east of Grand Wash and continuing across the Colorado Plateau. On the Plateau, a terrain of folded, faulted, and metamorphosed Precambrian rocks is overlain unconformably by a remarkably complete section of unmetamorphosed, essentially

flat-lying sedimentary rocks of Paleozoic through Mesozoic age; the present undisturbed nature of this column of rock demonstrates that not only was the whole of Paleozoic and Mesozoic time lacking in significant tectonic events, but that all of post-Mesozoic time has been similarly quiescent, with the exception of those periods when Tertiary volcanic rocks were extruded.

West of Grapevine Wash, however, the tectonic history has been profoundly different. The region today consists of alternating north-south-trending mountain ranges separated by deeply filled valleys; this topography has developed in response to a period of regional extension that allowed the valley floors to be dropped as structural basins along north-south-trending normal faults as individual mountain blocks rose between them. Subsequent erosion has cut deeply into the rocks that constitute the ranges, and has deeply buried the intervening valleys with the debris of that erosion. The major faults along which this motion occurred are, in most cases, concealed beneath the alluvial fill that lies in the valleys.

Erosion of the mountain blocks has been deep enough to have stripped off most of the Paleozoic and Mesozoic rock units that are so well exposed on the Colorado Plateau, exposing the Precambrian cores beneath.

The materials that have accumulated in the structural depressions are varied and stratigraphically complex. In addition to sediments derived from erosion of the mountain blocks, which in many parts of the Basin-and-Range Province have been subdivided into a number of Tertiary basin-filling formations, the basins also received masses of eruptive rocks derived from a complex sequence of Tertiary volcanic events, the timing of which may have been related to recurring episodes of displacement along the major faults. Thus, erosion, deposition, volcansim, and faulting have taken place consurrently through much of Tertiary time; the result is an extremely complex pattern of faulted, deformed basin fills which can be correlated only with difficulty from basin to basin. Many such sequences have been assigned to the Muddy Creek Formation.

Detailed maps of parts of the southern Basin-and-Range Province, such as those of Anderson (1977, 1978) show a bewilderingly complex pattern of closely spaced minor faults of every conceivable configuration. Such complexity is, of course, not expressed on smaller scale reconnaissance maps of lower resolution. We have chosen not to portray the full complexity of this structural pattern on those few portions of the larger regional map of Plate 1 for which information of such quality is available.

5.0 FOCUS ON DTR-1

5.1 GENERAL STATEMENT

The Dynamic Test Range - 1 lies in Detrital Wash, one of the broadest of the filled valleys in this part of the Basin-and-Range Province. The watershed of Detrital Wash extends

beyond the southern limit of the larger map area; the valley itself drains a complex terrain, consisting of a block of Precambrian high-grade metamorphic and acidic igneous rocks, intruded by a Tertiary acidic pluton and draped in a Tertiary sedimentary/volcanic complex, in the Black Mountains along the western margin of the valley; a thick sequence of superposed middle-Tertiary lavas and younger sedimentary rocks in the White Mountains along the northeast margin of the wash; and a poorly known Precambrian complex exposed in the Cerbat Mountains that rise along the southeast margin of the valley. The valley floor itself is underlain by an unknown thickness of Muddy Creek Formation, overlain in the valley axis by several hundred feet of the Chemehuevi Formation, a mass of sediment of highly variable grain size and lithology that was deposited in a closed basin that developed across the course of the Colorado River in Pleistocene (?) time. That basin ultimately was breached by a through-flowing Colorado River, and erosion removed all but a few remnants of Chemehuevi rocks as the river acquired its pre-dam configuration late in Pleistocene time. In the process of that incision a number of distinct Quaternary morpho-stratigraphic units have developed that appear on the map of DTR-1 and are described in some detail below.

5.2 DESCRIPTION OF ROCK UNITS (see fig. 4 and Plate 2)

5.21: Tm (Laney, 1973)
Tertiary Muddy Creek Formation (Mudstone Facies)
Light reddish-brown weakly to moderately cemented siltstone and claystone that grades into white bedded gypsum

5.22: Tmhl (Laney, 1973)
Tertiary Hualapai Limestone Member (Facies) of the Muddy Creek Formation
Gray to white, porous, contorted, thin to very thin limestone; locally contains individual nodules or discontinuous beds of chert.

5.23: Qc (Laney, 1973)
Quaternary Chemehuevi Formation
Light reddish-brown weakly cemented silt that contains sand and gravel beds; the gravel beds consist of subangular fragments of gneiss, schist, andesite, and basalt, and as much as 5% of rounded pebbles and cobbles of chert, quartzite, and granite. Materials of these compositions could not be transported to this site by a drainage network of the present configuration; these sediments must have been carried down the axis of the Colorado River at a time when the river flowed at a higher elevation.

5.24: Qg (Laney, 1973)
Quaternary (Terrace) Gravel
Light grayish-brown weakly cemented coarse-grained gravel of local origin; caps erosion surfaces of older units; generally less than 10 feet thick; mapped only in the area east of Detrital Wash.

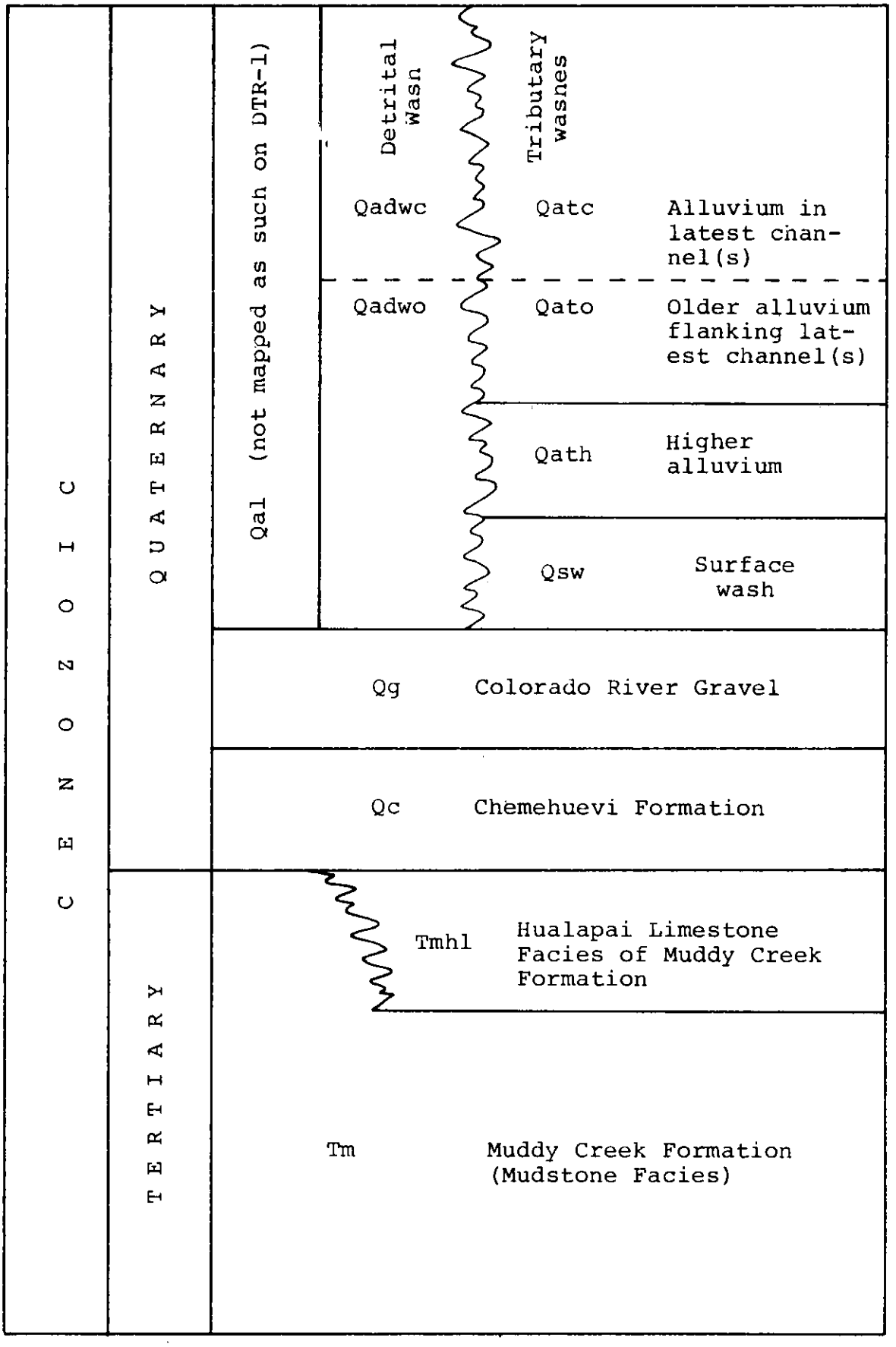

Figure 4: Schematic Stratigraphic Column for DTR-1

5.25: Qsw (this report)
Quaternary Surface Wash
This represents the surficial material that veneers alluvial and pediment surfaces, principally on the west side of Detrital Wash, that cannot conveniently be assigned to any other map unit. Thus, the debris that has moved downslope off the east flank of the Black Mountains has covered earlier rocks assigned to the Muddy Creek and Chemehuevi Formations; along much of the west side of Detrital Wash it has not been possible to determine the location of a contact between the Muddy Creek Formation and the overlying Chemehuevi Formation through the overlying veneer. East of Detrital Wash all such veneer is derived directly from the Chemehuevi Formation, and is mapped as Qc. Qsw west of Detrital Wash is not today actively accumulating, although it may be redistributed from time to time; indeed, it is being removed as incision of the present drainage pattern proceeds. East of Detrital Wash masses of gravel from the Chemehuevi may still be accumulating over the surface of the Chemehuevi Formation and, to a lesser extent, over exposures of Muddy Creek Formation. Some surficial material is, no doubt, moving downslope over the limited exposures of Muddy Creek Mudstone Facies that appear on the map of DTR-1, but has not accumulated in sufficient thickness to obscure the nature of the underlying rock and thus is not separately mapped.

5.26 Quaternary Alluvium

We make here, for the sake of mapping convenience consistent with the objectives of the contract, an artificial distinction between those morphostratigraphic units of alluvium that can be related directly to the present drainage network and those that are the products of a drainage system no longer extant (e.g. Qc, Qg, Qsw).

5.261 Tributary Alluvium vs Detrital Wash Alluvium

On the map of DTR-1 we make the distinction between alluvium derived from tributaries to Detrital Wash, whose source of detrital material is quite local, and alluvium deposited in the axis of Detrital Wash, which may be derived from a greater distance and owe its component lithologies to a broader range of bedrock types.

5.2611: Qath (this report)
Quaternary Alluvium in Tributaries, from Higher Terraces
This unit consists of materials locally derived that were deposited during a period when tributary valleys were graded to a higher elevation of the trunk stream. These materials are now being actively removed as tributary streams are incised to a lower position of Detrital Wash.

5.2612: Qato (this report)
Older Quaternary Alluvium in Tributaries
This unit consists of sediment, locally derived, that was deposited on the floors of tributary valleys in the recent past. This material has not been remobilized in the most recent

surface-runoff event to have visited each valley (as identified from air-photo coverage of September 20, 1978).

5.2613: Qatc (this report)
Quaternary Alluvium in the Youngest Channel of each Tributary
Sediment most recently mobilized, as identified from air-photo coverage of September 20, 1978.

5.2614: Qadwo (this report)
Older Quaternary Alluvium in Detrital Wash
This unit consists of sediment deposited on the floor of Detrital Wash in the recent past. This material has not been remobilized in the most recent surface-runoff event to have visited Detrital Wash, as identified from air-photo coverage of September 20, 1978.

5.2615: Qadwc (this report)
Quaternary Alluvium in the Youngest Channel of Detrital Wash
Sediment most recently mobilized, as identified from air-photo coverage of September 20, 1978.

5.3 STRUCTURAL GEOLOGY OF DTR-1

Laney (1973; see also U.S. Geological Survey 1972) has identified a south-plunging anticline, developed in sediments of the Muddy Creek and Chemehuevi Formations, the axis of which approximately parallels the axis of Detrital Wash. This structure is attributed by Laney (1973) to flowage of a mass of bedded halite that makes up part of the Mudstone Facies of the Muddy Creek Formation at this locality; the details of the configuration of this salt body have been determined from data recovered from 10 test wells (Laney, 1973; U.S. Geological Survey, 1972). The map of Plate 1 shows the approximate outline of this salt body in the subsurface. Similar structures have been described farther north along the Virgin Valley (U.S. Geological Survey, 1972), but lack of subsurface data has prevented those interested in the structures from identifying the thickness and extent of the salt body to the north.

The area of DTR-1 is too small to show the overall configuration of the salt anticline, as it falls wholly within the area underlain by the halite body and lies along the crest of the anticline. A number of dramatic smaller structures are well developed along the east flank of Detrital Wash just above where it enters Bonelli Bay; at this locality the Hualapai Limestone Facies, that here represents the uppermost unit of the Muddy Creek Formation, defines by its structural competence a cluster of tight domes, some no more than 50 m in diameter, that are not expressed either in the gypsiferous shales and siltstones of the underlying mudstone or in the fine sands and gravels of the overlying Chemehuevi Formation. Whether these small structures are related to development of the halite-cored anticline or were formed by flowage of the underlying gypsiferous siltstones is not clear. Elsewhere along the Muddy Creek - Chemehuevi contact where Hulalpai Limestone is absent, as along

the west flank of Detrital Wash, there is no evidence of such small-scale structures. Where Hualapai Limestone occurs outside the limits of the halite body in the subsurface, no such structures are apparent, except for the well-developed syncline in Tertiary rocks at Temple Bar, which Laney (1973) did not attribute to deformation of subsurface halite.

5.4 GEOLOGIC MAP OF DTR-1

Plate 2 is a geologic map of DTR-1, generated in the field on individual air photos produced for the contract. The information from the photos was later transferred to the topographic base map also provided for the contract. While minor revisions were made in Laney's (1973) map at 1:62,500, and while a great deal more detail is apparent at 1:6000, we acquired from Laney's work an important orientation to the local stratigraphy without which our work would have been far more difficult.

6.0 GEOLOGIC HISTORY

From remnants of unmetamorphosed sedimentary rocks exposed in the River Mountains just west of the western end of Lake Mead, it is clear that a Paleozoic-Mesozoic section much like that preserved today on the Colorado Plateau was laid down unconformably over a complexly deformed and metamorphosed Precambrian crystalline basement across the full width of the map area of Plate 1. In early Tertiary time a regional tensional stress-field was first imposed on the southern portion of what is now the Basin-and-Range Province (e.g. Stewart, 1971); a series of alternating north-south-trending mountain blocks and deep structural depressions developed in response to this stress, which abundant evidence indicates persists today, although students of Basin-and-Range tectonics disagree as to its contemporary configuration. During Tertiary time erosion stripped off much of the Paleozoic/Mesozoic sedimentary cover, reducing it to basin-fill detritus and exposing Precambrian rocks in the cores of the north-south-trending mountain blocks. Intervening valleys were filled with this detritus and with lavas of a wide range of compositions that were extruded through much of Tertiary time. Continued movement along the major normal faults and associated minor faults has deformed the Tertiary sequence, both on the mountain blocks and within the sediment-filled grabens. In many localities minor thrust faults have developed (e.g. Anderson, 1977, 1978); just north of Lake Mead a severely disturbed mass of rock preserves evidence of late-Tertiary strike-slip displacement (Anderson, 1973).

Some time during the late Tertiary (there is not yet firm agreement on details of the chronology) the Colorado River was established across several north-south-trending mountain ranges, thereby integrating drainage from a number of formerly isolated closed structural basins. Much evidence indicates that the tectonic and erosional processes that accompanied this development are as active now as they have ever been.

7.0 PETROLOGIC ANALYSES

7.1 GENERAL STATEMENT

As part of the requirements of the present contract, a number of samples of surficial sediment and soil were collected from within DTR-1; of these, 78 were delivered to the Geology Department of the University of Pennsylvania for petrologic analysis. The localities from which these samples were taken are plotted on the geologic map of Plate 2.

Each of the samples was analyzed for:

Moisture
pH
Organic concentration
carbonate concentration
particle-size distribution
mineralogy

These analyses were performed in the soil- and sediment-analysis laboratories of the Geology Department of the University of Pennsylvania. We summarize below the analytical procedures used for each of the above; the analyses themselves are presented in tabular form as appendices (section 10).

7.2 MOISTURE

Moisture content (expressed as percent) was determined as follows:

a) ± 100 g of wet sample (taken directly from plastic bag in which it was delivered) was weighed out.

b) sample was oven-dried @ 105° C for at least 48 hours.

c) dry sample was re-weighed

d) % moisture was calculated from the expression:

$$\% \text{ moisture} = 100 - \frac{\text{dry weight}}{\text{wet weight}} \times 100$$

Results of these determinations are tabulated in column 1 of Appendix 1 (section 10.2).

7.3 pH

pH was determined as follows:

a) each sample was mixed with an equal volume of double-de-ionized water.

b) each sample was agitated and allowed to sit 1 hour.

c) pH was measured with a pH meter.

pH values are tabulated in column 2 of Appendix 1 (section 10.2)

7.4 ORGANIC CONCENTRATION

The Walkley-Black method (see Allison, 1965) was used for determination of concentration of organic carbon:

a) A weighed sample of coarsely gound material was transferred to a flask.

b) 10 ml of 1N $K_2Cr_2O_7$ were added and the flask swirled gently.

c) 20 ml of concentrated H_2SO_4 were then added rapidly, the flask was swirled for 1 minute, and then set aside for about 30 minutes.

d) 200 ml of water and 3 drops of o-phenanthroline indicator were added, and the solution was titrated with o.5N $FeSO_4$ to a maroon endpoint.

e) Percent organic C was calculated according to the following formula, using a correction factor f = 1.33.

$$\text{Organic C, \%, } = \frac{(\text{milliequiv. } K_2Cr_2O_7 - \text{milliequiv. } FeSO_4) \times 0.003 \times 100}{\text{grams water-free soil}} \times (f)$$

Values for organic C are tabulated in column 3 of Appendix 1 (section 10.2)

7.5 CARBONATE CONCENTRATION

The gravimetric method (see Allison and Moodie, 1965) for loss of carbon dioxide was used for this determination:

a) A stoppered flask containing 50 ml of 3N HCl was weighed, and a weighed soil sample of known water content added slowly.

b) After effervescence subsided, the stopper was loosely replaced and the flask set aside.

c) At intervals of 30 minutes, the flask was unstoppered and swirled.

d) Within 2 hours, the reaction was complete; the flask and its contents were weighed.

e) Percent $CaCO_3$ equivalent was calculated as follows:

$$\text{weight of } CO_2 \text{ lost} = \text{difference in initial and final weights of (flask + stopper + acid + soil)}$$

$$CaCO_3 \text{ equivalent \%} = \frac{\text{grams } CO_2 \text{ lost}}{\text{grams water-free soil}} \times 2.274 \times 100$$

Values for carbonate concentration are tabulated in column 4 of Appendix 1 (section 10.2).

7.6 PARTICLE-SIZE ANALYSIS

Particle-size analysis was undertaken by conventional means. Weight-percent values for gravel (dia. > 2mm) were determined by dry-sieve separation. Values for sand, silt, and clay were determined by hydrometer wet-separation technique (see Day, 1965); corrected values were determined from the Stokes equation.

Particle-size information is presented in tabular form in Appendix 2 (section 10.3)

7.7 MINERALOGY

Even cursory field examination of the surficial materials at DTR-1 clearly demonstrates that those materials have been largely unaltered by pedogenic processes. This inference is strongly supported by the extremely low values reported for organic C (see App. 1, col.3).

While it is certainly true that these materials would be considered soils either by a pedologist or an engineer, most geologists would feel more comfortable describing them as surficial sediments, since the extent of pedogenic alteration they have undergone has been so slight as to be undetectable by conventional petrologic analyses.

The material at the surface of DTR-1 represents, in fact, a column of largely unconsolidated, unaltered sediment, ranging in age from Miocene(?)-Pliocene, in the case of the Muddy Creek Formation, to the several months preceding September 20, 1978, in the case of Qatc and Qadwc; these sediments are derived from parent materials of a broad range of mineralogies.

While it is possible that minor amounts of U, Th, and K might have been concentrated in parts of the Muddy Creek Formation by circulating ground water in the ± 10 million years since that sediment was deposited, it is unlikely that conditions have been appropriate or the lapse of time sufficient to have allowed such processes to have significantly affected the younger sediments. It thus seems inescapable that any minerals in these materials with concentrations of U, Th, and K high enough to be of interest must be derived from the source area(s) that contributed the bulk of the enclosing sediment.

Thus, we concluded that the component of the analyses specified in the contract most likely to yield useful information is the analysis for mineralogy; accordingly, we have made this analysis the most comprehensive.

Four size-class separates were analyzed for mineralogy:

7.71 GRAVEL MINERALOGY

The gravel that was separated by dry sieving in the first step of the particle-size analysis was examined under the binocular microscope and the individual grains identified by conventional low-magnification hand-specimen techniques. A semiquantitative tabulation of this analysis appears as Appendix 3 (section 10.4)

7.711 DISCUSSION

As can be seen from the data of Appendix 3, the gravel is decidedly immature, rock fragments exceeding individual mineral grains in most of the samples. With a better knowledge of the mineralogy of the various source areas, it might be possible to identify the provenance of each sample with some precision by reference to the mineralogy of the gravel fraction.

7.72 SAND MINERALOGY

A portion of the sand-size fraction was also analyzed under the binocular microscope; a semiquantitative tabulation of those data is presented as Appendix 4 (section 10.5).

7.721 DISCUSSION

The sand fraction appears mineralogically somewhat more mature than the gravel fraction, although rock fragments are still abundant. The gypsum identified in 19 of the samples may be secondary rather than detrital.

7.73 SILT-SIZE HEAVY MINERALS

Heavy minerals from a sample of the silt-size fraction were separated through a column of bromoform and identified in oil immersion under a petrographic microscope. The analyses are tabulated in Appendix 5 (section 10.6).

7.731 DISCUSSION

We do not yet know enough about the detailed mineralogy of the various source areas to allow us to use the data of heavy mineralogy as a diagnostic approach to provenance identification.

7.74 CLAY MINERALOGY

Each sample was suspended in water, and allowed to settle for 8 hours. The fine particles still in suspension (those less than about 2 microns in diameter) were decanted and filtered. Sediment trapped on the filter was then analyzed by X-ray diffraction, using Ni-filtered Cu radiation, and a scanning speed of 1°/minute. Scans from 5° to 20° 2θ were performed for each sample, and 15 representative samples were selected and further analyzed.

The 15 samples were scanned from 4° to 30° (or greater) 2θ,

at a speed of ½°/minute. Eight samples were treated with etnylene glycol and X-rayed again. Six samples were heated to 300° C and X-rayed, six to 400° C and X-rayed, and 2 to 600° C and X-rayed. The results are discussed below, and tabulated in Appendix 6 (section 10.7).

7.741 DISCUSSION

All samples contain montmorillonite, chlorite, illite, and kaolinite. In only one (o132 & ◊8; ◊8 & o132) can palygorskite be determined with some assurance; there are a number of other samples in which it is very tentatively identified. Palygorskite diffraction patterns show reflections at about 10.5, 6.4, 4.5, and 3.23 Å. Illite/muscovite reflections overlap the 4.5 Å reflection, and sometimes the 10.6 Å peak as well. In o132 & ◊8 the 6.4 Å reflection may be seen, as may the 3.23 Å reflection. These latter peaks are identified somewhat more tenuously in sample o177, and also in o33, where the 3.23 Å peak is so broad and diffuse that it resembles a blur rather than a peak. Sample o90 may also contain palygorskite, as may o62, o66, o105, o107, o108, o115, and o142, but abundances are very low compared to other minerals present. Relative abundances of palygorskite in the rest of the samples, if indeed the mineral is present, are below detection limits.

All 78 samples analyzed show reflections on the diffractograms in the area from about 15 Å to about 12 Å. Treatment with ethylene glycol and subsequent X-ray analysis showed that the broad blur of peaks shifted to the 17 Å region, indicating the presence of montmorillonite. Heating to 300° C caused the 12-15 Å peak(s) to shift to about 9.8 Å. Glycolation expands the montmorillonite lattice; heating to 300° C causes the lattice to begin a stepwise collapse as interlayer water is driven off.

Both heating and glycolation confirmed the presence of montmorillonite; judging from the very broad peak of the (001) reflection, the montmorillonite is probably variable in composition and may be interlayered with chlorite. With the removal of the 12-15 Å basal reflection of montmorillonite by heating or glycolation, a small 14 Å peak attributed to the (001)reflection of chlorite could be seen. Since this peak did not intensify upon heating, a characteristic of Mg-chlorites, the chlorite present is presumed to be Fe-chlorite.

A reflection at about 7.1 to 7.2 Å may be seen in all 78 analyses. This in part represents the chlorite (002) reflection, and in part the (001) reflection of kaolinite. That this peak is contributed by two minerals was confirmed by treatment with warm 1N HCl, which dissolves Fe-chlorite, but not kaolinite. Subsequent X-ray analysis showed that the 7 Å peak had diminished in intensity, but had not disappeared. The presence of kaolinite is also attested by the persistent presence of a reflection at 3.58 Å.

The 10 Å peak seen in all diffractograms is attributed to

muscovite/illite. The peak is often broad, and may include the basal reflection of palygorskite at 10.6 Å, but in most samples the two cannot be resolved and, as stated above, the presence of palygorskite cannot be confirmed. The 10 Å clay is most probably muscovite (2M), as all reflections for this polytype are apparent. Illite, a disordered muscovite (1Md), most strongly shows the basal reflection at 10 Å. (1M and 2M illites also exist, but they are really micas; illite is largely used as a field term.) It is likely that the montmorillonite discussed earlier is interlayered with the 10 Å clays. The relative proportions of the ordered mica (2M) to the disordered illite (1Md) cannot be assessed, but the presence of the latter is suggested by the broad peak at about 10 Å. This reflection becomes more intense upon heating for both the 2M and 1Md polytypes; this was observed in the analyses reported here.

The tables of Appendix 6 (section 10.7) indicate the minerals present, and an approximation of relative proportions. It is difficult to quantify the amount of each clay mineral present in terms of per cent. X-ray intensities are not truly proportional to the amount of each phase present due to a) variation in the degree of orientation of each sample; b) relative amounts of other, non-clay minerals present as a matrix; c) differences in the mass-absorption coefficient of the minerals analyzed; d) variation in quality of crystallinity; and e)the non-linearity of intensity vs ratio of two clay minerals. Since the majority of the diffractograms show a background of about 20 units (2") on the chart paper, intensities of the various peaks may be compared in a rough way as representing relative amounts, but these should not be taken to represent percentage of total sample, as the amount of quartz and calcite present varies from sample to sample. Those samples with a background of lower intensity cannot be compared with those of a higher intensity, as this effect may be due to differences in thickness of the sample and, in part, to the amount of iron present.

Although no quantitative estimates of the amounts of the clay minerals can be made without considerably more exacting procedures, it is not difficult to tell which samples have proportionately more illite/muscovite, which more kaolinite, and so on. The amount of montmorillonite seems fairly substantial in all cases, and the amount of chlorite appears to be low. The problems with palygorskite have been discussed earlier. In any case, the data of Appendix 6 represent reproducible semiquantitative assessments of the clay minerals identified in each sample. As such they can be used to characterize in part the clay-size mineralogy of the samples,and to draw instructive inferences as to the depositional, diagenetic, and pedogenic histories of the surficial materials of DTR-1.

8.0 RECOMMENDATIONS

Within a few minutes of our arrival at DTR-1 in January, 1979, a fundamental problem with the use of this locality as a calibration standard became apparent:

With the possible exception of the Hualapai Limestone, and the gypsum in the mudstone facies of the Muddy Creek Formation, all materials exposed at DTR-1 are sediments transported to the site of deposition as clastic particles. For exposures of Muddy Creek Formation, from which 1 of the 78 samples we analyzed was collected, the clastic material has remained in place for perhaps 10 million years, but for many of the younger, still-active sedimentary units the residence time of material in a given morphostratigraphic unit may be short indeed. Thus, sediment in localities mapped as Qatc and Qadwc on Plate 2 was deposited in the last climatic event (or events) to generate surface runoff in Detrital Wash and its tributaries prior to September 20, 1978, the date the air photos were taken. According to Park Service officials at Temple Bar, principal access to which is via a road that crosses the floor of Detrital Wash within the map area of Plate 2, runoff water flows on the floor of Detrital Wash and across the main road about three times a year, on the average. At each of these times, sediment on the valley floor is remobilized, retransported, and redeposited as a new Qadwc. The same is true of the unit Qatc. In fact, it is likely that the map units Qadwc and Qatc would be entirely different from those that appear on Plate 2, if they were identified on photos taken since the photo coverage of September 20, 1978, or even since the 78 samples analyzed here were collected January 1979.

If all the material in transit through the various intermittent stream channels were wholly locally derived, the gross mineralogy (and hence, perhaps, the concentrations of U, Th, and K) might not change appreciably from storm to storm; while this may be true of some of the shorter washes entering Detrital Wash from the east, it is certainly not true of the larger washes on the east, the washes draining the Black Mountains on the west, or the upper reaches of Detrital Wash itself, all of which drain terrains of diverse lithologies. Thus, the mineralogy of a succession of floods in Detrital Wash or one of the larger tributaries may vary profoundly depending on where in the watershed the storm occurs that generates the surface runoff.

Thus, all sediment assigned to the units Qadwc, Qadwo, Qatc, and Qato must be assumed to have a residence time on the valley floor(s) of the order of a few months. Of the 78 samples analyzed here, came from these 4 units. Sediment assigned to the map units Qath, Qg, Qc, and Qsw may be expected to have a longer residence time at a given locality, but we cannot estimate from information available how long that residence time might be.

It is unfortunate that DTR-1 should be located on a terrain so prone to redistribution of its surface materials, when one considers that one of the prerequisites of a test site should be mineralogical stability. Detrital is, indeed, the key word for an understanding of the local geology of DTR-1!

We offer the following proposals to either correct or compensate for this problem:

1. To compensate for the problem, the DTR-1 in Detrital Wash should be characterized in far more detail.

   With the analyses herein included, we now know far more about the mineralogy of the sediment in Detrital Wash than we do about the mineralogy of the various source areas.

   a) The watershed of Detrital Wash extends beyond the southern limit of the map of Plate 1; a new, detailed geologic map of the Detrital Wash watershed, at a scale of 1:62,500, should be produced, both to characterize the entire watershed in geologic terms, and to take advantage of the high quality of the best materials now available (e.g. Anderson, 1977, 1978; Laney, 1973). This will require some basic field mapping of the northern end of the Cerbat Mountains.

   b) The rock types exposed in the entire Detrital Wash watershed should be characterized in petrographic terms in sufficient detail to allow reasonable assessment to be made of the probable provenance of any sediment sample taken from the DTR-1. Such an assessment can rarely, if ever, be made uniquely, however, since detritus from many sources, including material in storage on the floor of any wash, may be mixed during even a minor surface-runoff event.

   Such lithologic characterization of the Detrital Wash watershed will require petrographic analysis of a minimum of 400 thin sections.

2. To correct the problem, a new DTR should be established, within the limits of the larger map of Plate 1, on which surficial materials are sufficiently stable to meet the stability requirements of a calibration site.

9.0 BIBLIOGRAPHY

The references listed here include those that were used in compilation of the map of Plate 1 (see explanation to fig. 2), as well as sources consulted in the process of acquiring background information for compiling that map and appropriate field orientation for undertaking the detailed study of DTR-1.

* * *

1. Allison, L.E., 1965, Organic carbon: section 90 in Methods of soil analysis, Part 2, American Society of Agronomy, Madison, Wisconsin.

2. Allison, L.E., and Moodie, C.D., 1965, Carbonate: section 91 in Methods of soil analysis, Part 2, American Society of Agronomy, Madison, Wisconsin.

3. Anderson, R.E., 1969, Notes on the Geology and Paleohydrology of the Boulder City Pluton, Southern Nevada: U.S. Geol. Survey Prof. Pap., n. 650-B, pp. B35-B40.

4. Anderson, R. E., 1971, Thin Skin distension in Tertiary Rocks of Southeastern Nevada: Geol. Soc. America Bull., v. 82, pp. 43-58.

5. Anderson, R.E., 1971, Thin skin distension in Tertiary rocks of Southeastern Nevada - Reply: Geol. Soc. America Bull., v. 82, p. 3533-3536.

6. Anderson, R.E., 1973, Large-Magnitude Late Tertiary strike-slip faulting North of Lake Mead, Nevada: U. S. Geol. Survey Prof. Paper, 794, 18 p.

7. Anderson, R.E., 1973, Late Cenozoic tectonic setting of Lake Mead, Nevada, Arizona, U.S.A.: Intern. Colloq. Seismic Effects of Reservoir Impounding, Royal Society, London.

8. Anderson, R.E., 1977, Geologic map of the Boulder City 15-minute quadrangle, Clark County, Nevada: U. S. Geol. Survey Map GQ-1395.

9. Anderson, R.E., 1978, Geologic Map of the Black Canyon 15-minute quadrangle, Mohave County, Arizona, and Clark County, Nevada: U. S. Geol. Survey Map GQ-1394.

10. Anderson, R.E., and Ekren, E.B., 1968, Widespread Miocene igneous rocks of intermediate composition, Southern Nye County, Nevada: in Nevada test site (E.B. Eckel, ed.), Geol. Soc. Amer., Mem. 110, p. 57-63.

11. Anderson, R.E. and Laney, R.L., 1975, The influence of Late Cenozoic stratigraphy on distribution of impoundment-related seismicity at Lake Mead, Nevada-Arizona: Jour. Research, U.S. Geol. Survey, v. 3, n. 3, p. 337-343.

12. Anderson, R.E., Longwell, C.R., Armstrong, R.L., and Marvin, R.F., 1972, Significance of K-Ar ages of Tertiary rocks from the Lake Mead Region, Nevada - Arizona: Geol. Soc. America Bull., v. 83, p. 273-288.

13. Armstrong, R.L., 1963, Geochronology and geology of the eastern Great Basin in Nevada and Utah: Yale Univ., Ph.D. thesis, 317 p.

14. Armstrong, R.L., 1968, Sevier orogenic belt in Nevada and Utah: Geol. Soc. Am. Bull v. 79, p. 429-458.

15. Armstrong, R.L., 1970, Geochronology of Tertiary igneous rocks, eastern Basin and Range province, USA: Geochim. et. Cosmochim. Acta, v. 34, no. 2, p. 203-232.

16. Armstrong, R.L., Ekren, E.B., McKee, E.H., and Noble, D.C., 1969, Space-time relations of Cenozoic silicic volcanism in the Great Basin of the western United States: Am. Jour Sic., v. 267, no. 4, p. 478-490.

17. Baker, V.R., 1977, Stream-channel response to floods, with examples from Central Texas: Geol. Soc. Am. Bull., v. 88, p. 1057-1071.

18. Bastin, E.S., 1923, Origin of certain rich silver ores near Chloride and Kingman, Arizona: U.S. Geol. Survey Bull., v. 750, pp. 17-39.

19. Bentley, C.B., 1969, Geohydrologic reconnaissance of Lake Mead National Recreation area - Mount Davis to Davis Dam, Arizona: U.S. Geol. Survey admin. rpt., 34 p. (unpublished; prepared under contract with National Park Service).

20. Bentley, C.B., 1970, Geohydrologic reconnaissance of Lake Mead National Recreation Area - Opal Mountain to Davis Dam, Nevada: U.S.G.S. admin. rpt., 36 p. (unpublished; prepared under contract with National Park Service).

21. Bentley, C.B., 1971, Geohydrologic reconnaissance of Lake Mead National Recreation Area - Hoover Dam to Mount Davis, Arizona: U.S.G.S. admin. rpt., 37 p.

22. Bingler, E.C. and Bonham, H.F., Jr., 1972, Reconnaissance geologic map of the McCullough Range and adjacent areas, Clark County Nevada: Nevada Bur. Mines and Geology Map 45.

23. Blackwelder, Eliot, 1934, Origin of the Colorado River: Geol. Soc. Am. Bull., v. 45, p. 551-566.

24. Blair, W.N., 1978, Gulf of California in Lake Mead area of Arizona and Nevada during late Miocene time: A.A.P.G. Bull., v. 62, no. 7, p. 1159-1170.

25. Blair, W.H., McKee, E.H., and Armstrong, A.K., 1977, Age and environment of deposition: Hualapa: Limestone member of the Muddy Creek Formation: Geol. Soc. of Am. Abstr. with programs, v. 9, no. 4, p. 390.

26. Bowyer, B., Pampeyan, E.H., and Longwell, C.R., 1958, Geologic map of Clark County, Nevada: U.S. Geol. Survey and Nevada State Bureau of Mines, Map MF 138.

27. Brock, W.G., 1973, Characterization of the Muddy Mountain - Keystone thrust contact and related deformation (M.S. thesis): College Station, Texas A.& M.Univ., 179 p.

28. Brock, W.G. and Engelder, T., 1977, Deformation associated with the movement of the Muddy Mountain overthrust in the Buffington window, southeastern Nevada: Geol. Soc. America Bull., v. 88, p. 1667-1677.

29. Bucknam, R.C., Anderson, R.E., 1979, Estimation of fault - scarp ages from a scarp-height - slope-angle relationship: Geology v. 7, no. 1, p. 11-14.

30. Burchfiel, B.C., and Davis, G.A., 1968, Source terrain of the Keystone thrust plate, southern Nevada and southeastern California: Geol. Soc. Am. Program with Abstracts, Ann. Mtg., p. 41-42.

31. Burke, K., 1978: "Amount, timing, and characteristics of Cenozoic uplift along the southwestern edge of the Colorado Plateau: A case of tectonic heredity"; Conf. on Plateau Uplift: Mode and Mechanism, Lunar and Planetary Institute Contr. 329, p. 8-9.

32. Callagham, E., 1939, Geology of the Searchlight District, Clark County, Nevada: U.S. Geol. Survey Bull., v. 906, pp. 135-188.

33. Campbell, I. and Schenk, E.T., 1950, Camptonite dikes near Boulder Dam, Arizona: Am. Min., v. 35, p. 671-727.

34. Carder, D.S., 1945, Seismic investigations in the Boulder Dam area, 1940-1944, and the influence of reservoir loading on local earthquake activity: Bull. Seism. Soc. America, v. 35, p. 175-192.

35. Carder, D.S., and Small, J.B. 1948, Level divergencies, seismic activity, and reservoir loading in the Lake Mead Area, Nevada and Arizona: Am. Geophys. Union Trans., v. 29, p. 767-771.

36. Chapman, D. S., et al., 1978, "Geophysical characteristics of the Colorado Plateau and its transition to the Basin and Range province in Utah", Conf. on Plateau Uplift: Mode and Mech., Lunov and Planetary Institute Contr. 329, p. 10-12.

37. Christiansen, R.L., and Lipman, P.W., 1972, Cenozoic volcanism and plate-tectonic evolution of the western United States: II Late Cenozoic: Royal Soc. of London Philosophical Transactions, ser. A, v. 217, p. 249-284.

38. Colbert, E. H.,1974, Mesozoic vertebrates of northern Arizona: Geol. Soc. America, Rocky, Mtn. Sect., pp. 208-219.

39. Conley, J.N., 1974, Review of the development of oil and gas resources of northern Arizona: Geol. Soc. America, Rocky Mtn. Sect., pp. 393-406.

40. Cooley, M.E., et al., 1967, Arizona Highway geologic map: Ariz. Geol. Soc. Map.

41. Damon, P.E. 1965, Correlation and chronology of ore deposits and volcanic rocks: Univ. of Arizona Geochronology Lab., Am. prog. rept; 1. C00-689-50, 75 p.; 2. C00-689-100, 75 p.; 3. COO-689-130, 77 p.

42. Damon, P.E., Shafigullah, M, and Scarborough, R.B., 1978, Revised chronology for critical stages in the evolution of the lower Colorado River: Geol. Soc. Am. Abstr. with Programs, v. 10, no. 3, p. 101.

43. Darton, N.H. and others, 1924, State Geologic Map of Arizona: Arizona Bur. Mines, in coop. with U.S.G.S.

44. Day, P.R., 1965, Particle fractionation and particle-size analysis: Section 43 in: Methods of Soil Analysis American Society of Agronomy, Madison, Wisconsin.

45. Dickey, B.D., Carr, W.J., and Bull, W.B., Geologic map of the Parker Northwest, Calif.; Parker, Calif.-Ariz.; and parts of the Whipple Mountains Southwest, Calif. and Whipple Wash., Calif., quadrangle: U.S.G.S. map I-1124, in Press.

46. Diment, W.H., Stewart, S.W., and Roller, J.C., 1961, Crustal structure from the Nevada Test Site to Kingman, Ariz., from seismic and gravity observations: Jour. Geophys. Res., v. 66, p. 201-214.

47. Dings, M.G., 1951, The Wallapai Mining District, Cerbat Mountains, Mohave County, Arizona: U.S. Geol. Survey Bull., v. 978-E, pp. 123-163.

48. Dutton, C.E., 1882, Tertiary history of the Grand Canyon district: U.S. Geol. Surv. Mon. 2, 264 p.

49. Eberly, LiD., and Stanley, T.B., 1978, Cenozoic stratigraphy and geologic history of Southwestern Arizona: Geol. Soc. Am. Bull., v. 89, p. 921-940.

50. Eckel, E.B., 1968, Nevada Test Site: Geol. Soc. America Memoir 110.

51. Ekren, E.B., Rogers, C.L., Anderson, R.E., and Orkild, P.P., 1968, Age of Basin and Range normal faults in Nevada Test Site and Nellis Air Force Range, Nev., in Nevada Test Site: Geol. Soc. Amer. Mem. 110. p. 247-250.

52. Epis, R.C., and Chapin, C.C., 1975, Geomorphic and tectonic implications of the post-Laramide, late Eocene erosion surface in the southern Rocky Mountains: Geol. Soc. Am. Memoir 144, p. 45-74.

53. Fleck, R.J., 1970, Age and possible origin of the Las Vegas Valley shear zone, Clark and Nye Counties, Nevada: Geol. Soc. Amer. Abs. with Programs (Rocky Mtn. Sec.), v. 2, no. 5, p. 333.

54. Geodata International, Inc., 1976, Lake Mead Dynamic Test Range for calibration of airborne gamma radiation measuring systems: Geodata Int'l., Inc., 973, Denton Drive, Dallas, Texas.

55. Gerson, R., 1977, Sediment transport for desert watersheds in erodible materials: Earth Surface Processes, v. 2, p. 343-361.

56. Gibbs, J.F., and Roller, J.C., 1966, Crustal structure determined by seismic-refraction measurements between the Nevada Test Site and Ludlow, California: U.S. Geol. Survey Professional Paper 550-D, 125 p.

57. Gilbert, G.K., 1875, Report on the geology of portions of Nevada, Utah, California, and Arizona: U.S. Geog. and Geol. Surv. west of 100th Mer., vol. 3, pp. 17-187.

58. Gillespie, J.B., Bentley, C.B., and Kan, W., 1966, Basic hydrologic data of the Hualapai, Sacramento, and Big, Sandy Valleys, Mohave County Arizona: Arizona State Land Dept. Water-Resources Rpt. 26, 39 p.

59. Gillespie, J.B. and Bentley, C.B., 1971, Geohydrology of Hualapai and Sacramento Valleys, Mohave County, Arizona: U.S. Geol Survey Water - Supply Paper 1899-H, pp. H1-H37. (Ariz. map index no. 335).

Goetz, A.F.H., et al., see No. 119.

60. Goff, F.E., 1979, "Wet" Geothermal Potential of the Kingman-Williams Region, Arizona: LA-7757 MS Informal Report, UC-66a, 25 p.

61. Gray, R.S., 1959, Cenozoic geology of Hindu Canyon, Mohave County, Arizona (M.S. thesis): Tucson, Arizona Univ., 64 p.

62. Gromme, C.S., McKee, E.H., Blake, M.C., 1972, Paleomagnetic correlations and potassium-argon dating of middle tertiary ash-flow sheets in the eastern Great Basin, Nevada and Utah: Geol. Soc. America Bull., v. 83, p. 1619-1638.

63. Hale, F.A., Jr., 1918, Manganese deposits of Clark County, Nev.: Eng. and Min. Jour., v. 105, pp. 775-777.

64. Hamblin, W.K., 1963, Transition between the Colorado Plateau and the Basin and Range in southern Utah and northern Arizona, in: Abstracts for 1962: Geol. Soc. Am. Spec. Paper 73, p. 85.

65. Hamblin, W.K., 1965, Origin of "reverse drag" on the downthrown side of normal faults: Geol. Soc. Amer. Bull, v. 76, n. 10, p. 1145-1164.

66. Hamblin, W.K., 1975, The geologic boundary between the Colorado Plateau and the Basin and Range province: Geol. Soc. of Am. Abstr. with Programs, v. 7, p. 1097.

67. Hansen, S.M., 1962, The geology of the Eldorado mining district, Clark County, Nevada: Ph.D. thesis, Missouri Univ., 328 p.

68. Hansen, S.M., and Proctor, P.D., 1963, Geology of the Eldorado Mining district, Clark County, Nevada (abstr): in Abstracts for 1962, Geol. Soc. Amer., Spec. Paper 73, p. 165-166.

69. Hart, O.M. and Hetland, D.L., 1953, Preliminary report on uranium-bearing deposits in Mohave County: U.S. AEC RME-4026.

70. Haury, P.S., 1947, Examination of zinc-lead mines in the Wallapai mining district, Mohave County, Arizona: U.S. Bur. Mines Rept. Inv. 4101.

71. Helmstaedt, H. and Schulze, D.J., 1978, "Petrologic constraints for upper mantle models of the Colorado Plateau", Conf. on Plateau Uplift: Mode and Mechanism, Lunar and Planetary Institute Contr. 329, p. 16-18.

72. Hernon, R.M., 1938, The Cerbat Mountains: Arizona Bur. Mines Bull. 145, pp. 110-117.

73. Hewett, D.F., 1931, Geology and ore deposits of the Goodsprings quadrangle, Nevada: U.S. Geol. Survey, Prof. Paper 162.

74. Hewett, D.F., 1933, Sedimentary manganese deposits: in Ore deposits of the Western States (Lindgren volume) pp. 488-489, Am. Inst. Min. Met. Eng.

75. Hewett, D.F., Callaghan, E., Moore, B.N., Nolan, T.B., Rubey, W.W., and Schaller, W.T., 1936, Mineral Resources of the Region around Boulder Dam: U.S. Geol. Survey Bull., v. 871, 197 p.

76. Hewett, D.F., and Webber, B.N., 1931, Bedded deposits of manganese oxides near Las Vegas, Nevada: Nevada Univ. Bull., v. 25, n. 6, pp. 5-17.

77. Hill, J.M., 1916, Notes on some mining districts in eastern Nevada: U.S. Geol. Survey Bull. 648.

78. Howard, C.S., 1948, Quality of water in the Upper Colorado River Basin, Trans. Am. Geophys Union, v. 29, p. 375-378.

79. Hunt, C.B., 1969, Geologic history of the Colorado River: U.S. Geol. Survey Prof. Paper 669, Sec. C, pp. 59-130.

80. Hunt, C.B., 1974, Natural Regions of the United States and Canada: W.H. Freeman and Co., S.F., Cal. 725 p.

81. Hunt, C.B., McKelvey, V.E., and Wiese, J.H., 1942, The Three Kids Manganese District, Clark County, Nevada: U.S. Geol. Survey Bull., v. 936-L, pp. 297-319.

82. Ives, J.C., 1861, Report upon the Colorado River of the west: Washington, U.S. Govt. Printing Office.

83. Johnson, L.R., 1965, Crustal structure between Lake Mead, Nevada, and Mono Lake, Calif.: J. Geophys. Res. 70, 2863-2872.

84. Jones, A.E., 1944, Earthquake magnitudes, efficiency of stations, and perceptibility of local earthquakes in the Lake Mead Area: Bull. Seism. Soc. America, v. 34, pp. 161-173.

85. Jones, E.L., Jr., 1920, Deposits of manganese ore in Nevada: U.S. Geol. Survey Bull. 710.

86. Kane, M.F., 1963, Precambrian rock densities and isostatic processes in Clark County, Nevada (abstr.): in Abstracts for 1962, Geol. Soc. Amer., Spec. Paper 73, p. 184.

87. Keller, G.R., et al., 1978, Regional crustal structure of the Colorado Plateau: Conf. on Plateau Uplift: Mode and Mechanism, Lunar and Planetary Institute Contr. 329, p. 26.

88. King, P.B., 1977, The evolution of North America - revised edition, Princeton Univ. Press, 197 p.

89. King, W.H. and Trengove, R.R., 1950, Investigation of the Fannie Ryan and Boulder City manganese deposits, Clark County, Nevada: U.S. Bur. Mines Rept. Inv. 4712 (Nevada map index no. 108).

90. Laney, R.L., 1973, Geohydrologic reconnaissance of Lake Mead National Recreation Area - Hoover Dam to Temple Bar, Arizona: Administrative report to U.S. Dept. of the Interior Geological Survey, 42 p. (Unpublished; prepared under contract for National Park Service.)

91. Lansen, Carl, 1931, Geology and ore deposits of the Oatman and Katherine districts, Arizona: Ariz. Bureau of Mines Bull. 131, Geol. Ser. 6 (Univ. Bull. v. 2, no. 2), 126 p., 30 figs.

92. Lara, J.M. and Sanders, J.I., 1970, The 1963-64 Lake Mead Survey: U.S. Bureau Reclamation Rep. REC-OCE-70-21, 174 p.

93. LaRue, E.L., 1925, Waterpower and flood control of Colo. River below Green River, Utah: U.S. Geol. Survey Water Supply paper 556, 176 p.

94. Lasky, S.G., and Webber, B.N., 1942, Manganese deposits in the Artillery Mountains region, Mohave County, Arizona: U.S. Geol. Sur. Bull. 936-R.

95. Lee, W.H.K. and Matamoros, E.E., 1975, Catalogue of earthquakes in the Lake Mead area, Nevada-Arizona, for the period from July 10, 1972 to December 6, 1973: U.S. Geol. Survey Open File Rept. 75-15, 31 p.

96. Lee, W.T., 1908, Geologic Reconnaissance of a part of Western Arizona: U.S. Geol. Survey Bull., v. 352, 96 p.

97. Leighton, F.B., 1954, Origin of vermiculite deposits, Southern Virgin Mountains, Nevada (Abstract): Econ. Geol., v. 49, p. 809; Geol. Soc. America Bull., v. 65, p. 1277.

98. Livaccari, R.F., 1979, Late Cenozoic tectonic evolution of the western United States: Geology, v. 7, p. 72-75.

99. Longwell, C.R., 1921, Geology of the Muddy Mountains, Nevada, with a section to the Grand Wash Cliffs, in Western Arizona: Am. Jour. Sci., v. 50, p. 39-62.

100. Longwell, C.R., 1922, The Muddy Mountain Overthrust in Southeastern Nevada: Jour. Geol., v. 30, p. 63-72.

101. Longwell, C.R., 1925, The pre-Triassic unconformity in Southern Nevada: Am. Jour. Sci., v. 10, p. 93-106.

102. Longwell, C.R., 1926, Structural studies in Southern Nevada and Western Arizona: Geol. Soc. America Bull., v. 37, p. 551-584.

103. Longwell, C.R., 1928, Geology of the Muddy Mountains, Nevada: U.S. Geol. Surv. Bull., v. 798, 152 p.

104. Longwell, C.R., 1936, Geology of the Boulder Reservoir floor, Arizona-Nevada: Geol. Soc. America Bull., v. 47, p. 1393-1476.

105. Longwell, C.R., 1945, Low-angle normal faults in the Basin and Range Province: Amer. Geophys. Union, Trans., v. 26, pt. 1, p. 107-118.

106. Longwell, C.R., 1946, How old is the Colorado River? Am. Jour. Sci., v. 244, p. 817-855.

107. Longwell, C.R., 1949, Structure of the Northern Muddy Mountain Area, Nevada: Geol. Soc. America Bull., v. 60, p. 923-968.

108. Longwell, C.R., 1951, Megabreccia developed downslope from large faults: Am. Jour. Sci., v. 249, p. 343-355. (Lake Mead region)

109. Longwell, C.R., 1960, Possible explanation of diverse structural patterns in southern Nevada: Am. Jour. Sci., v. 258-A (Bradley vol.), p. 192-203.

110. Longwell, C.R., 1963, Reconnaissance geology between Lake Mead and Davis Dam, Arizona - Nevada: U.S. Geol Surv. Prof. Pap., no. 374-E, 51 p.

111. Longwell, C.R., 1971, Measure of the lateral movement on Las Vegas shear zone, Nevada (abs.): Geol. Soc. Am. Abs. with Programs, v. 3, no. 2, p. 152.

112. Longwell, C.R., 1974, Large-scale lateral faulting in Southern Nevada: Geol. Soc. Am. Abstr. with Programs, v. 6., p. 209.

113. Longwell, C.R., Pampeyan, E.H., Bowyer, B., and Roberts, R.J., 1965, Geology and mineral deposits of Clark County, Nevada: Nevada Bur. Mines Bull. 62, 218 p.

114. Loring, A.K., 1976, The age of basin-range faulting in Arizona: Arizona Geol. Soc. Digest, v. 10, p. 229-257.

115. Lovejoy, E.M.P., 1969, Grand Wash problem at Grand Canyon: Geol. Soc. Am., Abs. with Programs for 1969, v. 1, pt. 5, p. 46.

116. Lucchitta, Ivo, 1966, Cenozoic geology of the upper Lake Mead area adjacent to the Grand Wash Cliffs, Arizona (Ph.D. thesis): Penn State Univ.

117. Lucchitta, I., 1972, Early History of the Colorado River in the Basin and Range Province: Geol. Soc. America Bull., v. 83, p. 1933-1948.

118. Lucchitta, I., 1974, Structural evolution of northwest Arizona and its relation to adjacent Basin and Range Province structures: Geol. Soc. America, Rocky Mtn. Sect., p. 336-354.

119. Goetz, A.F.H., Billingsley, F.C., Gillespie, A.R., Abrams, M.J., Squires, R.L., Shoemaker, E.M., Lucchitta, I., Elston, D.P., 1975, Application of ERTS images and image processing to regional geologic problems and geologic mapping in northern Arizona: Jet Propulsion Laboratory Technical Report 32-1597.

120. Lucchitta, Ivo., Development of landscape of northwest Arizona: The country of plateaus and canyons: in Evolution of the Arizona landscape: University of Arizona press, in press.

121. Lucchitta, Ivo, Late-Cenozoic uplift of the SW Colorado Plateau and adjacent lower Colorado River region: draft manuscript.

122. Lucchitta, Ivo, and McKee, E.H., 1975, New geochronologic constraints on the history of the Colorado River and the Grand Canyon: Geol. Soc. America Abs. with Programs, v. 7, no. 3, p. 343.

123. Lunar and Planetary Institute, 1978, Plateau uplift: mode and mechanisms: Lunar and Planetary Institute contribution 329, 60 p. + p. F1 - F12 + p. i-x + 2 maps.

124. Mannion, L.E., 1963, Virgin Valley salt deposits, Clark County, Nevada; in: Symposium on Salt, Cleveland, 1962: Cleveland, Northern Ohio Geol. Soc., p. 166-175.

125. McKee, E.D., 1951, Sedimentary basins of Arizona and adjoining states: Geol. Soc. Am. Bull., v. 62, no. 5, p. 481-506.

126. McKee, E.H., 1971, Tertiary igneous chronology of the Great Basin of Western United States - Implications for tectonic models: Geol. Soc. America Bull., v. 82, p. 3497-3502.

127. McKee, E.H., and Anderson, C.A., 1971, Age and chemistry of Tertiary volcanic rocks in north central Arizona and relation of the rocks to the Colorado Plateaus: Geol. Soc. Amer. Bull., v. 82, p. 2767-2782.

128. McKee, E.D., and McKee, E.H., 1972, Pliocene uplift of the Grand Canyon region: Time of drainage adjustment: Geol. Soc. Am. Bull., v. 83, no. 7, p. 1923-1932.

129. McKee, E.D., Wilson, R.F., Breed, W.J., and Breed, C.S., eds., 1967, Evolution of the Colorado River in Airzona: Mus. Northern Arizona Bull. 44, 68 p.

130. McKelvey, V.E., Wiese, J.H., and Johnson, V.H., 1949, Preliminary report on the bedded manganese of the Lake Mead Region, Nevada-Arizona: U.S. Geol. Surv. Bull., v. 948, pp. 83-101.

131. Mead, T.C. and Carder, D.S., 1941, Seismic investigations in the Boulder Dam area in 1940: Bull. Seism. Soc. Am., v. 31, p. 321-324.

132. Mears, A.I., 1979, Flooding and sediment transport in a small alpine drainage basin in Colorado: Geol. Mag., 7:1, p. 53-57.

133. Metzger, D.G., 1968, The Bouse Formation (Pliocene) of the Parker-Blythe-Cibola area, Arizona and California in Geological Survey Research 1968: U.S. Geol. Survey Prof. Paper 600-D, p. D126-D136.

134. Mindling, A., 1971, A summary of data relating to land subsidence in Las Vegas Valley: Desert Research Institute Report. (Unpublished report to the U.S. Atomic Energy Comm., 55 p.)

135. Moore, R.B., 1978, "Cenozoic igneous rocks of the Colorado Plateau", Conf. on Plateau uplift: Mode and Mechanism, Lunar and Planetary Institute Contr. 329, p. 28-30.

136. Morgan, J.R., 1968, Structure and stratigraphy of the northern part of the South Virgin Mountains, Clark County, Nevada: Albuquerque, New Mexico Univ., M.S. thesis.

137. Nickell, F.A., 1942, Development and use of engineering geology: Am. Assoc. Petr. Geol. Bull., v. 26, p. 1797-1826.

138. Otton, J.K., 1977, Geology of uraniferous tertiary rocks in the Artillery Peak - Date Creek Basin, west-central Arizona: in Campbell, J.A., ed., Short papers of the U.S. Geol. Survey Uranium-thorium Symposium, 1977: U.S. Geol. Survey Circ. 753, p. 35-36.

139. Otton, J.K., and Brooks, W.E., 1978, "Tectonic History of the Colorado Plateau margin, Date Creek Basin and adjacent areas, West-central Arizona": Conf. on Plateau Uplift: Mode and Institute Contr. 329, p. 31-33.

140. Peterson, M.S., Rigby, J.K. and Hintze, L.F., 1973, Historical Geology of North America: Wm. C. Brown Co., Dubuque, Iowa, 193 p.

141. Peirce, H.W., 1972, Red Lake salt mass: Arizona Bur. Mines Field Notes, v. 2, no. 1, p. 45.

142. Peirce, H.W., 1976, Tectonic significance of Basin and Range thick evaporite deposit: Arizona Geological Society Digest, v. 10, p. 325-339.

143. Peirce, H.W., Damon, P.E., and Snafigullah, M., 1978, "'Plateau Uplift' in Arizona - a conceptual review", Conf.on Plateau Uplift: Mode and Mechanism, Lunar and Planetary Institute Contr. 329, p. 37-39.

144. Piper, A.M., and Poland, J.F., 1943, Character and structure of volcanic rocks near Kingman, Arizona, with respect to water-yielding capacity: U.S. Geol. Surv. open-file report, 14 p.

145. Ransome, F.L., 1904, Description of the Globe quadrangle (Ariz.): U.S.G.S. Geol. Atlas, Folio III.

146. Ransome, F.L., 1907, Preliminary account of Goldfield, Bullfrog, and other mining districts in Southern Nevada: U.S. Geol. Survey Bull., v. 303, 98 p.

147. Ransome, F.L., 1923, Geology of the Oatman gold district, Arizona - a preliminary report: U.S. Geol. Survey Bull. 743, 58 p.

148. Ransome, F.L., 1923, Ancient high-level potholes near the Colorado River (abs.): Science, new ser., v. 57, p. 593.

149. Ransome, F.L., 1923, Geology of the Boulder Canyon and Black Canyon dam sites and reservoir sites on the Colorado River, a report (unpublished) to the Director of the U.S.G.S., Wash., D.C.

150. Ransome, F.L., 1931, Report on the geology of the Hoover Dam site and vicinity, a report (unpublished) to the Chief Engineer, U.S. Bureau of Reclamation, Denver, Colorado.

151. Raphael, J.M., 1954, Crustal disturbance in the Lake Mead area: U.S. Bur. Reclamation, Eng. Monogr. 21, 14 p.

152. Reeside, John B., Jr., and Bassler, H., 1922, Stratigraphic section in southwestern Utah and northeastern Arizona, U.S. Geol. Survey, Prof. Paper 129, p. 53-77.

153. Reiter, M. et al., 1978, "Geothermal characteristics of the Colorado Plateau", Conf. on Plateau Uplift: Mode and Mechanism, p. 43 (see note).

154. Rogers, A.M. and Lee, W.H.K., 1976, Seismic study of earthquakes in the Lake Mead, Nevada-Arizona Region: Bull. Seism. Soc. Am., v. 66, n. 5, p. 1657-1681.

155. Rogers, A.M., and Gallanthine, S.K., 1974, Seismic study of earthquakes in the Lake Mead Region, Final Report to U.S.G.S., Contract 14-08-0001-13069 under ARPA Order No. 1648, 70 p.

156. Roller, J.C., 1964, Crustal structure in the vicinity of Las Vegas, Nevada, from seismic and gravity observations, U.S.G.S. Prof. Paper 475-D, 108 p.

157. Roller, J.C., and Healy, J.H., 1963, Seismic refraction measurements between Santa Monica Bay and Lake Mead: J. Geophys. Res. v. 68, p. 5837-5849.

158. Schmitt, H., 1933, Summary of the geological and metallagenetic history of Arizona and New Mexico: in Ore deposits of the western states, J.W. Finch, ed., Amer. Inst. of Mining and Metal. Eng., Rocky Mountain Fund, p. 316-326.

159. Scholz, C.H., Barazangi, Muawia, and Sabar, M.L., 1971, Late Cenozoic evolution of the Great Basin, western United States, as an ensialic interarc basin: Geol. Soc. Am. Bull., v. 82, p. 2979-2990.

160. Schrader, F.C., 1909, Mineral deposits of the Cerbat Range, Black Mountains, and Grand Wash Cliffs, Mohave County, Arizona: U.S. Geol. Survey, Bull. v. 397, 226 p.

161. Secor, D.R., 1963, Geology of the central Spring Mountains, Nevada: Ph.D. dissert., Stanford Univ., Stanford, Calif, 152 p.

162. Shackelford, T.J., 1976, Structural geology of the Rawhide Mountains, Mohave County, Arizona: unpublished Ph.D. thesis, University of Southern California, Los Angeles, Calf.

163. Shakel, D.W., 1978, Plate tectonic rubric for late Cenozoic transcurrent faulting in Arizona: Geol. Soc. of Am. Abstr. with Programs, v. 10, p. 146.

164. Shawe, D.R., 1965, Strike-slip control of Basin-Range structure indicated by historical faults in Western Nevada: Geol. Soc. Am. Bull., v. 76, p. 1361-1378.

165. Sheppard, R.A., and Gude, A.J., 1972, Big Sandy Formation near Wikieup, Mohave County, Arizona: U.S. Geol. Survey Bull. 1354-C, p. C1-C10.

166. Shoemaker, E.M., 1975, Late Cenozoic faulting and uplift of the Colorado Plateau: Geol. Soc. of Am. Abstr. with Programs, v. 7, p. 1270.

167. Silver, L.T., and McGethin, T.R., 1978, "The nature of the basement beneath the Colorado Plateau and some implications for plateau uplifts." Conf. on Plateau Uplift: Mode and Mechanism, Lunar and Planetary Institute Contr. 329, p. 45-46.

168. Sklar, M., 1938, Petrology of the volcanic rocks of the region around Boulder Dam, M.S. thesis (unpublished), Calif. Inst. Tech.

169. Smith, P.B., 1970, New evidence for Pliocene marine embayment along the Lower Colorado River area, California and Arizona: Geol. Soc. America Bull., v. 81, p. 1411-1420.

170. Smith, W.O., Vetter, C.P., Cummings, G.B., et al., 1960, Comprehensive Survey of Sedimentation in Lake Mead, 1948-9: U.S.G.S. Prof. Paper No. 295, 254 p.

171. Spurr, J.E., 1903, Descriptive geology of Nevada south of the Fortieth Parallel and adjacent portions of California: U.S. Geol. Survey Bull. no. 208, 229 p.

172. Stanley, R.S., and Morse, J.D., 1974, Fault zone characteristics of two well-exposed overthrusts: the Muddy Mountain thrust, Nevada, and the Champlain thrust at Burlington, Vermont: Geol. Soc. America, Abs. with Programs, v. 5, p. 78.

173. Stewart, J.H., 1971, Basin and Range structure - a system of horsts and grabens produced by deep-seated extension: Geol. Soc. Am. Bull., v. 82, p. 1019-1044.

174. Stewart, J.H., and Carlson, J.E., 1974, Preliminary geologic map of Nevada, U.S.G.S. Misc. Field Studies, Map. MF-609.

175. Stewart, John H. and Carlson, John E., 1977, Geologic map of Nevada: Nev. Bur. of Mines and Geology, Univ. of Nevada, Reno, NV. Map. 57.

176. Stewart, J.H., Albers, J.P., and Poole, F.G., 1968, Summary of regional evidence for right-lateral displacement in the western Great Basin: Geol. Soc. Am. Bull., v. 79, p. 1407-1414.

177. Stock, Chester, 1921, Later Cenozoic mammalian remains from the Meadow Valley region, southeastern Nevada: Am. Jour Sci., 5th ser., v. 2, p. 250-264.

178. Stump, E., 1978, Structural elements of the southern Basin and Range: Geol. Soc. of Am., Abs. with Progs., v. 10, p. 149.

179. Suneson, N., and Lucchita, I., 1978, Bimodal volcanism along the eastern margin of the Basin and Range Province, western Arizona: Geol. Soc. America Abs. with Progs., v. 10, n. 3, p. 149.

180. Thomas, B.E., 1949, Geology and ore deposits of the Wallapai district, Arizona: Calif. Inst. Tech., Ph.D. thesis, 187 p.

181. Thomas, B.E., 1949, Ore deposits of the Wallapai district, Arizona: Econ. Geol., v. 44, p. 663-705.

182. Thomas, B.E., 1953, Geology of the chloride quadrangle, Arizona: Geol. Soc. Am. Bull., v. 64, p. 391-420.

183. Thompson, G.A. and M.L. Zoback, 1978, "Geophysics of the Colorado Plateau", Conf. on Plateau Uplift: Mode and Mechanism, Lunar and Planetary Institute Contr. 329, p. 52-54.

184. Tschanz, C.M., 1960, Regional significance of some lacustrine limestones in Lincoln County, Nevada, recently dated as Miocene, in Short papers in the Geological Sciences: U.S. Geol. Survey Prof. Paper 400-B, p. B293.

185. Twenter, F.R., 1962, Geology and promising areas for ground-water development in the Hvalapai Indian Reservation, Arizona: U.S. Geol. Survey water supply paper 1576-A, 38 p.

186. U.S. Bureau of Reclamation, 1950, Geological investigations, Arizona-Nevada: U.S. Bur. Reclamation Bull. 1, pt. 3, Boulder Canyon Project Final Report.

187. U.S. Geological Survey, 1971, Aeromagnetic map of the Gold Butte-Chloride area, Arizona and Nevada: U.S. Geol. Survey, Geophys, Invest. Map, n. GP-757.

188. U.S. Geological Survey, 1972, Geol. Survey research 1972: U.S. Geol. Survey Prof. Paper 800-A, p. A43-A46.

189. Vanderburg, W.C., 1937, Reconnaissance of mining districts in Clark County, Nevada: U.S. Bur. Mines, Inf. Circ. 6964.

190. Volborth, A., 1960, Rapakivi-type Precambrian granites from Gold Butte, Clark County, Nevada (Abstr.): 21st Internat. Geol. Cong., Copenhagen, Rept., p. 126-127.

191. Volborth, A., 1960, Allanite pegmatites from Red Rock, Washoe County, Nevada, compared with allanite pegmatites in southern Nevada and California: 21st Internat. Geol. Cong., Copenhagen, Rept., p. 167 (abs.).

192.Volborth, A., 1962, Rapakivi-type granites in the Precambrian complex of Gold Butte, Clark County, Nevada: Geol. Soc. America Bull., v. 73, p. 813-832.

193. Volborth, A., 1973, Geology of the granite complex of the Eldorado, Newberry, and northern Dead Mountains, Clark County, Nevada: Nevada Bur. Mines and Geology Bull. 80.

194. Westergaard, H.M., and Adkins, A.W., 1934, Deformation of earth's surface due to weight of Boulder Reservoir: U.S. Bur. Reclamation, Tech. Mem. 422, 34 p.

195. Wilson, E.D., 1933, Geology and mineral deposits of southern Yuma County, Arizona: Ariz. Bur. Mines Bull. 134, Geol. ser. 7, 236 p.

196. Wilson, E.D., 1940, Pre-Cambrian of Arizona basin ranges: 6th Pac. Sci. Cong., Pr. 1939, vol. 1, p. 321-330.

197. Wilson, E.D., 1962, A resume of the geology of Arizona: Ariz. Bur. Mines Bull. 171, 140 p.

198. Wilson, E.D. and Moore, R.T., 1959, Geology of Mohave County, Arizona: Arizona Bur. Mines Map.

199. Wilson, E.D. and Moore, R.T., 1969, Geologic map of Arizona: Ariz. Bur. of Mines and U.S. Geol. Survey.

200. Wright, L.A., and Troxel, B.W., 1969, Chaos structure and Basin and Range normal faults - Evidence for a genetic relationship: in Abstracts with Programs, Part 7, Geol. Soc. Amer., p. 326.

201. Young, R.A., 1966, Cenozoic geology along the edge of the Colorado Plateau, in northwestern Arizona: Ph.D. thesis, Washington Univ., St. Louis, Mo., 115 p.

202. Young, R.A. 1966, Cenozoic geology along the edge of the Colorado Plateau in northwestern Arizona (abs.): Dissertation Abstracts, v. 27, no. 6, p. 1994-1995.

203. Young, R.A., 1970, Geomorphological implications of pre-Colorado and Colorado tributary drainage in the western Grand Canyon region. Plateau, v. 42, no. 3, p. 107-117.

204. Young, R.A., 1978, Nature of Cenozoic tectonism, volcanism and erosion along the south-western edge of the Colorado Plateau in Arizona: Conf. on Plateau Uplift: Mode and Mechanism, p. 56-58.

205. Young, R.A., 1978, Field trip guide: in Conference on plateau uplift: Mode and Mechanism: Lunar and Planetary Institute Contribution 329, p. F-1 - F-12, plus maps and illustrations.

206. Young, R.A. and Brennan, W.J., 1974, Peach Springs Tuff: its bearing on structural evolution of the Colorado Plateau and development of Cenozoic drainage in Mohave County, Arizona: Geol. Soc. America Bull., v. 85, p. 83-90.

207. Young, R.A., and McKee, E.H., 1978, Early and middle Cenozoic drainage and erosion in west-central Arizona: G.S.A. Bull. v. 89, no. 12, p. 1745-1750.

208. Zoback, M.L., and Thompson, G.A., 1978, Basin and range rifting in northern Nevada: Clues from a mid-Miocene rift and its subsequent offsets: Geology, v. 6, p. 111-116.

10.0 APPENDICES

10.1 EXPLANATION OF TERMS USED

We have been delivered a collection of 78 samples, each uniquely identified by a sample number. A prefix, either ◊ or o, was used to identify the type of analyses to be performed on the samples.

Of the 78 samples, 5 are designated only by a ◊, and 67 only by a o. Six samples are designated by both a ◊ number and a o number. The samples were identified in the field and on the map (Plate 2) according to three circumstances as follows:

◊ Samples acquired for both petrographic analysis (11) (University of Penna.), chemical analysis (Bendix), and identified in the field by a semipermanent* marker.

o Samples acquired for both petrographic analysis and chemical analysis (228).

o
O Samples acquired for chemical analysis only (150).

In the table that follow, ◊ numbers are listed first, followed by ◊ &o numbers, followed by o numbers. Each of the ◊ &o numbers is repeated as a o&◊ number in the appropriate place in the o sequence, so that readers seeking information on a sample from either array can find it without tedious cross-referencing.

Thus, although only 78 analyses were conducted, the tables that follow show data for 84 (78 + 6) samples.

10.2 APPENDIX 1: Moisture, pH, organic C, and carbonate (see sections 7.1-7.5)

Moisture is expressed in % by weight.

pH is expressed in conventional pH units.

Organic C is expressed in % by weight.

Carbonate is expressed in % by weight of $CaCO_3$ equivalent.

*A stake driven into the ground – not a concrete monument. The identification should last for approximately a year or two.

APPENDIX 1: Moisture, pH, Organic C, and Carbonate

	% Moisture	pH	Organic C	% $CaCO_3$ equiv.
◊1	4.47	9.0	<.1	4.1
◊2	4.81	8.7	<.1	2.9
◊3	3.35	8.5	<.1	3.9
◊4	3.84	8.6	<.1	3.2
◊5	3.70	8.7	<.1	5.3
◊6 & o29	4.06	8.7	<.1	1.5
◊7 & o82	2.93	8.8	<.1	1.2
◊8 & o132	7.74	8.7	.1	4.9
◊9 & o140	4.79	9.0	<.1	5.6
◊10 & o89	4.28	8.6	.1	6.8
◊11 & o35	3.63	8.2	<.1	9.1
o27	5.14	9.0	<.1	2.2
o28	3.34	8.9	<.1	1.3
o29 & ◊6	4.06	8.7	<.1	1.5
o30	3.08	8.9	<.1	1.4
o31	4.67	8.8	<.1	2.0
o32	4.58	8.6	<.1	1.7
o33	3.17	8.9	<.1	3.6
o34	3.10	8.8	<.1	6.0
o35 & ◊11	3.63	8.2	<.1	9.1
o36	8.32	8.6	.1	13.9
o37	3.51	8.3	<.1	10.8
o57	2.63	8.9	<.1	1.9
o58	3.63	8.8	<.1	2.8
o59	4.21	8.7	<.1	3.5
o60	3.58	8.7	.1	3.0
o61	2.71	8.8	<.1	2.5
o62	2.80	8.9	<.1	10.0

APPENDIX 1, continued

	% Moisture	pH	Organic C	% $CaCO_3$ equiv.
o63	2.90	8.9	<.1	3.6
o64	3.35	8.8	<.1	4.2
o65	3.00	9.0	<.1	11.0
o66	2.41	9.0	<.1	12.6
o67	3.93	8.5	.2	11.5
o68	5.46	8.6	<.1	9.1
o80	3.44	8.9	<.1	2.0
o81	2.65	8.9	<.1	2.4
o82 & ◇7	2.93	8.8	<.1	1.2
o83	3.59	8.7	<.1	1.6
o84	2.30	8.7	<.1	1.6
o85	1.99	8.8	<.1	1.3
o86	4.18	8.6	<.1	1.8
o87	2.58	8.8	<.1	4.4
o88	2.77	8.4	<.1	6.1
o89 & ◇10	4.28	8.6	.1	6.8
o90	7.13	8.5	.1	14.7
o91	8.27	8.7	.15	10.9
o104	10.3	8.6	<.1	11.8
o105	4.27	9.0	<.1	1.0
o106	5.18	8.9	<.1	1.1
o107	4.91	8.8	<.1	1.1
o108	4.90	8.9	<.1	7.1
o109	3.53	8.9	<.1	2.2
o110	4.40	8.8	<.1	2.4
o111	2.10	8.3	<.1	3.2
o112	3.70	8.7	<.1	3.2
o113	3.86	8.7	<.1	3.4

APPENDIX 1, continued

	% Moisture	pH	Organic C	% $CaCO_3$ equiv.
o114	2.05	8.8	<.1	2.1
o115	5.26	8.5	.1	8.4
o130	5.87	8.7	<.1	3.7
o131	5.88	8.6	<.1	5.4
o132 & ◇8	7.74	8.7	.1	4.9
o133	6.38	8.8	<.1	2.4
o134	3.79	8.7	<.1	6.3
o135	4.62	8.7	<.1	4.1
o136	3.78	8.9	<.1	3.1
o137	4.49	8.9	<.1	6.6
o138	3.48	8.8	<.1	2.8
o139	5.74	8.8	<.1	5.7
o140 & ◇9	4.79	9.0	<.1	5.6
o141	5.79	8.7	<.1	3.7
o142	6.16	8.6	<.1	4.7
o165	6.13	8.7	.1	4.3
o166	3.93	8.8	<.1	2.4
o167	5.67	8.8	<.1	2.2
o168	5.55	8.8	.1	2.4
o169	5.02	8.6	<.1	2.7
o170	4.54	8.7	<.1	2.9
o171	3.96	8.8	<.1	2.0
o172	4.75	8.2	<.1	2.5
o173	4.29	8.1	<.1	6.3
o174	3.66	8.3	<.1	2.6
o175	4.74	8.8	<.1	4.7
o176	7.20	8.8	.1	5.4
o177	7.83	8.5	<.1	4.3

10.3 APPENDIX 2: Particle-size analysis (see section 7.6)

Gravel is expressed as % by weight of the entire sample.

Each of the finer size classes is expressed as % by weight of the non-gravel fraction of the sample.

Abbreviations:

cms	coarse to medium sand
fs	fine sand
vfs	very fine sand
csi	coarse silt
msi	medium silt
fsi	fine silt
vfsi	very fine silt

APPENDIX 2: Particle-size analysis

	% GRAVEL	% of fines cms 0-2ϕ	fs 2-3ϕ	vfs 3-4ϕ	csi 4-5ϕ	msi 5-6ϕ	fsi 6-7ϕ	vfsi 7-8	clay >8ϕ
◇1	65.2	90.75	0.75	1.0	1.25	0.5	1.25	2.0	2.5
◇2	54.5	85.0	0.5	1.75	1.0	1.75	0.75	3.5	5.75
◇3	63.8	88.25	1.0	0.5	1.25	1.25	0.25	2.0	5.5
◇4	42.3	87.0	0.75	1.0	0.0	0.75	3.0	2.0	6.5
◇5	49.4	90.0	2.25	0.25	1.5	0.5	0.0	1.25	4.25
◇6 & o29	7.0	85.0	2.75	1.75	1.25	1.0	1.75	0.5	3.5
◇7 & o82	29.3	84.5	2.0	4.75	1.0	0.25	0.5	1.5	5.5
◇8 & o132	51.8	58.5	6.5	5.25	3.0	2.0	3.25	6.25	15.25
◇9 & o140	36.9	90.0	0.75	0.75	0.5	0.5	1.0	1.5	5.0
◇10 & o89	17.4	81.0	7.75	1.5	0.75	0.5	0.75	0.75	7.0
◇11 & o35	38.4	91.25	1.25	1.25	0.25	1.0	0.0	0.75	4.25
o27	8.2	92.0	0.50	0.25	0.0	0.5	1.25	0.25	5.25
o28	14.1	93.25	0.75	0.50	0.0	1.5	0.0	0.5	3.5
o29 & ◇6	7.0	85.0	2.75	1.75	1.25	1.0	1.75	0.5	3.5
o30	21.9	94.25	0.25	0.25	0.5	0.0	0.0	0.0	4.75
o31	2.4	92.0	0.5	2.0	0.0	0.0	0.0	0.0	5.5
o32	6.0	92.0	1.0	0.25	0.5	0.5	0.25	0.0	4.5
o33	29.8	92.0	1.0	0.25	0.0	0.0	1.0	0.0	5.75
o34	71.3	90.75	0.75	0.5	0.25	0.25	0.0	0.0	7.5
o35 & ◇11	38.4	91.25	1.25	1.25	0.25	1.0	0.0	0.75	4.25
o36	13.4	83.75	2.75	4.25	0.75	0.0	0.25	0.25	9.0
o37	55.7	85.75	1.5	2.25	0.25	0.75	0.5	1.0	8.0
o57	44.3	92.75	0.5	1.25	0.0	0.0	0.25	0.75	4.5
o58	42.3	90.5	1.75	0.5	0.5	1.25	0.5	0.0	4.75
o59	34.7	82.25	3.75	4.0	1.0	0.25	0.0	0.75	8.0
o60	33.6	85.5	4.0	2.25	0.75	0.0	0.0	0.0	7.5
o61	48.7	92.5	0.0	0.25	1.0	0.0	0.25	0.5	5.5
o62	57.4	92.75	0.5	1.25	0.25	0.25	0.0	0.25	4.75

	% GRAVEL	% of fines cms 0-2ϕ	fs 2-3ϕ	vfs 3-4ϕ	csi 4-5ϕ	msi 5-6ϕ	fsi 6-7ϕ	vfsi 7-8ϕ	clay >8ϕ
o63	22.9	92.0	1.0	0.75	0.25	0.5	0.0	0.25	5.25
o64	45.2	93.5	1.0	0.25	0.5	0.0	0.5	0.25	4.0
o65	53.4	91.25	0.25	0.5	0.0	0.0	0.75	0.5	6.75
o66	27.9	90.5	1.75	0.25	1.25	0.75	0.0	0.25	5.25
o67	35.1	87.5	1.5	0.0	0.0	0.25	o.5	0.25	10.0
o68	33.1	66.2	5.5	8.3	3.0	4.0	1.0	4.5	7.5
o80	25.3	82.5	1.25	3.75	0.75	4.25	0.5	0.5	6.5
o81	24.4	90.0	0.5	2.0	0.0	0.0	0.0	0.0	6.5
o82 &◇7	29.3	84.5	2.0	4.75	1.0	0.25	0.5	1.5	5.5
o83	24.1	87.0	1.0	2.0	0.5	0.75	0.75	0.0	8.0
o84	45.7	87.0	1.0	1.75	0.5	0.25	1.25	0.75	7.5
o85	45.5	89.75	0.25	2.0	1.75	1.25	0.5	0.5	4.0
o86	33.6	92.25	0.75	0.0	0.0	0.0	0.5	0.5	6.0
o87	42.1	92.5	0.0	0.5	0.25	0.0	0.25	0.0	6.5
o88	46.2	93.75	1.25	0.5	0.75	0.0	0.0	0.0	3.75
o89 &◇10	17.4	81.0	7.75	1.5	0.75	0.5	0.75	0.75	7.0
o90	29.8	73.0	7.0	0.5	2.0	2.0	1.25	6.5	7.75
o91	22.5	75.0	5.0	0.0	0.75	1.0	3.25	4.5	10.5
o104	24.5	66.0	7.75	0.75	3.5	2.0	0.25	4.0	15.75
o105	15.9	90.5	2.0	0.75	0.5	0.75	0.5	0.5	4.5
o106	18.0	89.25	0.75	2.25	0.25	0.50	1.25	0.75	5.0
o107	27.3	90.5	2.25	1.75	0.5	0.25	0.25	0.25	4.25
o108	66.8	90.25	1.25	1.0	0.0	0.0	0.75	0.5	6.25
o109	55.5	92.5	0.75	1.0	0.75	1.25	0.0	0.5	3.25
o110	24.2	94.5	0.5	0.5	0.25	0.5	0.5	0.25	3.0
o111	38.6	89.5	1.25	0.75	0.5	0.25	0.25	0.75	6.75
o112	13.0	86.0	2.0	2.0	0.75	1.25	0.5	0.75	6.75
o113	38.6	71.25	6.3	12.0	0.75	1.25	1.0	2.5	5.0

APPENDIX 2, continued

	% GRAVEL	% of fines cms 0-2	fs 2-3ϕ	vfs 3-4ϕ	csi 4-5ϕ	msi 5-6ϕ	fsi 6-7ϕ	vfsi 7-8ϕ	clay >8ϕ
o114	86.3	86.25	1.25	2.75	0.0	0.75	0.75	1.75	6.5
o115	63.3	75.25	4.25	5.0	2.5	3.5	0.0	1.75	7.25
o130	41.9	74.25	5.75	7.0	3.0	3.0	0.0	0.75	6.25
o131	28.5	88.0	1.75	1.25	0.25	0.0	1.0	0.25	7.5
o132 & ◇8	51.8	58.5	6.5	5.25	3.0	2.0	3.25	6.25	15.25
o133	33.4	81.25	6.0	4.0	0.0	1.0	0.5	1.0	6.25
o134	55.3	92.5	0.5	0.75	0.0	0.0	0.0	0.0	6.25
o135	66.3	91.25	1.0	0.75	0.5	0.5	0.5	0.75	4.75
o136	51.3	91.0	1.5	1.0	0.25	0.0	0.75	0.5	5.0
o137	65.0	89.75	0.5	2.25	0.0	0.5	0.0	1.5	5.5
o138	65.4	92.25	0.25	0.75	0.5	0.0	0.5	0.75	5.0
o139	26.5	86.75	3.25	2.0	0.0	0.5	0.75	0.5	6.25
o140 & ◇9	36.9	90.0	0.75	0.75	0.5	0.5	1.0	1.5	5.0
o141	13.1	85.0	3.0	2.75	0.25	0.25	1.25	0.5	7.0
o142	50.7	68.0	5.0	6.5	1.5	1.5	2.0	3.0	12.5
o165	29.0	76.25	4.0	5.5	1.75	1.0	1.25	2.0	8.25
o166	40.3	87.5	2.5	0.5	1.5	1.0	0.75	0.25	6.0
o167	10.7	87.0	1.25	1.25	0.5	0.75	0.5	1.25	7.5
o168	27.9	88.0	2.25	0.5	1.25	1.0	0.0	1.75	5.25
o169	23.4	85.5	3.25	1.25	0.5	0.75	1.25	0.75	6.75
o170	44.1	83.0	2.0	3.75	1.25	1.5	1.0	2.75	4.75
o171	39.4	92.75	0.5	0.25	0.25	1.25	0.25	1.0	3.75
o172	7.3	90.5	0.5	1.5	0.0	0.75	1.5	0.75	4.5
o173	41.0	92.0	0.25	0.25	0.0	0.5	0.75	1.25	5.0
o174	70.8	85.0	2.75	2.75	0.0	0.75	1.25	1.0	6.5
o175	36.3	88.0	2.0	1.5	0.25	0.25	0.5	1.5	6.0
o176	15.5	79.75	4.5	3.25	0.0	0.5	0.25	4.25	7.5
o177	41.7	83.75	2.0	4.25	0.5	0.0	2.0	1.0	6.5

10.4 APPENDIX 3: Gravel mineralogy (see section 7.71)

Values listed are visual estimates of volume %

The plot is organized into two categories: mineral grains and rock fragments.

Abbreviations:

gr	granite
bas	basalt
ls	limestone
qtz. w/ sm.incl.	quartz grains that include small mineral inclusions
wea. rhy.	weathered rhyolite

APPENDIX 3: Gravel Mineralogy

	MINERALS		ROCK FRAGMENTS				
	Quartz	Biotite	gr.	bas.	ls.	qtz. w/ sm.incl.	wea. rhy.
◇1	15		30	<5		50	≈1
◇2	5			few		90	<5
◇3	20		10	few	<5	≈75	
◇4	10		15		5	65	5
◇5	20		40	5-10	<1	30	
◇6 & o29	5-10		10-15		<1	80	
◇7 & o82			5			95	
◇8 & o132	5		15			70	10
◇9 & o140			60-70			15	15-20
◇10 & o89	10		20-25	35	<1	25	<5
◇11 & o35	10		30	30	<1	25	5
o27			30			60	10
o28			25			65	10
o29 & ◇6	5-10		10-15		<1	80	
o30			60			40	
o31			60			30	10
o32			45			50	5
o33	15		15		≈1	70	
o34	5		50		≈1	45	
o35 & ◇11	10		30	30	<1	25	5
o36	25		40			35	
o37	15		50			35	
o57	15		25			60	
o58			60			38	≈2
o59			65			35	
o60	25		25			50	
o61			35			65	
o62			50			50	

APPENDIX 3, continued

	Quartz	Biotite	gr.	bas.	ls.	qtz. w/ sm.incl.	wea. rhy.
o63	15		15			70	
o64	20		35			40	5
o65	15		50		≈1	30-35	<5
o66	10		40			50	
o67	5		75			20	≈1
o68	10		25+			60	<5
o80	10		10			75	5
o81	10		10			80	
o82 & ◇7			5			95	
o83			5			95	
o84	10		10			80	
o85	5		25			70	
o86	10		20			70	<1
o87	15		40			40	5
o88	10		40		≈2	30	≈18
o89 & ◇10	10		20-25	35	<1	25	<5
o90	5		70		5	20	
o91			75	<1		20	5
o104			<5			>95	
o105			<5			>95	
o106	5	<1	<5			90	
o107					2	95+	≈2
o108	5		5		<1	90	
o109	10		10			80	
o110	10		20	<1	5	65	
o111	10		30		<5	55	<5
o112	10		≈25		2	≈65	
o113	5		15			80	

APPENDIX 3, continued

	Quartz	Biotite	gr.	bas.	ls.	qtz. w/ sm.incl.	wea. rhy.
o114			50			50	
o115			80		15	5	
o130						>98	
o131			<5		2	95	
o132 & ◇8	5		15			70	10
o133	10					85	5
o134	10					80	10
o135	15-20		10		≈1	75	
o136	10		20		5	60	
o137			15		5	80	
o138	10		40		<1	50	
o139	5		85			5	5
o140 & ◇9			60-70			15	15-20
o141			60	≈7	5	≈28	
o142	10-20		10			70-80	
o165	10		5		5	80	
o166	10-15		20-25		5	60-70	
o167	10-15				<5	85	
o168	<5				≈1	95+	
o169	5				5	90	
o170	5		5		10	80	
o171	20		5-10		<5	70	
o172			5		<1	90	5
o173	30		15-20	<1	<5	45	5
o174	10		35	<1	<1	40	15
o175	10		20			65	5
o176	5		40	<1		55	
o177	20-25		20		<5	≈50	5-10

10.5 APPENDIX 4: Sand mineralogy (see section 7.72)

Values listed are visual estimates of volume %.

The plot is organized into the following categories, reading from left to right:

quartz
feldspars
micas
rock fragments
accessory minerals

Abbreviations:

qtz	quartz
FSP	feldspars
or	orthoclase
pl	plagioclase
mus	muscovite
bio	biotite
wea	weathered mica
gr	granite
bas	basalt
ls	limestone
epi	epidote
hbd	hornblende
gyp	gypsum

In some cases, it was not possible to identify the feldspars specifically. Those values are plotted on the line that separates the orthoclase feldspars from the plagioclase feldspars.

Similarly, micas not assignable either to mus or bio are plotted on the line separating the two species.

APPENDIX 4: Sand mineralogy

		FSP		MICAS			RX FRAGS					
	qtz	or	pl	mus	bio	wea	gr	bas	ls	epi	hbd	gyp
◇1	50	2			2		40	5	≈1		1	
◇2	85						10	≈1	5			
◇3	80	5					15	≈1	≈1			
◇4	60	2	18	5	1		2	5	5		2	<1
◇5	55		15		1		25		2		2	<1
◇6 & o29	45-50	20			2	2	25		>1		3	
◇7 & o82	50	20		3	2		20				5	
◇8 & o132	≈70	15		>1			15				1	
◇9 & o140	≈50	5					10	20	10		5	2
◇10 & o89	70-75	5		2	2		>1	10	3		3	2
◇11 & o35	90	5					5					
o27	≈70	10			2	3	10		<1		2	1
o28	85	5			3	2	5					
o29 & ◇6	45-50	20			2	2	25		>1		3	
o30	≈90				5		5		<1		<1	1
o31	90				3	3	2				2	
o32	90					2	3		<1		5	
o33	80	5					10+	2+	<1			
o34	90	2	4				3		<1		1	
o35 & ◇11	90	5					5					
o36	75	3				2	20					
o37	≈90					<1	5				3	
o57	≈70					2	25				5	
o58	60	5		2	1		30		1			1
o59	≈80					5	15				1	<1
o60	≈80					1	20	<1			<1	
o61	≈80				2	1	15				3	
o62	90	2				2	5		2			

	ytz	or	pl	mus	bio	wea	gr	bas	ls	epi	hbd	gyp
o63	75					<1	20		2		2	
o64	85	1					10		4			
o65	80	5			<1		10		4	<1		
o66	≈60						40		2			
o67	≈65	<1					35		<1			<1
o68	75-80						20		1			1
o80	90	<1			3	2	5		<1			
o81	≈90	<1			2		5		1		2	1
o82 & ◇7	50	20		3	2		20				5	
o83	90+					5	<1		<1		<1	1
o84	≈90					2	5		2		2	
o85	95					<	2				3	
o86	95+						<1		1		2	
o87	95+	<1			<1		<1		1		<1	
o88	50						45		5		<1	
o89 & ◇10	70-75	5		2	2		>1	10	3		3	2
o90	95	5					<1		<1		<1	
o91	≈55	<1				< 1	20	5	20			
o104	95	5			2		3					
o105	95+				<1	<1	<1		<1		3+	<1
o106	≈90	<1			1		3				5	<1
o107	95+	<1			1		<1		<1		2	<1
o108	95+	<1				<1	3		1			<1
o109	95+						1		1		1	
o110	≈80	2			<1		15		2		<1	
o111	65	2	3				25		5		<1	
o112	85	2					10		3			
o113	95	<1					2				2	

APPENDIX 4, continued

	qtz	or	pl	mus	bio	wea	gr	bas	ls	epi	hod	gyp
o114	90						5		5			
o115	≈70	2	2				10	10	5		3	
o130	≈85				5	2	10					
o131	90-95						<1		5		2	
o132 & ◇8	≈70	15			>1		15				1	
o133	≈95	2	2			<1	<1				2	
o134	90	<1				<1	<1	5	<1		3	
o135	85-90	3					10		<1		<1	
o136	≈95					<1	5		1		<1	
o137	≈90				<1	<1	10				<1	
o138	≈90				<1		10				<1	
o139	≈55	5					5	30	5		<1	
o140 & ◇9	≈50	5					10	20	10		5	2
o141	≈80	2					15		2		<1	
o142	≈85	5				<1	10		<1			<1
o165	85-90					<1	5		5		2	
o166	85-90				5		2		5		2	
o167	≈90				<1		<1		<1		10	
o168	80						5		10		5	
o169	85	<1				5	<1				10	<1
o170	≈90					<1	5		5		1	
o171	95+	<1				1					<1	
o172	95	<1					<1	5	<1		<1	
o173	≈60	2				25	3	2	5		<1	
o174	75						15		10		<1	
o175	80	2					3	5	5			
o176	95						5		<1		<1	
o177	85-90						10		2			

10.6 APPENDIX 5: Silt-size heavy minerals (see section 7.73)

X indicates presence of a given mineral. No effort was made to approximate relative abundances of the heavy-mineral species identified.

Abbreviations:

bio	biotite
zir	zircon
op	opaque minerals, non-differentiated
pyr	pyroxene
amph	amphibole
apa	apatite
mon	monazite
stauro	staurolite

APPENDIX 5: Silt-size heavy minerals

	bio	zir	op	pyr	amph	apa	mon	stauro	sphene	garnet
◊ 1	X	X	X	X		X	X			
◊ 2	X		X	X		X				X
◊ 3	X	X	X	X		X	X			X
◊ 4	X		X	X		X				
◊ 5	X	X	X	X		X	X			
◊ 6 & o29	X	X	X	X		X				
◊ 7 & o82	X		X	X						X
◊ 8 & o132	X	X	X	X		X	X			
◊ 9 & o140	X	X	X	X		X				
◊10 & o89	X	X	X	X		X				
◊11 & o35	X	X	X	X		X	X			
o27	X	X	X	X		X				
o28		X	X	X						
o29 & ◊6	X	X	X	X		x				
o30		X	X	X						
o31	X	X	X	X						
o32	X	X	X	X		X				
o33	X	X	X	X			X			
o34	X	X	X	X		X				
o35 & ◊11	X	X	X	X		X	X			
o36	X	X	X	X		X				
o37	X		X	X						
o57	X	X	X	X						
o58	X		X	X		X				
o59	X		X	X						
o60	X	X	X	X						
o61	X	X	X	X						
o62	X		X	X	X				X	

APPENDIX 5, continued

	bio	zir	op	pyr	amph	apa	mon	stauro	sphene	garnet
o63	X	X	X	X			X			
o64	X	X	X	X	X					
o65	X	X	X	X		X	X			
o66	X		X	X		X	X			X
o67	X	X	X	X						
o68	X	X	X	X						
o80	X	X	X	X						
o81	X	X	X	X						
o82 & ◇7	X		X	X						X
o83	X	X	X	X		X	X	X		
o84	X	X	X	X		X	X			
o85	X	X	X	X		X	X			
o86	X	X	X	X			X			
o87	X	X	X	X		X				
o88	X	X	X	X		X	X			
o89 & ◇10	X	X	X	X		X				
o90	X	X	X	X						X
o91	X	X	X	X		X				
o104		X	X	X		X				
o105	X	X	X	X		X				
o106	X		X	X						X
o107	X	X	X	X				X		
o108	X	X	X	X		X	X			
o109	X	X	X			X	X			X
o110	X	X	X				X			X
o111	X	X	X	X		X				
o112	X	X	X	X		X	X			X
o113	X	X	X	X		X	X			X

	bio	zir	op	pyr	amph	apa	mon	stauro	sphene	garnet
o114	X	X	X	X			X			
o115	X	X	X	X		X				X
o130	X	X	X	X	X	X	X			
o131	X	X	X	X		X				
o132 & ◇8	X	X	X	X		X	X			
o133	X	X	X	X	X	X	X			
o134		X	X	X		X	X			
o135	X	X	X	X		X				X
o136	X	X	X	X		X	X			
o137	X	X	X	X		X	X			
o138	X	X	X	X		X	X			
o139	X	X	X	X	X	X				
o140 & ◇9	X	X	X	X		X				
o141	X	X	X	X		X				
o142	X	X	X	X		X				X
o165	X	X	X	X						
o166		X	X	X		X				
o167			X	X			X			
o168	X	X	X	X		X	X	X		
o169	X	X	X	X		X				
o170	X	X	X	X		X	X			
o171	X	X	X	X		X				
o172	X	X	X	X		X				
o173	X	X	X	X		X				X
o174	X		X	X		X				X
o175	X	X	X	X		X				
o176	X	X	X	X		X	X			
o177	X	X	X	X		X				

10.7 APPENDIX 6: Clay mineralogy (see section 7.74)

Symbols plotted on the table represent an approximation of the relative abundances of the clay minerals identified by X-ray diffraction.

The values are related to height of peak above baseline. Baseline ranges from 20 to 25 units above 0 on the diffractogram paper.

SYMBOL	DESCRIPTION	PEAK HEIGHT
++	relatively very large amount	>85 units
+	relatively large amount	55-85 "
+/o	rel. large to rel. moderate amount	45-55 "
o/+	rel. moderate to rel. large amount	45 "
o	rel. moderate amount	35-45 "
o/-	rel. moderate to rel. small amount	30-35 "
-/o	rel. small to rel. moderate amount	30 "
-	rel. small amount	<30 "
tr	barely detectable	

APPENDIX 6: Clay mineralogy

	Montmor-illonite	Chlorite	Illite/ muscovite	Kaolinite	Paly-gorskite
◊ 1	+	-	+/o	o/-	
◊ 2	+/o	-	+	o	
◊ 3	+	-	+/o	o	
◊ 4	+	-	+	o	
◊ 5	+	-	+	o	
◊ 6 & o29	o/+	-	o/+	-/o	
◊ 7 & o82	+	-	o	-/o	
◊ 8 & o132	o/-	-	+/o		+/o
◊ 9 & o140	+	-	o	-/o	tr?
◊10 & o89	+	-	o	-	tr?
◊11 & o35	+	-	+/o	o/-	tr?
o27	o	-	+	o/-	
o28	+/o	-	o	o	
o29 & ◊6	o/+	-	o/+	-/o	
o30	+	-	o	o/-	
o31	+	-	o	o/-	
o32	o/+	-	o/-	-	
o33	++	-	o/-	+	-?
o34	+/o	-	++	+	
o35 & ◊11	+	-	+/o	o/-	tr?
o36	+	-	o/-	-	
o37	+/o	-	+/o	o/+	
o57	+	-	o	-/o	
o58	+	-	o	o	
o59	+	-	+	-/o	
o60	+	-	+	-	
o61	+	-	+	o	
o62	o/+	-	o/+	-/o	tr?

APPENDIX 6, continued

	Montmorillonite	Chlorite	Illite/muscovite	Kaolinite	Palygorskite
o63	+	-	+/o	o	
o64	+	-	+	o/+	
o65	+	-	o	o	
o66	+	-	o	o	tr?
o67	o	-	o/-	o/-	
o68	+/o	-	o	tr?	
o80	+	-	+/o	o	
o81	+	-	o	-	
o82 & ◇7	+	-	o	-/o	
o83	+	-	+/o	-	
o84	+	-	o	-	
o85	+	-	+	o	
o86	+	-	+/o	o/-	
o87	+	-	+	o	
o88	+	-	+/o	o/-	
o89 & ◇10	+	-	o	-	tr?
o90	+/o	-	+	-	tr?
o91	+	-	+	o	
o104	++	-	o/-	+	
o105	+/o	-	o	o/-	tr?
o106	+	-	o	-/o	
o107	+	-	+/o	-/o	tr?
o108	+	-	+	o	tr?
o109	+	-	+	o/-	
o110	o	-	+	-/o	
o111	+/o	-	+	o	
o112	+/o	-	o	o/-	
o113	o	-	+/o	tr?	

APPENDIX 6, continued

	Montmorillonite	Chlorite	Illite/ muscovite	Kaolinite	Palygorskite
o114	+	-	+/o	o/-	
o115	+	-	o	o/-	tr?
o130	o	-	o	-	
o131	+	-	+	o	
o132 & ◇8	o/-	-	+/o		+/o
o133	+/o	o/-	+/o	-/o	
o134	+	-	+/o	-/o	
o135	+	-	+	o	
o136	+	-	+	o	
o137	+/o	-	+/o	o/-	
o138	+	-	+	o	
o139	+	-	o	o/-	
o140 & ◇9	+	-	o	-/o	tr?
o141	o/+	-	o	o/-	
o142	o	-	+	-	tr?
o165	o	-	+/o	o/-	
o166	+/o	-	o/+	o	
o167	+	-	+/o	o	
o168	+/o	-	+	o	
o169	o	-	o	o/-	
o170	+	-	o	-	
o171	+	-	+	o/-	
o172	+	-	+	o/-	
o173	+	-	+	o/-	
o174	+	-	+/o	o/-	
o175	+/o	-	o	-	
o176	o/+	-	o	o	
o177	o/-	-	+	-	-

APPENDIX 6.1

10.7.1 GEOCHEMICAL ANALYSES

Geochemical Analysis (Winter 1979)

Map Location*	Sample Number	%K	ppm eU	ppm eTh	Latitude	Longitude
1	MIK 797	1.75	3.1	8.1	36.0374	114.4690
2	798	2.52	3.5	10.8	.0373	.4681
3	799	2.67	3.6	10.0	.0371	.4670
4	800	2.64	3.8	10.6	.0370	.4661
5	801	2.52	3.3	11.9	.0369	.4651
6	802	2.43	2.7	9.3	.0367	.4641
7	803	2.22	2.7	8.2	.0366	.4632
8	804	2.45	2.8	12.3	.0364	.4622
9	805	2.57	3.4	10.7	.0363	.4613
10	806	2.40	3.2	11.3	.0361	.4602
11	807	1.96	3.7	12.3	.0360	.4592
12	808	2.98	4.0	11.8	.0358	.4581
13	809	2.36	5.6	9.6	.0356	.4572
14	810	2.39	5.6	11.1	.0361	.4694
15	811	2.67	2.5	11.9	.0360	.4683
16	812	2.24	2.5	12.1	.0358	.4673
17	813	2.25	2.5	11.2	.0357	.4664
18	814	2.61	2.2	8.8	.0355	.4654
19	815	2.69	2.6	9.1	.0353	.4644
20	816	1.32	5.1	6.9	.0352	.4635
21	817	2.14	2.8	11.3	.0350	.4625
22	818	2.83	3.4	11.9	.0350	.4615
23	819	3.07	2.0	7.9	.0348	.4605
24	820	2.86	2.5	11.1	.0347	.4596
25	821	2.41	3.2	11.8	.0345	.4585
26	822	2.55	4.4	15.6	.0343	.4575
27	823	2.25	2.5	9.7	.0348	.4694
28	824	2.24	2.8	10.9	.0345	.4687
29	825	2.02	2.5	11.9	.0344	.4666
30	834	2.16	2.4	11.1	.0342	.4633
31	835	1.99	2.1	9.4	.0341	.4640
32	836	2.25	2.4	10.5	.0340	.4693
33	837	3.20	2.4	9.5	.0337	.4624
34	838	3.04	2.3	9.6	.0335	.4614
35	839	2.91	2.8	10.4	.0333	.4604
36	840	2.33	4.4	10.9	.0332	.4595
37	841	2.69	3.5	9.5	.0330	.4581
38	842	2.07	1.8	9.4	.0329	.4698
39	843	2.18	2.0	10.5	.0327	.4687
40	844	2.04	3.0	12.2	.0326	.4677
41	845	2.30	1.8	8.6	.0325	.4667
42	846	2.29	2.2	10.8	.0324	.4657
43	847	2.14	2.8	12.9	.0322	.4647
44	848	2.93	2.2	13.7	.0320	.4639
45	849	3.21	2.5	12.4	.0319	.4630

Map Location*	Sample Number	%K	ppm eU	ppm eTh	Latitude	Longitude
46	MIK 850	3.13	2.7	10.2	36.0317	114.4619
47	851	2.85	2.0	10.1	.0316	.4611
48	852	2.33	7.2	9.3	.0316	.4602
49	853	2.43	3.4	10.7	.0314	.4589
50	854	2.10	2.3	10.4	.0310	.4701
51	855	2.23	2.0	9.9	.0309	.4691
52	856	2.13	4.8	12.2	.0293	.4589
53	857	2.16	2.0	11.6	.0300	.4705
54	858	2.06	2.3	11.3	.0298	.4694
55	859	2.42	3.1	11.0	.0284	.4602
56	860	2.33	3.3	12.3	.0283	.4592
R-1	861	2.99	3.3	14.7	.0549	.4545
R-2	862	3.17	2.2	12.0	.0543	.4502
R-3	863	3.24	2.1	11.2	.0520	.4595
R-4	864	3.05	2.2	11.3	.0514	.4554
R-5	865	3.00	2.5	12.4	.0508	.4512
R-6					.0497	.4685
R-9					.0479	.4563
R-10					.0473	.4521
57	676	2.06	2.2	11.7	.0284	.4708
58	677	2.78	3.6	17.6	.0282	.4598
59	678	2.11	2.9	14.7	.0282	.4687
60	679	2.54	3.0	14.3	.0280	.4676
61	680	2.80	2.8	18.1	.0279	.4666
62	681	2.97	2.6	12.4	.0278	.4659
63	682	2.86	2.5	16.4	.0276	.4653
64	683	2.58	3.7	12.4	.0274	.4643
65	684	2.16	4.2	13.5	.0272	.4631
66	685	2.71	4.9	12.1	.0270	.4621
67	686	2.18	4.3	13.7	.0268	.4607
68	694	2.21	3.6	13.2	.0266	.4597
69	693	2.08	2.9	11.2	.0273	.4711
70	687	1.99	3.4	18.0	.0271	.4700
71	688	1.86	3.4	11.8	.0257	.4609
72	689	2.63	4.8	13.6	.0256	.4599
73	690	2.11	2.2	11.9	.0258	.4714
74	691	2.24	3.6	15.1	.0257	.4703
75	692	2.38	3.2	9.8	.0244	.4613
76	695	2.34	3.2	15.7	.0241	.4603
77	696	2.16	1.9	11.5	.0240	.4718
78	697	2.18	5.0	14.8	.0224	.4617
79	698	2.14	5.4	14.7	.0222	.4606
80	699	2.60	2.0	15.8	.0225	.4721
81	700	2.67	2.8	15.0	.0225	.4709
82 (B-7)	701	2.53	2.6	16.9	.0223	.4697
83	702				.0221	.4686
84	703	2.57	2.4	12.3	.0220	.4678
85	704	2.62	2.5	12.8	.0219	.4672
86	705	3.07	2.1	11.9	.0217	.4663
87	706	3.13	2.7	9.5	.0215	.4652

Map Location	Sample Number	%K	ppm eU	ppm eTh	Latitude	Longitude
88	MIK 707	2.87	4.0	12.5	36.0213	114.4641
89	(B-10) 708	2.55	3.7	13.0	.0211	.4630
90	709	2.22	5.0	15.6	.0210	.4620
91	710	2.47	4.2	14.4	.0208	.4610
92	711	2.71	2.5	13.3	.0207	.4725
93	712	2.68	3.8	13.2	.0193	.4634
94	713	2.81	3.2	11.0	.0191	.4623
95	714	2.39	5.6	13.4	.0190	.4614
96	715	2.63	2.3	10.8	.0195	.4728
97	716	2.79	3.9	13.6	.0177	.4636
98	717	2.60	4.4	15.1	.0175	.4626
99	718	2.26	3.5	11.8	.0173	.4616
100	719	2.64	2.6	11.9	.0183	.4731
101	720	2.91	5.0	13.9	.0166	.4641
102	721	2.55	6.1	12.5	.0163	.4629
103	722	2.84	4.2	9.7	.0161	.4620
104	723	2.31	3.1	10.5	.0171	.4733
105	724	2.63	2.2	10.8	.0169	.4722
106	725	2.57	3.4	15.5	.0168	.4714
107	726	2.56	2.9	9.8	.0166	.4703
108	727	3.23	2.0	9.5	.0161	.4697
109	728	2.96	2.2	15.0	.0162	.4691
110	729	3.25	1.8	10.6	.0160	.4691
111	730	2.78	3.4	13.1	.0158	.4672
112	731	2.71	2.2	10.4	.0158	.4660
113	732	3.07	3.5	13.3	.0153	.4645
114	733	3.61	2.3	10.7	.0150	.4633
115	734	2.31	5.5	13.3	.0148	.4623
116	735	2.63	2.6	12.6	.0152	.4741
117	736	2.61	2.4	11.8	.0150	.4730
118	737	2.54	3.5	11.5	.0135	.4656
119	738	2.53	2.3	9.8	.0131	.4658
120	739	3.18	2.9	11.3	.0129	.4630
121	740	2.54	2.8	12.9	.0140	.4743
122	741	2.61	2.7	12.9	.0137	.4734
123	742	2.40	3.3	9.4	.0122	.4654
124	743	2.20	3.1	11.1	.0120	.4642
125	744	2.28	2.3	9.5	.0118	.4632
126	745	2.42	2.6	14.3	.0126	.4748
127	746	2.61	2.8	12.6	.0124	.4738
128	747	2.40	3.1	14.5	.0106	.4645
129	748	2.35	2.8	14.8	.0104	.4636
130	749	2.22	2.4	11.9	.0114	.4750
131	750	2.33	3.2	19.0	.0112	.4741
132	(B-8) 751	3.00	3.0	19.3	.0111	.4730
133	752	3.04	2.3	12.9	.0109	.4718

Map Location*	Sample Number	%K	ppm eU	ppm eTh	Latitude	Longitude
134	753	3.03	2.0	13.9	36.0109	114.4718
135	754				.0104	.4699
136	755	3.10	2.1	12.9	.0104	.4679
137	756	3.26	1.8	11.4	.0102	.4685
138	757	3.26	1.7	12.5	.0100	.4679
139	758	2.41	1.9	11.6	.0099	.4669
140 (B-9)	759	2.46	3.6	14.7	.0094	.4649
141	760	2.51	3.3	8.9	.0094	.4649
142	761	2.96	2.7	11.4	.0093	.4639
143	762	2.34	3.1	11.0	.0101	.4755
144	763	2.28	4.3	19.8	.0099	.4745
145	764	2.49	3.8	11.7	.0083	.4662
146	765	2.41	5.4	14.1	.0081	.4653
147	766	2.45	4.2	12.0	.0080	.4644
148	767	2.46	3.3	13.8	.0089	.4758
149	768	2.49	2.7	11.4	.0087	.4749
150	769	2.48	2.8	12.1	.0069	.4657
151	770	3.54	2.5	13.3	.0067	.4647
152	771	2.43	3.7	13.8	.0075	.4766
153	772	2.57	2.6	12.2	.0073	.4756
154	773	2.55	2.6	12.0	.0071	.4740
155	774	2.64	3.3	12.0	.0069	.4736
156	775	2.58	2.6	12.1	.0067	.4726
157	776	2.62	2.9	10.3	.0065	.4715
158	777	3.19	3.1	10.7	.0064	.4707
159	778	2.99	3.2	10.4	.0061	.4697
160	779	2.93	3.0	11.6	.0060	.4688
161	780	2.76	3.2	10.2	.0058	.4678
162	781	2.19	3.2	9.8	.0056	.4668
163	782	2.13	3.5	8.3	.0054	.4658
164	783	2.35	3.3	7.9	.0052	.4648
165	784	2.51	3.4	13.8	.0062	.4770
166	785	2.72	2.9	12.4	.0060	.4760
167	786	2.72	2.3	11.8	.0058	.4750
168	787	2.64	2.6	12.8	.0057	.4739
169	788	2.56	2.8	14.2	.0054	.4730
170	789	2.62	3.1	9.7	.0052	.4720
171	790	3.40	2.2	10.5	.0051	.4710
172	791	2.99	2.9	11.3	.0049	.4701
173	792	2.38	3.2	9.8	.0047	.4691
174	793	2.82	3.1	10.4	.0044	.4681
175	794	2.72	3.5	10.6	.0043	.4672
176	795	2.39	2.9	9.5	.0041	.4662
177	796	3.21	3.6	12.3	.0039	.4652
R-26	659	2.51	2.9	14.4	.0052	.4799
R-27	660	2.48	3.9	14.3	.0043	.4754
R-28	661	2.56	2.1	10.0	.0036	.4765
R-29	662	2.70	3.6	12.2	.0023	.4676
R-30	672	2.13	3.8	12.4	.0020	.4633

Map Location*	Sample Number	%K	ppm eU	ppm eTh	Latitude	Longitude
R-31	MIK 663	2.39	2.9	11.5	36.0016	114.4808
R-32	664	2.47	2.7	12.0	.0009	.4763
R-33	665	2.79	2.3	15.4	.0002	.4724
R-34	666	2.55	4.8	14.9	.9994	.4684
R-35	673	1.86	3.6	10.1	.9987	.4642
R-36	667	2.11	2.8	12.2	.9981	.4816
R-37	668	2.26	2.8	12.4	.9973	.4772
R-38	669	3.01	2.2	12.1	.9967	.4733
R-39	670	3.42	1.7	11.1	.9960	.4694
R-40	671	2.23	2.9	9.5	.9953	.4651
R-41	651	2.04	5.4	19.7	.9946	.4826
R-42	652	2.62	2.8	10.0	.9938	.4781
R-43	653	2.76	2.0	11.3	.9932	.4742
R-44	654	3.44	2.7	14.6	.9925	.4702
R-45	674	1.52	2.2	5.5	.9918	.4660
R-46	655	2.22	3.3	11.6	.9911	.4835
R-50	675	1.70	3.0	8.5	.9883	.4668
B-1	861	2.99	3.3	14.7	.0075	.4701
B-2	862	3.17	2.2	12.0	.0129	.4688
B-3	863	3.24	2.1	11.2	.0217	.4663
B-4	864	3.06	2.2	11.3	.0274	.4648
B-5	865	3.00	2.5	12.4	.0343	.4628
B-6	825	2.02	2.5	11.9	.0344	.4667

* Reference is to Plates 2A and 2B, "Geology DTR-1 Environs" prepared by International Exploration on behalf of LKB Resources, Inc. (1979)

Geochemical Analysis (Fall - Winter 1977)

Map Location*	Sample Number	%K	ppm eU	ppm eTh	Latitude	Longitude
1-I	1	2.09	3.04	11.21	36.0064	114.4673
1-G	2	2.64	3.13	10.82	.0066	.4687
1-F	3	2.26	2.35	11.30	.0068	.4698
1-E	4	2.77	3.00	10.64	.0069	.4705
1-A	5	2.12	2.00	11.40	.0070	.4715
1-B	6	2.28	2.98	13.03	.0071	.4725
1-C	7	2.65	2.11	10.06	.0073	.4732
1-D	8	2.61	2.67	11.19	.0074	.4741
1-H	9	2.34	2.83	10.72	.0077	.4752
2-I	10	2.39	4.85	13.39	.0081	.4676
2-G	11	2.45	2.76	11.10	.0080	.4683
2-F	12	2.66	3.46	12.57	.0081	.4694
2-E	13	2.75	2.93	12.77	.0082	.4702
2-A	14	2.40	2.41	11.25	.0084	.4709
2-B	15	2.76	2.27	11.36	.0085	.4718
2-C	16	2.80	1.89	9.24	.0086	.4726
2-D	17	2.51	2.67	12.47	.0087	.4738
2-H	18	2.54	3.19	12.74	.0089	.4750
3-G	19	2.30	3.61	11.54	.0092	.4677
3-F	20	2.33	4.52	12.07	.0094	.4689
3-E	21	2.89	2.22	10.84	.0095	.4696
3-A	22	2.63	2.24	9.46	.0098	.4704
3-B	23	2.62	2.86	13.71	.0098	.4710
3-C	24	2.76	2.49	10.72	.0101	.4718
3-D	25	2.55	2.50	11.55	.0104	.4731
3-H	26	2.57	2.53	12.43	.0106	.4743
3-I	27	1.99	3.14	10.10	.0095	.4662
4-I	28	2.07	3.25	10.02	.0101	.4658
4-G	29	2.35	2.39	8.86	.0104	.4674
4-F	30	2.48	3.52	11.98	.0103	.4683
4-E	31	3.05	2.49	12.37	.0107	.4692
4-A	32	2.90	2.55	10.83	.0110	.4699
4-B	33	2.67	2.32	12.61	.0111	.4707
4-C	34	2.73	2.33	12.88	.0112	.4717
4-D	35	2.45	2.95	10.02	.0114	.4727
4-H	36	2.09	3.05	11.72	.0117	.4739
5-I	37	2.04	2.77	9.05	.0107	.4649
5-G	38	2.25	3.00	12.49	.0115	.4660
5-F	39	2.58	2.23	9.12	.0121	.4682
5-E	40	2.96	2.26	11.06	.0123	.4689
5-A	41	2.53	2.27	13.14	.0124	.4687
5-B	42	2.54	2.25	9.37	.0126	.4704
5-C	43	2.49	2.16	11.29	.0128	.4711
5-D	44	2.14	2.66	10.16	.0135	.4725
5-H	45	2.47	3.00	12.13	.0134	.4735
6-I	46	2.09	2.71	10.18	.0127	.4652

Map Location*	Sample Number	%K	ppm eU	ppm eTh	Latitude	Longitude
6-G	47	2.30	3.20	12.36	36.0131	114.4673
6-F	48	2.87	2.63	11.92	.0133	.4685
6-E	49	2.59	2.26	10.09	.0134	.4692
6-A	50	2.59	3.57	12.16	.0137	.4690
6-B	51	2.63	2.71	11.81	.0140	.4706
6-C	52	2.39	2.85	12.71	.0144	.4714
6-D	53	2.16	2.76	12.50	.0147	.4724
6-H	54	2.09	2.71	10.18	.0148	.4736
7-I	55	2.26	2.58	11.74	.0155	.4666
7-G	56	2.69	2.80	10.76	.0155	.4679
7-F	57	2.50	2.26	10.66	.0157	.4690
7-E	58	2.67	2.54	14.47	.0159	.4700
7-A	59	2.74	2.59	15.61	.0159	.4707
7-B	60	2.60	3.11	14.60	.0163	.4714
7-C	61	2.39	2.61	13.41	.0166	.4725
7-D	62	2.16	3.53	14.65	.0167	.4733
7-H	63	2.32	3.19	11.89	.0169	.4746
8-I	64	2.52	2.82	12.87	.0168	.4658
8-G	65	2.74	2.99	13.06	.0170	.4670
8-F	66	2.56	2.38	10.62	.0172	.4681
8-E	67	2.76	2.96	14.50	.0172	.4691
8-A	68	2.77	2.61	13.08	.0173	.4696
8-B	69	2.58	2.97	14.03	.0174	.4704
8-C	70	2.50	2.72	11.28	.0176	.4711
8-D	71	2.15	2.78	13.71	.0178	.4720
8-H	72	2.16	2.91	12.90	.0180	.4732
9-I	73	2.41	2.67	11.16	.0180	.4657
9-G	74	2.51	2.79	11.47	.0181	.4668
9-F	75	2.77	2.60	9.81	.0183	.4676
9-E	76	2.85	2.68	12.02	.0184	.4682
9-A	77	2.88	2.73	13.38	.0186	.4692
9-B	78	2.72	2.69	11.49	.0187	.4699
9-C	79	1.99	3.28	12.46	.0189	.4707
9-D	80	2.21	2.90	13.09	.0191	.4718
9-H	81	1.81	3.03	11.50	.0193	.4730
10-I	82	2.37	4.78	12.93	.0190	.4645
10-G	83	2.47	4.02	12.01	.0193	.4656
10-F	84	2.69	2.37	9.72	.0197	.4662
10-E	85	2.69	2.46	11.43	.0198	.4674
10-A	86	2.86	2.30	10.00	.0201	.4683
10-B	87	2.09	5.33	13.51	.0203	.4689
10-C	88	2.46	2.20	9.75	.0204	.4696
10-D	89	2.53	2.57	10.28	.0206	.4707
10-H	90	2.37	3.45	12.90	.0208	.4721
11-I	91	2.64	4.22	11.45	.0204	.4632
11-G	92	2.54	4.16	9.97	.0206	.4643
11-F	93	2.43	3.19	11.46	.0214	.4653

Map Location*	Sample Number	%K	ppm eU	ppm eTh	Latitude	Longitude
11-E	94	2.91	2.59	10.66	36.0217	114.4666
11-A	95	2.87	2.28	9.97	.0220	.4675
11-B	96	2.26	4.16	13.86	.0222	.4682
11-C	97	2.50	2.61	10.68	.0223	.4690
11-D	98	2.41	3.21	14.80	.0225	.4702
11-H	99	2.46	3.08	13.12	.0228	.4716
12-I	100	2.02	3.53	11.77	.0221	.4629
12-G	101	2.60	3.10	11.46	.0222	.4638
12-F	102	2.82	2.69	10.81	.0229	.4649
12-E	103	2.64	2.64	10.22	.0233	.4661
12-A	104	2.28	3.39	11.03	.0235	.4669
12-B	105	2.38	3.55	11.70	.0238	.4678
12-C	106	2.33	3.15	12.05	.0237	.4688
12-D	107	1.91	2.41	10.90	.0242	.4701
12-H	108	2.02	2.92	12.96	.0243	.4712
13-I	109	2.24	3.29	12.52	.0238	.4619
13-E	110	2.29	3.32	12.13	.0240	.4634
14-I	111	2.64	4.22	11.45	.0249	.4637
13-F	112	2.54	3.32	12.29	.0251	.4649
13-E	113	2.79	3.21	13.06	.0255	.4654
13-A	114	2.71	2.76	13.47	.0257	.4668
13-B	115	2.40	2.95	11.41	.0258	.4675
13-C	116	2.05	2.45	10.68	.0261	.4687
13-D	117	1.90	2.79	12.87	.0263	.4699
13-H	118	1.87	3.32	15.36	.0247	.4614
14-G	119	2.56	4.48	11.20	.0258	.4626
15-I	120	2.38	2.98	9.98	.0266	.4632
14-F	121	2.90	2.62	12.21	.0267	.4645
14-E	122	2.86	2.77	13.13	.0270	.4653
14-A	123	2.51	3.04	14.95	.0272	.4660
14-B	124	2.31	2.83	14.07	.0273	.4667
14-C	125	2.38	2.71	11.00	.0276	.4678
14-D	126	2.11	2.48	8.94	.0277	.4688
14-H	127	2.02	2.65	10.13	.0270	.4619
15-G	128	2.20	3.85	9.40	.0275	.4627
15-F	129	2.79	2.57	12.40	.0272	.4638
15-E	130	2.85	2.12	9.57	.0281	.4648
15-A	131	2.82	2.65	9.41	.0285	.4654
15-B	132	2.60	2.80	12.29	.0285	.4662
15-C	133	2.60	2.30	9.58	.0286	.4674
15-D	134	2.07	2.55	9.89	.0289	.4686
15-H	135	1.93	2.33	8.72	.0278	.4601
16-I	136	2.21	3.83	8.74	.0285	.4610
16-G	137	2.10	3.58	9.20	.0294	.4620
16-F	138	2.28	3.38	9.36	.0296	.4631
16-E	139	2.74	2.25	8.08	.0297	.4638
16-A	140	2.92	2.69	12.26	.0300	.4648

Map Location*	Sample Number	%K	ppm eU	ppm eTh	Latitude	Longitude
16-B	141	2.81	2.86	11.76	36.0301	114.4655
16-C	142	2.19	2.58	13.59	.0304	.4671
16-D	143	2.03	2.99	12.37	.0305	.4682
16-H	144	2.09	3.18	11.55	.0300	.4591
17-I	145	2.37	2.66	9.76	.0302	.4605
17-G	146	2.51	3.55	11.20	.0303	.4615
17-F	147	2.80	2.93	12.09	.0305	.4626
17-E	148	2.91	2.68	10.79	.0307	.4635
17-A	149	2.81	2.91	13.12	.0310	.4644
17-B	150	2.05	2.85	11.29	.0312	.4653
17-C	151	2.20	2.32	9.81	.0314	.4664
17-D	152	2.04	2.84	12.24	.0318	.4678
17-H	153	1.83	2.75	11.02	.0319	.4578
18-I	154	1.78	3.42	14.30	.0321	.4591
18-G	155	2.61	3.51	12.06	.0322	.4602
18-F	156	2.91	2.80	11.31	.0322	.4605
18-E	157	2.73	2.65	11.76	.0323	.4612
18-A	158	2.83	2.37	9.53	.0325	.4623
18-B	159	1.94	2.60	10.44	.0327	.4631
18-C	160	1.91	2.89	13.20	.0330	.4659
18-D	161	1.90	2.51	11.38	.0332	.4650
18-H	162	1.80	3.15	13.64	.0335	.4662
19-I	163	2.09	3.22	11.65	.0333	.4570
19-G	164	2.34	2.95	13.34	.0338	.4585
19-F	165	2.69	3.00	11.75	.0340	.4591
19-E	166	2.83	2.29	11.99	.0342	.4604
19-A	167	2.85	2.57	10.53	.0345	.4613
19-B	168	1.95	2.34	10.99	.0348	.4622
19-C	169	1.53	2.13	7.88	.0350	.4629
19-D	170	2.04	2.45	11.28	.0352	.4645
19-H	171	2.04	2.73	11.37	.0356	.4658

*Reference is to Figures 5.1 and 5.3 "Soil Sample Location Map" prepared by Bendix Field Engineering Corporation (1977)

APPENDIX 6.2

10.7.2 DATA TABULATION *
(Eleven Sites)

	◊1	◊2	◊3	◊4	◊5	◊6	◊7	◊8	◊9	◊10	◊11
Map Location	B-1	B-2	B-3	B-4	B-5	29	82	132	140	89	35
APPENDIX 1											
% Moisture	4.47	4.81	3.35	3.84	3.70	4.06	2.93	7.74	4.79	4.28	3.63
pH	9.0	8.7	8.5	8.6	8.7	8.7	8.8	8.7	9.0	8.6	8.2
Organic C	<.1	<.1	<.1	<.1	<.1	<.1	<.1	.1	<.1	.1	<.1
% $CaCO_3$ equiv.	4.1	2.9	3.9	3.2	5.3	1.5	1.2	4.9	5.6	6.8	9.1
APPENDIX 2											
% Gravel	65.2	54.5	63.8	42.3	49.4	7.0	29.3	51.8	36.9	17.4	38.4
% of fines											
cms 0-2ϕ	90.75	85.0	88.25	87.0	90.0	85.0	84.5	58.5	90.0	81.0	91.25
fs 2-3ϕ	0.75	0.5	1.0	0.75	2.25	2.75	2.0	6.5	0.75	7.75	1.25
vfs 3-4ϕ	1.0	1.75	0.5	1.0	0.25	1.75	4.75	5.25	0.75	1.5	1.25
csi 4-5ϕ	1.25	1.0	1.25	0.0	1.5	1.25	1.0	3.0	0.5	0.75	0.25
msi 5-6ϕ	0.5	1.75	1.25	0.75	0.5	1.0	0.25	2.0	0.5	0.5	1.0
fsi 6-7ϕ	1.25	0.75	0.25	3.0	0.0	1.75	0.5	3.25	1.0	0.75	0.0
vfsi 7-8	2.0	3.5	2.0	2.0	1.25	0.5	1.5	6.25	1.5	0.75	0.75
clay 8ϕ	2.5	5.75	5.5	6.5	4.25	3.5	5.5	15.25	5.0	7.0	4.25
APPENDIX 3 Minerals											
Quartz	15	5	20	10	20	5-10		5		10	10
Biotite											
Rock Fragments											
gr.	30		10	15	40	10-15	>5	15	60-70	20-25	30
bas.	<5	few	few		5-10					35	30
ls.			<5	5	<1	<1				<1	<1
qtz. w/ sm.incl.	50	90	≈75	65	30	80	95	70	15	25	25
wea. rhy.	=1	<5		5				10	15-20	<5	5

	◊1	◊2	◊3	◊4	◊5	◊6	◊7	◊8	◊9	◊10	◊11
APPENDIX 4											
FSP											
qtz	50	85	80	60	55	45-50	50	≈70	≈50	70-75	90
or	2		5	2		20	20	15	5	5	5
pl				18	15						
MICAS											
mus				5			3	>1		2	
bio	2			1	1	2	2			2	
wea						2					
RX FRAGS											
gr	40	10	15	2	25	25	20	15	10	>1	5
bas	5	≈1	≈1	5					20	10	
ls	≈1	5	≈1	5	2	>1			10	3	
epi											
hbd	1			2	2	3	5	1	5	3	
gyp				<1	<1				2	2	
APPENDIX 5											
bio	X	X	X	X	X	X	X	X	X	X	X
zir	X		X		X	X		X	X	X	X
op	X	X	X	X	X	X	X	X	X	X	X
pyr	X	X	X	X	X	X	X	X	X	X	X
amph											
apa	X	X	X	X	X	X		X	X	X	X
mon	X		X		X			X			X
stauro											
sphene											
garnet		X	X				X				
APPENDIX 6											
Montmor-illonite	+	+/o	+	+	+	o/+	+	o/-	+	+	+
Chlorite	-	-	-	-	-	-	-	-	-	-	-
Illite/ muscovite	+/o	+	+/o	+	+	o/+	o	+/o	o	o	+/o
Kaolinite	o/-	o	o	o	o	-/o	-/o		-/o	-	o/-
Paly-gorskite								+/o	tr?	tr?	tr?

	◊1	◊2	◊3	◊4	◊5	◊6	◊7	◊8	◊9	◊10	◊11
APPENDIX 6.1											
Sample No. MIK	861	862	863	864	865	825	701	751	759	708	839
%K	2.99	3.17	3.24	3.06	3.00	2.02	2.53	3.00	2.46	2.55	2.91
ppm eU	3.3	2.2	2.1	2.2	2.5	2.5	2.6	3.0	3.6	3.7	2.8
ppm eTh	14.7	12.0	11.2	11.3	12.4	11.9	16.9	19.3	14.7	13.0	10.4
Latitude 36.	0075	0129	0217	0274	0343	0344	0223	0111	0094	0211	0333
Longitude 114.	4701	4688	4663	4648	4628	4666	4697	4730	4649	4630	4604

* This Data Tabulation is a recompliation of analysis results previously presented in Appendices 1-6 and Appendix 6.1. It is presented here for the reader's ease of reference. An explanation of terms used has been previously provided in each referenced Appendix. The eleven sites presented are identified in the field by a semi-permanent marker (see Section 10.1).

APPENDIX 6.3

10.7.3 GROUND READINGS*
(Five Sites)

* These readings were taken by personnel of Bendix Field Engineering Corporation using a fully equipped ground vehicle (DTR-1 vehicle). Readings were taken between February 19, 1979 and April 3, 1979.

Weather Data (1979)

Date	Time	Temperature	Humidity	Pressure	Wind Direction	Wind Speed
Feb 18	12:30 pm	56° F	40%	29.20 in.	0°	5-10 mph
	3:35 pm	57° F	33%	29.15 in.	10°	2-5 mph
Feb 24	12:05 pm	54° F	43%	30.75 in.	0°	5-10 mph
	4:15 pm	55° F	34%	31.15 in.	355°	4 mph
Feb 25	12:00 pm	58° F	30%	30.90 in.	0°	2-3 mph
	5:35 pm	50° F	32%	31.00 in.	225°	1-2 mph
Feb 26	12:00 pm	62° F	29%	30.55 in.	30°	5-15 mph
	3:20 pm	63° F	22%	30.65 in.	270°	*5-20 mph
Feb 27	10:55 am	60° F	36%	31.00 in.	0°	0-10 mph
	2:30 pm	62° F	24%	30.95 in.	30°	5-10 mph
Mar 26	10:45 am	70° F	27%	30.55 in.	180°	**15-25 mph
	1:55 pm	76° F	24%	30.95 in.	180°	**15-20 mph
Apr 2	10:35 am	60° F	28%	30.80 in.	45°	8 mph
	2:10 pm	62° F	24%	30.80 in.	0°	7 mph
Apr 3	11:30 am	58° F	30%	31.00 in.	0°	10 mph
	3:40 pm	62° F	20%	31.00 in.	60°	2-3 mph

* Wind speed and direction were changing all day

** Gusty

%K

Day (1979)	1	2	3	4	5	Repeat	Repeat Station	Daily Averag
Feb 18	1.98	1.95	1.93	2.09	1.35	1.86	1	1.92
Feb 24	1.88	2.02	1.97	1.90	1.37	1.36	5	1.37
Feb 25		2.06	2.04	1.96	1.39			1.86
Feb 26	1.90	2.02	1.95	1.92	1.41	1.34	5	1.38
Feb 27	1.99	2.06	2.08	3.04	1.34	1.36	5	1.35
Mar 26	2.88	2.85	2.94	2.95	2.10	2.97	1	2.92
Apr 2	2.86	2.99	2.92	2.95	2.07	2.05	5	2.06
Apr 3	2.85	3.00	2.95	3.02	2.14	2.10	5	2.12

Uncertainty %K

Day (1979)	1	2	3	4	5	Repeat	Repeat Station	Daily Averag
Feb 18	.10	.10	.11	.10	.08	.11	1	.11
Feb 24	.10	.11	.11	.10	.08	.08	5	.08
Feb 25		.10	.11	.10	.08			.10
Feb 26	.10	.10	.10	.10	.08	.08	5	.08
Feb 27	.10	.10	.10	.10	.08	.08	5	.08
Mar 26	.14	.13	.14	.13	.10	.14	1	.14
Apr 2	.14	.13	.14	.13	.11	.10	5	.11
Apr 3	.14	.13	.14	.13	.11	.11	5	.11

ppm eTh

Day (1979)	1	2	3	4	5	Repeat	Repeat Station	Daily Average
Feb 18	8.48	7.52	10.42	8.00	8.35	10.80	1	9.64
Feb 24	10.03	9.91	10.19	9.38	7.78	7.92	5	7.85
Feb 25		8.57	9.18	8.39	7.93			8.52
Feb 26	9.41	8.66	9.16	8.23	7.63	7.41	5	7.52
Feb 27	9.21	8.36	9.01	8.06	7.46	7.60	5	7.53
Mar 26	13.53	12.63	13.55	11.95	11.23	13.72	5	12.47
Apr 2	13.70	12.78	13.15	11.78	11.24	11.21	5	11.23
Apr 3	13.47	12.67	13.55	11.90	11.49	11.33	5	11.41

Uncertainty ppm eTh

Day (1979)	1	2	3	4	5	Repeat	Repeat Station	Daily Average
Feb 18	.17	.17	.18	.16	.15	.18	1	.18
Feb 24	.17	.18	.18	.17	.15	.15	5	.15
Feb 25		.16	.17	.16	.15			.16
Feb 26	.17	.17	.17	.16	.14	.14	5	.14
Feb 27	.17	.16	.17	.16	.14	.14	5	.14
Mar 26	.21	.21	.21	.20	.18	.22	1	.20
Apr 2	.21	.21	.21	.20	.18	.18	5	.18
Apr 3	.21	.21	.21	.20	.18	.18	5	.18

ppm eU

Day (1979)	1	2	3	4	5	Repeat	Repeat Station	Daily Average
Feb 18	2.31	2.87	2.44	2.26	2.53	2.52	1	2.42
Feb 24	2.47	2.99	2.79	2.71	2.32	2.51	5	2.42
Feb 25		2.39	2.61	2.56	2.46			2.51
Feb 26	2.48	2.55	2.45	2.53	2.41	2.20	5	2.31
Feb 27	2.49	2.35	2.37	2.27	2.35	2.00	5	2.18
Mar 26	2.80	2.49	2.61	2.22	2.22	2.28	1	2.54
Apr 2	2.70	2.33	2.69	2.42	2.47	2.26	5	2.37
Apr 3	2.91	2.42	2.63	2.38	2.21	2.45	5	2.33

Uncertainty ppm eU

Day (1979)	1	2	3	4	5	Repeat	Repeat Station	Daily Average
Feb 18	.20	.20	.22	.20	.19	.22	1	.21
Feb 24	.21	.23	.22	.21	.18	.18	5	.18
Feb 25		.20	.21	.20	.18			.20
Feb 26	.21	.21	.21	.21	.18	.17	5	.18
Feb 27	.21	.20	.21	.20	.17	.17	5	.17
Mar 26	.26	.23	.25	.22	.20	.24	1	.25
Apr 2	.25	.23	.24	.23	.20	.20	5	.20
Apr 3	.25	.24	.25	.23	.20	.20	5	.20

Soil Moisture Weight %

Day (1979)	1	2	3	4	5	Repeat	Repeat Station	Daily Average
Feb 18	2.9	2.9	3.3	2.9	5.7	2.9	1	2.9
Feb 24	3.0	3.1	3.0	4.8	4.9	5.0	5	5.0
Feb 25	3.0	3.1	2.8	4.1	4.8			3.6
Feb 26	3.7		1.9	1.9	4.3	2.7	5	
Feb 27	2.1	2.2	2.1	1.9	4.1	4.8	5	4.5
Mar 26	3.16	3.18	3.21	3.5	3.9	2.88	1	3.02
Apr 2	2.97	3.26	2.81	3.12	3.73	3.81	5	3.77
Apr 3		2.7	2.95	2.84	3.17	2.84	5	3.01

APPENDIX 6.4

10.7.4 CIRCLE OF INVESTIGATION

GENERAL

The purpose of this segment of the project was to use the surficial concentration of the radio-elements K,U & Th over a region and the functional relationship between surface activity and airborne gamma ray detector observations in order to calculate the radio-element concentration that would be perceived at various altitudes above a line within the region. Surficial concentrations were based on geochemical analysis results (K,U, & Th) from 384 sample sites within the region. Airborne gamma ray spectrometry data (K,U, & Th count rates, positional coordinates, and altitudes) was obtained along 21 flight lines over the region.

METHOD

SUMMARY OF THE METHOD

The geochemical data being too sparse and unevenly distributed to permit its use for detailed calculations, the first task was to generate detailed pseudo-geochemical data from the actual geochemical results via the intermediary of the radiometric data.

The second task was to generate a set of 2-dimensional digital convolution filters, each specific to a given altitude and radio-element, such that the convolution of the filter with an underlying grid of radio-element concentration values would give the perceived concentration of the radio-element at a point at the center of the filter.

The third task was to apply each of the 36 filters (12 altitudes x 3 elements) to each of 40 points along a standard line within the test region. The result being 36 profiles of perceived concentrations.

DETAILS OF THE METHOD

GENERATION OF PSEUDO-GEOCHEMICAL DATA

The mean values of K,U & Th concentration with the region were found by averaging the geochemical results. The mean count rates over the region for K,U & Th were found from the radiometric data. This provided a calibration factor for the region for each element, giving CONCENTRATION/COUNT. (See page 98: NOTE. The parameters labelled "N USED" or "N VALUES USED" give the number of count rate samples actually used to calculate the average count rates. All count rate samples taken over water or within approximately 250' of the shore line were excluded from calculation of the averages as they were biased by the presence of water over which no corresponding zero-value geochemical results existed. Their inclusion would, therefore, have resulted in spuriously low average count rates and hence spuriously high perceived concentrations.)

The count rates along each radiometric survey line were then converted to %K, ppm U or ppm Th by multiplying by their respective calibration factors. A detailed regular grid of elemental concentration was then interpolated for each element (grid cell size: 50' x 50' ground distance; 0.1" x 0.1" map distance at scale=1:600).

The grid cell size chosen (50' x 50') is less than the recommended minimum of 1/6 x flight altitude for the 100' and 200' profiles. It is, however, more than adequate for these altitudes when the low spatial frequency of variation of the geochemical data is considered. For example, the variation of radio-element concentration, as derived from the radiometric measurements, is essentially linear over distances of the order of 50'. Hence the concentrations within a 50' cell are adequately described by a single value at its centre.

(NOTE These grids were contoured at the same scale as the radiometric and geochemical maps in order to validate the calibration and gridding processes. The resulting maps are available for inspection.)

GENERATION OF CONVOLUTION FILTERS

Kosanke and Koch (1978) provide an equation of the form:

$$dI = N*C*Fun(X,Y,Z)*dA \qquad (1)$$

Where:

dI=Photo peak intensity in a gamma ray detector.
N=a normalization constant.
C=the gamma ray activity of an element of the ground surface.
Fun(X,Y,Z)=A function of the spatial coordinates of the detector with respect to the surface element.
dA=the area of the surface element.

On the reasonable assumption that dI is proportional to count rate which is in turn proportional to perceived concentration of radio-element; and that C is proportional to actual radio-element concentration, then we can state that:

$$dP=N'*C'*Fun(X,Y,Z)*dA \qquad (2)$$

Where:

dP=perceived concentration.
N'=a different normalization constant.
C'=ground radio-element concentration.

Filters were generated for each element at each of 12 altitudes by calculating the summed perceived concentration from an array of surface elements.

The array was a square block of N x N cells centered beneath the point of observation. Each cell was 50' square, and defined as having unit concentration of the radio-element concerned. Beginning with N=1 (X=Y=0, Z=Altitude), then continuing with larger squares (N=2,3,4 ... etc.) the contribution of each square was calculated and the total contribution accumulated. The process terminated when a value of N was reached whose added contribution was less than 1% of the previously accumulated total.

For an altitude of 100' the terminal value of N was 25. For 1200' the terminal value was 95.

The individual contribution of all cells in the final square was retained and these values became the filter weights by normalizing their sum to unity. The

value of weight at a point offset by I & J from the central weight is given by:

$$W(I,J)=Fun2(I,J)/SFun(N) \qquad (3)$$

Where:

Fun2=the perceived concentration function for a single surface element

SFun=the sum of Fun2 for I=-N/2 to +N/2; J=-N/2 to +N/2

GENERATION OF PROFILES

The standard line along which the profiles were to be generated was specified by the latitudes and longitudes of its end points. The coordinates of these end points in the reference frame of the interpolated grid were calculated.

The coordinates of 41 points equispaced along the line and including the end points were then calculated. These were the points at which the filters were to be applied.

Except by random chance, a line point would not fall on a grid point, therefore, the center point for each successive filter application was taken as the grid point closest to the line point. The maximum error of placement of a filter was then 25' on the ground. This is considered tolerable as; i) the same set of points was used for all 36 profiles; ii) the areal extent of the filters varied from 600' square (100' altitude) to 4700' square (1200' altitude); and, iii) the precision of the spatial data provided (0.0001 degrees lat/lon) is only within $\pm$18'.

The filters were applied to the interpolated radio-element concentration grids to generate the profiles. The perceived concentration at each point on which the filter is centered is given by:

$$PC(IG,JG)=SUM(IG-I,JG-J)) \quad \begin{matrix} I=-N/2 \text{ to } +N/2 \\ J=-N/2 \text{ to } +N/2 \end{matrix} \qquad (4)$$

Where:

PC(IG,JG)=Perceived concentraton at grid point IG,JG
G=The matrix of grid values.
W=The matrix of filter weights.
N=The size of the filter (N is always an odd number)

The profile data was plotted as presented.

REFERENCE:
Kosanke K. L., Koch C. D.
"An aerial radiometric data modelling program."
IEEE Transactions on Nuclear Science, Vol.NS-25, No.1, Feb. 1978

CALIBRATION FACTORS

Line	Number of Samples: Overall	Number of Samples: N Values Used (K,U,T,)	Average Count Rates (Stripped Counts Per Second): K	U	T
10	401	230	454.92	70.59	119.34
130	397	280	328.05	75.76	114.97
131	494	330	341.87	71.87	122.21
132	472	290	371.87	71.72	127.73
133	387	210	364.32	71.56	123.86
134	402	220	359.90	68.77	127.64
135	414	270	364.53	72.34	124.19
136	439	270	386.24	71.87	124.47
137	398	230	409.67	65.83	120.73
138	389	230	386.58	67.93	120.36
139	427	250	431.02	65.64	119.48
141	396	250	430.62	71.52	113.77
142	379	260	426.84	67.91	115.65
143	442	310	428.39	81.27	113.14
144	425	300	420.15	84.12	115.45
145	418	280	395.88	86.19	112.89
146	491	360	365.04	90.88	107.88
147	487	370	362.51	88.09	106.84
148	559	450	337.79	88.12	106.99
149	514	390	362.36	87.04	108.73
150	521	420	351.69	94.52	104.63

Overall Average Count Rates: K = 380.86, U = 78.54, T = 115.53

Total N Values Used (K,U,T) = 6200

Average Concentrations From Geochem Data: %K = 2.51, ppmU = 2.98
ppmT = 12.14

Calibration Ratios: cps/K% = 151.738, cps/ppmU = 26.355
cps/ ppmT = 9.516

AVERAGE PROFILE CONCENTRATIONS

Altitude in Feet	%K	ppm U	ppmTh
100	3.191	2.801	12.805
200	3.142	2.818	12.844
300	3.093	2.842	12.863
400	3.050	2.865	12.881
500	3.013	2.886	12.898
600	2.979	2.906	12.915
700	2.948	2.925	12.928
800	2.919	2.942	12.939
900	2.896	2.955	12.944
1000	2.869	2.965	12.939
1100	2.847	2.972	12.927
1200	2.823	2.974	12.903

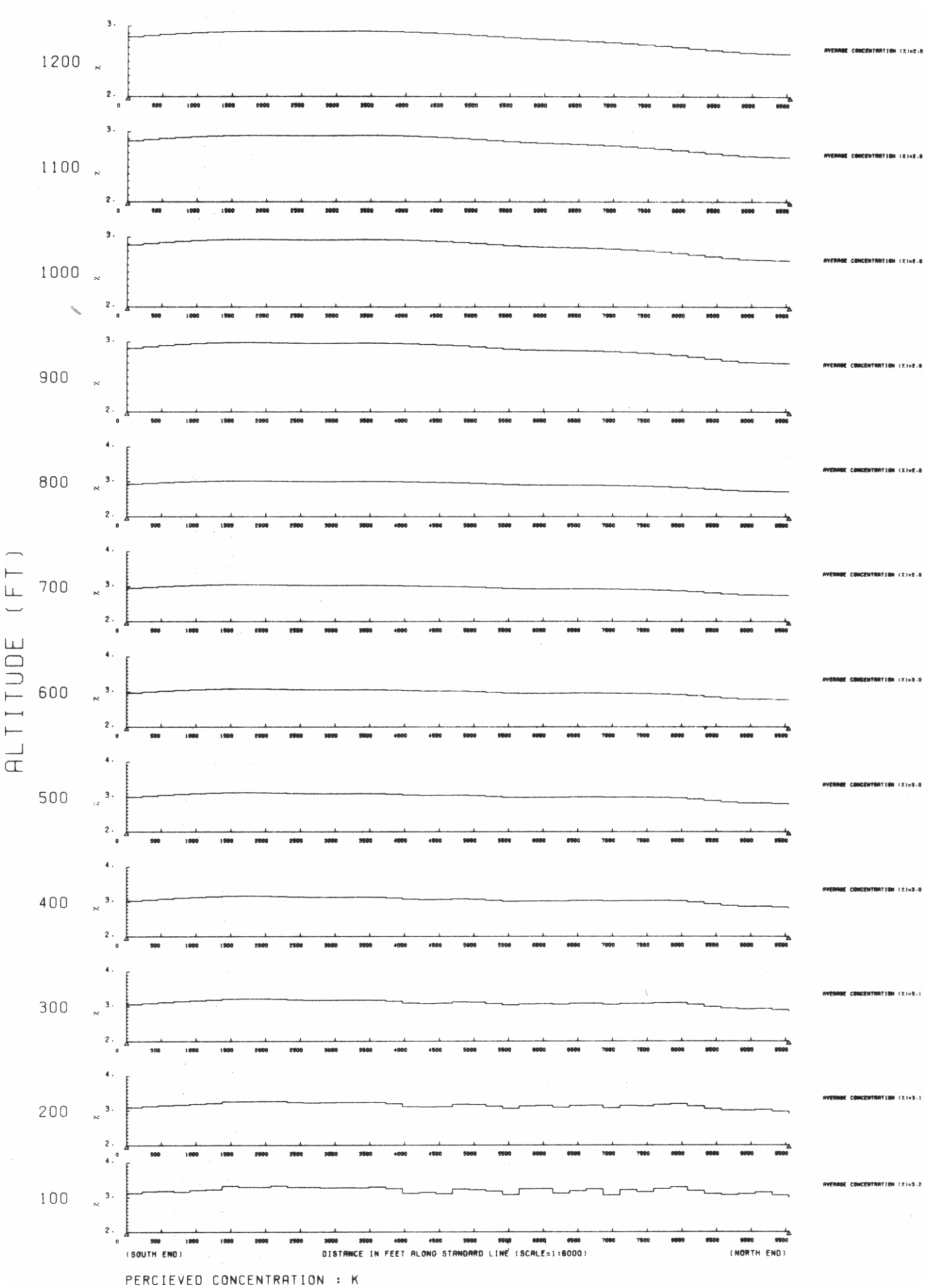
ALTITUDE (FT)
1200
1100
1000
900
800
700
600
500
400
300
200
100
(SOUTH END)
DISTANCE IN FEET ALONG STANDARD LINE (SCALE=1:6000)
(NORTH END)
PERCIEVED CONCENTRATION : K

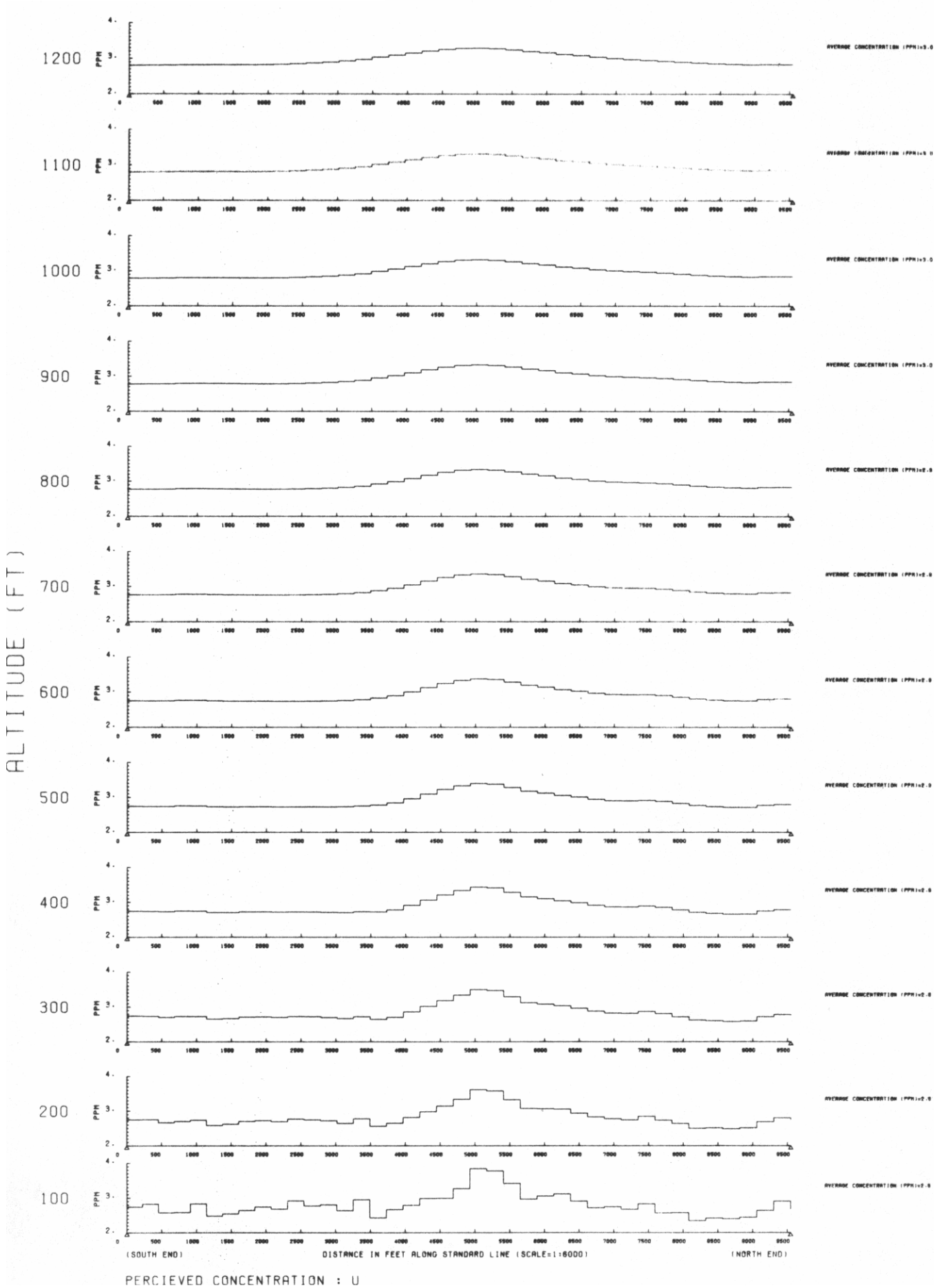

PERCIEVED CONCENTRATION : U

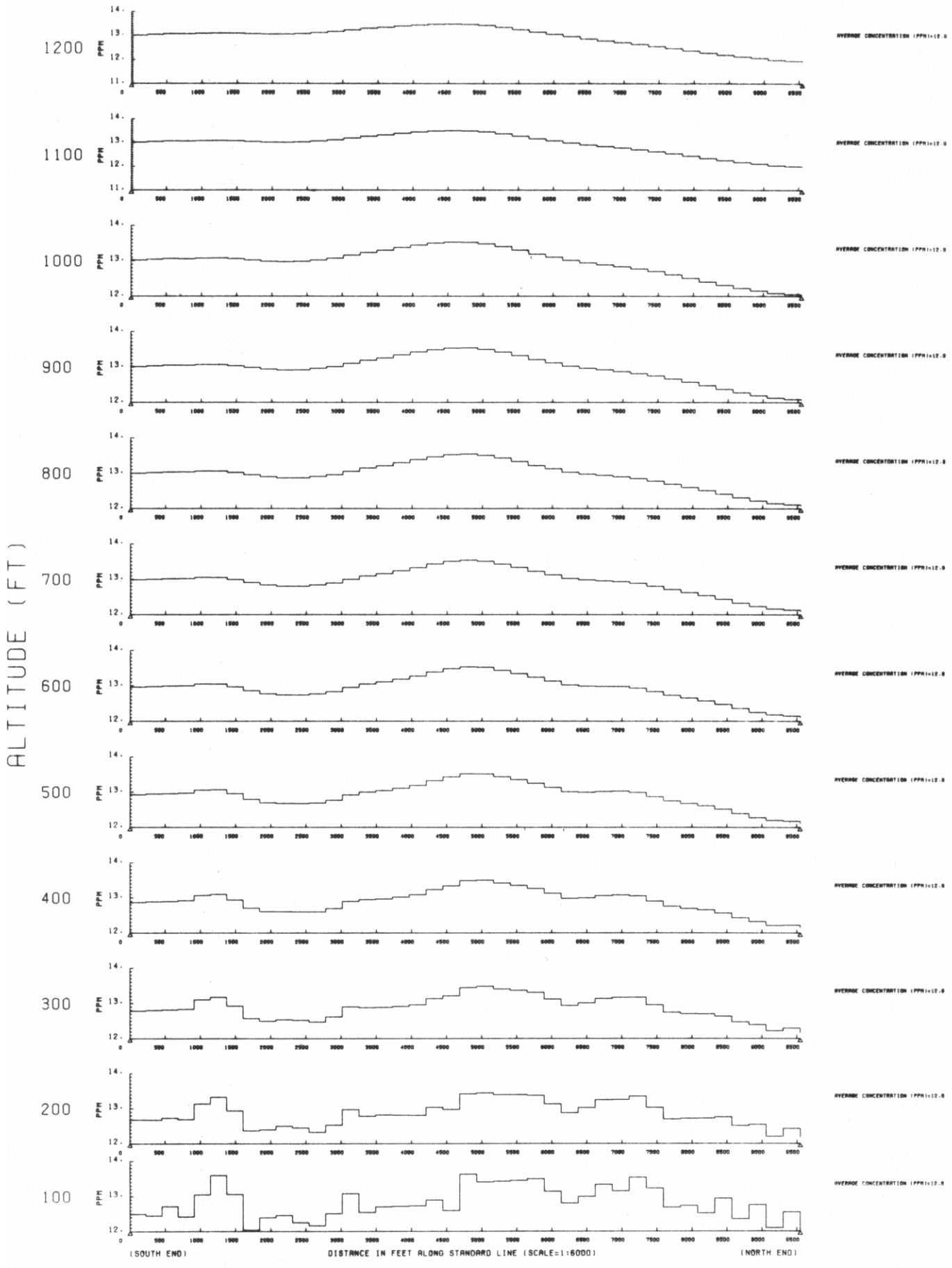

PERCIEVED CONCENTRATION : T

APPENDIX 7

10.8 AERIAL SURVEY

10.8.1 AIRBORNE SYSTEM

AERIAL SURVEY

GENERAL

The aerial radiometric and magnetic survey of the test range was conducted during the period from February 25 to February 28, 1979. The survey consisted of 22 traverses and 5 tie lines. Traverse lines were flown at 250 foot intervals at a azimuth of 128° from north. Flight altitude was 100 feet and the average airspeed was 60 MPH.

The radiometric and magnetic data are presented in the form of contour maps and stacked profiles. A line index of the area surveyed is presented in Figure 1.

THE AIRBORNE SYSTEM

ROTARY-WING AIRCRAFT

A Silkorsky S58T Twin Turbine helicopter (N870W) was utilized as survey platform for the airborne radiometric survey. (see Figure 2)

All equipment was located within the cabin of the aircraft with the exception of the magnetometer which was rigidly mounted to the exterior. (see Figure 3)

INSTRUMENTATION

The primary system components include the following: (see Figure 4)

(1) Terrestrial Gamma-Ray Sensor
(2) Atmospheric Gamma-Ray Sensor
(3) Magnetometer
(4) Barometric Pressure Altimeter
(5) Radar Altimeter
(6) Temperature Sensor
(7) Data Acquisition System
(8) Recording System
(9) 35 mm Tracking Camera

Terrestrial Sensor

This sub-system consists of two identical Scintrex GSA-77 Sensors, each containing seven crystals measuring 7 inches in diameter X 4' inches thick. The seven NaI (Tl) crystals in each sensor are arranged with six crystals mounted in a circle around one in the center. Each sensor incorporates an ultrastable high voltage supply, seven preamplifiers, a temperature control unit and a detector signal mixing circuit.

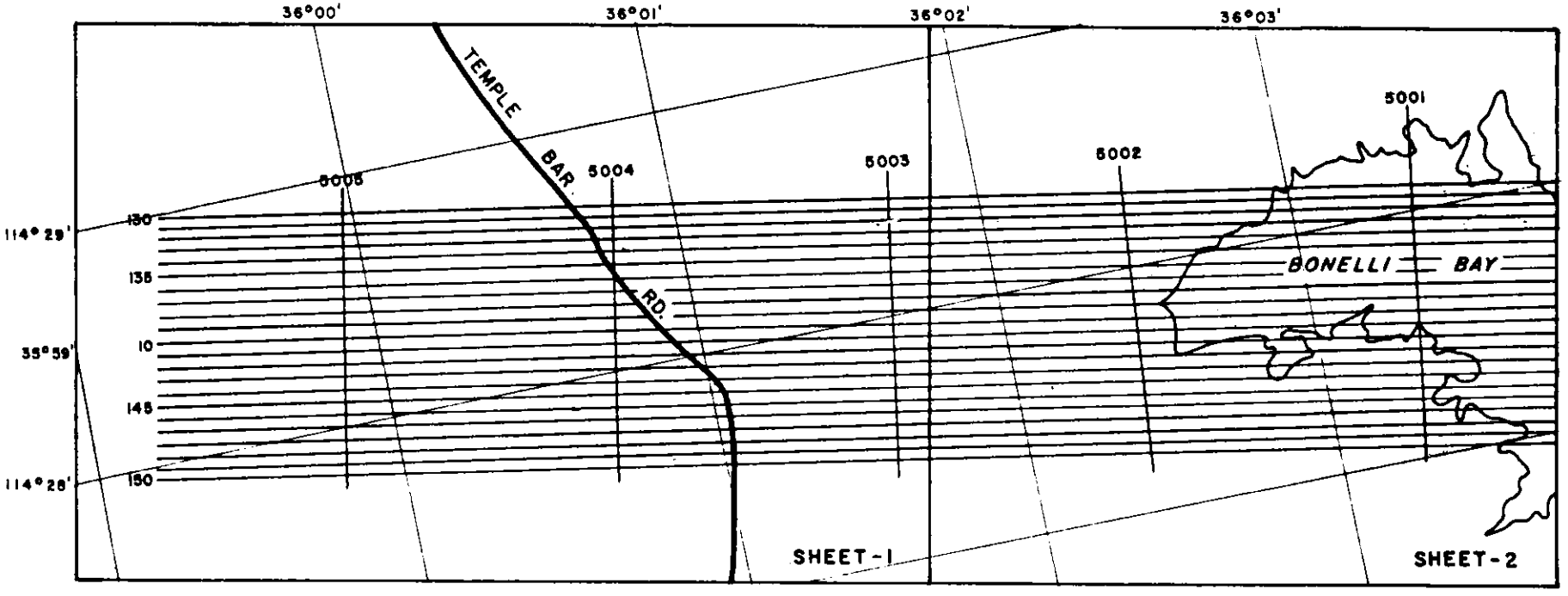

FIGURE 1 — AERIAL SURVEY LINE INDEX

The detectors are housed in an appropriately insulated container. A heating element inside each container provides temperature stabilization to maintain detector balance. A temperature range control offers six switch-selectable temperature settings, and a temperature meter permits continued monitoring. A temperature setting of 27.5 ^{o}C was maintained for most of the survey.

The central detector in each sensor contains a light emitting diode which allows the injection of a stabilization pulse which can be monitored and stabilized at any location on the pulse height spectrum. Although two such stabilization sources are available (one in each sensor) only one is used at any given time. A location above 6 MeV is used for this LED pulse.

Each of the two sensors provides a sensitive volume of 1077 inches^3 and weighs 350 lbs. These sensors draw power from the 28V helicopter system when in flight. When not flying, the sensor heaters are plugged into an external 115V power source through a 28V D.C. converter to maintain temperature control.

Atmospheric Sensor

This sub-system is mounted directly over a lead slab measuring 12 inches X 12 inches X 3 inches such that its field of view is limited to a solid angle of approximately 2π in the upward direction.

The detector consists of one 9 inch diameter X 5 inch thick NaI (Tl) crystal having a total sensitive volume of 318 inches^3, and containing a light emitting diode system to provide a stabilization pulse. The weight of the atmospheric detector, including the lead shield is approximately 300 lbs.

Magnetometer

A modified ASQ-10 fluxgate magnetometer was employed in this system, with the observed magnetic field measurements obtained in units of 0.1 gamma.

Barometric Altitude Transducer

The barometric pressure instrumentation consists of an elastic pressure sensing element acting as a prime mover for positioning an electro-mechanical transducer.

Radar Altimeter

A Minneapolis Honeywell altimeter is used to measure helicopter to ground distance. The antennae are mounted on the underside of the

helicopter. Altitude measurements are recorded to 1.0 foot. The recording range is 0-5,000 feet with an accuracy of ± 5 feet + 3% at actual altitude.

Temperature Sensor

A platinum resistance thermometer was utilized to record outside air temperature with an accuracy of 0.01 ^{o}C.

Data Acquisition System

Signals from the terrestrial and atmospheric sensors are amplified, digitized and stored in the digital processor contained in the 1024 channel pulse height analyzer. Each sensor calibration is such that a 400 channel block contains gamma-ray intensity information for the energies 0-3 MeV and 3-6 MeV. The last 112 channels in each block are reserved for storing the stabilization pulses for the individual LED's. Two independent digital stabilizers are latched onto their appropriate LED pulse to achieve stability of the entire gamma-ray energy calibration. An oscilliscope display is available to monitor the accumulation of gamma-ray pulses during each acquisition period.

Data from the magnetometer, temperature probe, barometric altimeter, radar altimeter, clock and the preset data is fed through an A/D converter into the 1024 channel digital processor.

Recording System

The collected data is fed through a magnetic tape control to the tape unit. The data is recorded in 7 track BCD code at 556 BPI density. After each readout cycle, the system is automatically reset and a new data acquisition cycle is begun.

A permanent record of the following information is obtained for each acquisition cycle.

1. Acquisition Identification
   Four sets of six digit presettable data for
   a. Julian Day
   b. Line Number
   c. Reference number (Job No.)
   d. Azimuth (flight direction)
2. Record number - (Sequential Record Count)
3. Time of day (correlates with camera fiducials)
4. Temperature
5. Barometric Altitude
6. Radar Altitude
7. Scan Time (presettable - 2.0 seconds for this project)
8. Observed aeromagnetic reading
9. Live time in milliseconds for both terrestrial and atmospheric sensors
10. Full gamma-ray spectrum for each sensor package

SYSTEM CALIBRATION AND NORMALIZATION

The airborne gamma-ray system used for the aerial survey of the test range was calibrated and normalized in accordance with BFEC Specification 1250A (General Procedure and Documentation for Normalization and Calibration of Airborne Gamma-Ray Systems). The data for the calibration and normalization was collected on the following dates: Walker Field Calibration Pads, November 8, 1978; Lake Mead Dynamic Test Range, February 24, 26, 27, 1979; High Altitude Flights, February 22, 1979. On April 4, 1979, LKB Resources, Inc. submitted its Calibration and Normalization Reports to BFEC. On May 18, 1979, BFEC issued a Performance Evaluation of the Airborne Gamma-Ray System used in the survey. That report is referenced as Calibration Report Number 027.

FIG.-2 S-58T HELICOPTER

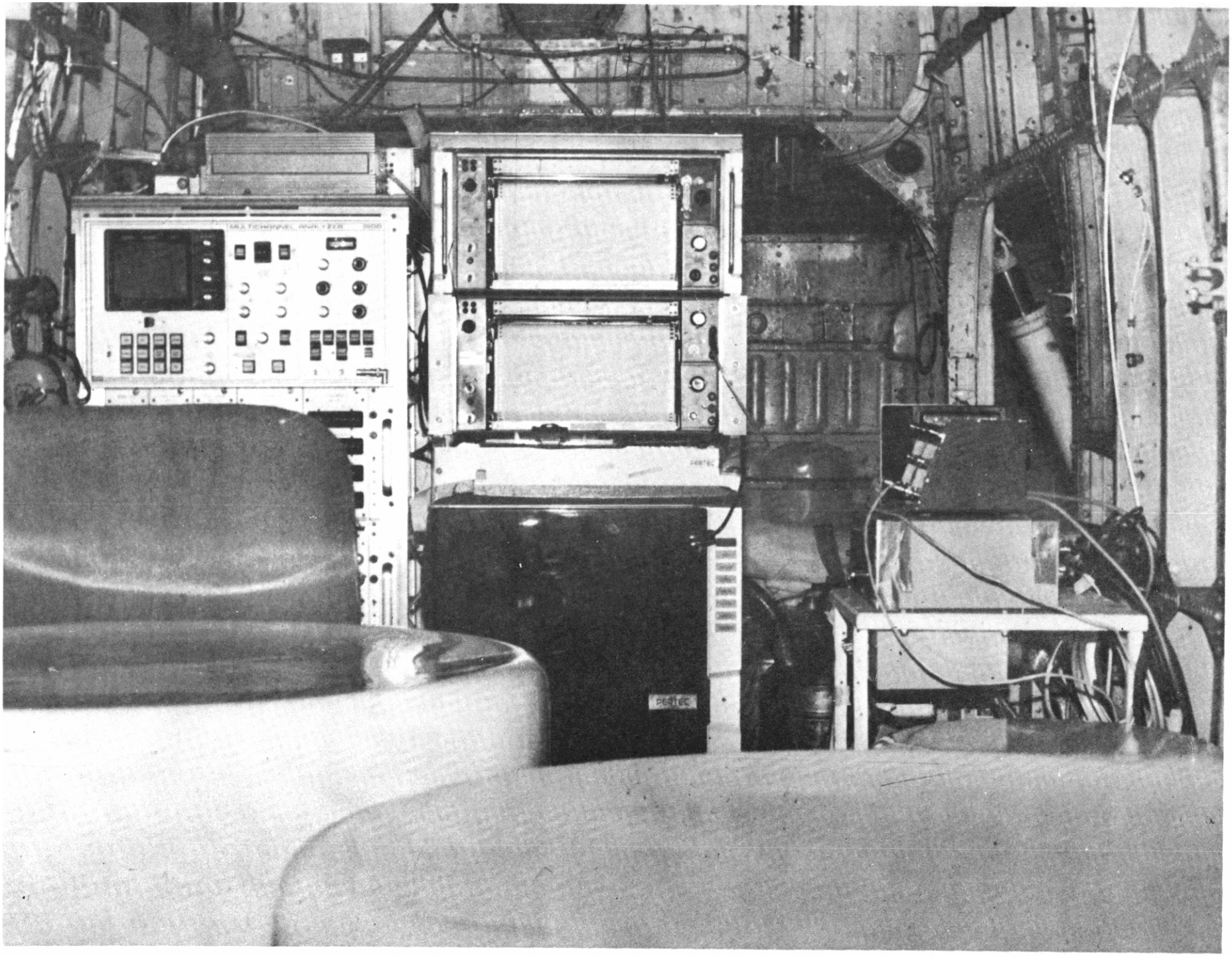

FIG.-3 S-58T HELICOPTER (CABIN LAYOUT)

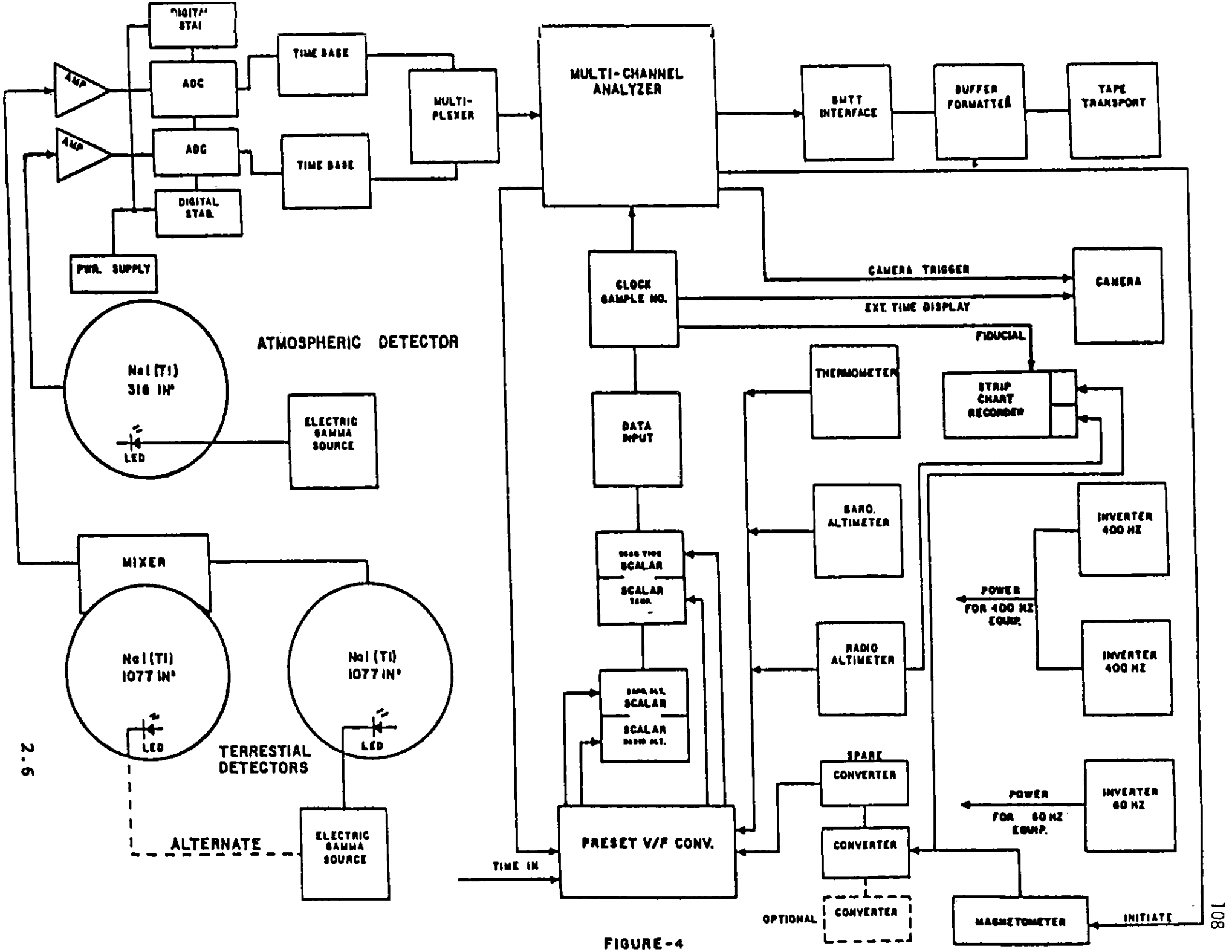

FIGURE-4
SYSTEM BLOCK DIAGRAM

10.8.2 DATA REDUCTION METHODS

DATA REDUCTION

GENERAL

Figure 5 outlines the processing sequence followed to locate, identify and reduce the gamma-ray survey data. The following sections describe the main data reduction steps consisting of the following principal operations:

(1) Path recovery and geologic correlation
(2) Digital data edit
(3) Radiometric corrections
(4) Magnetics adjustment
(5) Statistical analysis

PATH RECOVERY

The aircraft track was established by manual identification and correlation of the 35mm tracking camera imagery with a 1:6000 scale photo mosaic of the test range. The film images were identified and the UTM X, Y coordinates scaled from a super-imposed grid.

The coordinate data was edited by plotting the recovered path from the scaled X, Y coordinates. This was accomplished via the card edit plot program. The plotted path was inspected, any erratic variations were checked and if found in error, corrected and replotted.

The edited positional data was then transferred to the geologic map sheets from which the geologic rock units were read and correlated with the digital data by means of the common fiducial number.

DIGITAL DATA EDIT

The airborne data tapes are processed by the edit program which decodes and translates the recorded data. The multi-channel spectra for both atmospheric and terrestrial gamma-ray sensors are summed over the entire time interval required to traverse the surveyed line. The resulting spectrum is smooth enough to fit a least squares polynominal to the potassium and thorium photopeaks so as to accurately locate the channels corresponding to the peak centroids. The energy per channel is determined and the channel limits corresponding to the primary energy band are computed.

K = 1.365 - 1.575 MeV
U = 1.650 - 1.860 MeV
T = 2.400 - 2.805 MeV

The computation of the photopeak limits effectively compensates for any spectrum drift.

The counts/channel within each photopeak are summed, as are the total count (.4 - 3.0 MeV) and the cosmic counts (3.0 - 6.0 MeV). The summed counts are all normalized to counts per second by dividing each sum by the recorded net live time.

The ancilliary data (barometric, radar, temperature and magnetometer) are all converted to appropriate units and tested for validity. The standard deviation of the median values of the first and second differences and of the absolute values are computed for groups of 56 samples. All samples within a given group for which three or more data words deviate more than six times the standard deviation of the appropriate median are flagged as being of suspect data quality. The suspect data words are replaced by linearly interpolated values.

Program outputs consist of a raw spectral data file and a single record data file containing the summed, normalized raw spectral data. In addition, a comprehensive edit listing is generated which is reviewed for possible additional edit corrections and further provides a detailed list of the magnetic field data which is utilized for the determination of the magnetic level corrections.

RADIOMETRIC CORRECTIONS

The reformatted data, having been summed and normalized to counts per second, was further processed to remove the effects of aircraft background, cosmic radiation and atmospheric bismuth. In addition, the Compton scattering of the higher energy levels into the lower spectral windows was corrected using the spectral stripping method. The net reduced count was then tested for statistical adequacy and normalized to 100 feet altitude at standard temperature and pressure.

Background Corrections

The effects of aircraft background and cosmic radiation was removed by computing their contribution to each of the primary energy windows, from empirically derived correction parameters.

The parameters, defining the contribution of these non-terrestrial radiation sources to the airborne gamma-ray measurements were determined from data obtained from high altitude overwater flights.

To derive the cosmic and aircraft background correction parameters several assumptions must be made:

(1) The background radiation, emanating from onboard sources, is a constant.

(2) Atmospheric and terrestrial radiation are effectively eliminated by flying at high altitudes over deep bodies of water.

(3) The observed count rate varies linearly with respect to the cosmic count as measured by summing over the energy band from 3.0 to 6.0 MeV.

Using these assumptions, the spectrums obtained are considered to be composed of only two components, cosmic radiation and aircraft background.

The count rate for any given window may then be expressed by the following equation:

(1) $C_{ij}=B_i + R_i \, Cos_j$

where:

i, j are the subscripts identifying the window and observation respectively.

C_{ij} is the mean count for window i, ovservation j

B_i is the background constant corresponding to window i.

R_i is the cosmic ratio corresponding to window i

Cos_j is the summed cosmic count corresponding to observation j.

A system of observation equations was formed for each of the principal windows and solved simultaneously for the most probable values of the cosmic and background correction parameters.

Compton Scatter Corrections

The effects of the Compton scattering of the higher energy radiation into the lower energy bands of interest were removed by computing the scattered radiation count utilizing the following correction equations.

(1) $Tc = To - bUc$

(2) $U_C = U_O - Tc\alpha o - Tc\alpha_1 H$

(3) $K_C = K_O - T_C \, B_O - Uc\beta$

where:

U_C = Corrected uranium count

U_O = Uranium count corrected for aircraft background and cosmic radiation

T_O = Thorium count corrected for aircraft background and cosmic radiation

T_c = Thorium count corrected for aircraft background, cosmic radiation and scattered uranium at 2.43 MeV appearing in the thorium window

K_o = Potassium count carrected for aircraft background and cosmic radiation

K_c = Corrected potassium count

b = Fraction of uranium counts appearing in the thorium window (R. L. Grasty - A Calibration Procedure for an Airborne Gamma-ray Spectrometer)

α_o = Stripping ratio (uranium counts per thorium count at zero altitude)

α_1 = Rate of change of the uranium stripping ratio with altitude H

B_o = Stripping ratio (potassium counts per thorium count at zero altitude)

γ = Stripping ratio (potassium counts per uranium count)

The stripping ratios α_o, B_o, γ_o and b were determined from data obtained at the Walker Field test pads. The five test pads, each having known concentrations of K, U, T, provided the necessary redundant data for the solution of the stripping ratios $_o$, B_o, γ and the system sensitivities K1, K2, K3. The several equations relating the count rates with their corresponding concentrations are as follows:

(4) $T = K_1 \times Tppm + Uc \times b$

(5) $U = K_2 \times Uppm + Tc \times \alpha_o$

(6) $K = K_3 \times K_{pct} + Tc\ B_o + Uc\ \gamma_o$

where:

T, U, K = Observed counts corrected for the local background as measured at Matrix Pad No. 1.

Tppm, Uppm, Kpct = Concentration values after subtracting the Matrix Pad concentration values.

α_o, B_o, γ_o, b = Unknown stripping ratios
K_1, K_2, K_3 = Unknown sensitivities

Atmospheric Bismuth Correction

The atmospheric detector data was sampled at the same time interval as the terrestrial detector data, 1.0 seconds per scan. However, the relative precision of the atmospheric data is significantly less than the terrestrial data. This results from the fact that the volume of the atmospheric detector is approximately one seventh that of the terrestrial system.

Since the precision index varies directly as the square root of the number of observations, the atmospheric precision was increased by averaging over a 49 sample period. This period provides a seven fold increase in the precision of the atmospheric data which approaches the precision of the terrestrial sensor.

The averaged atmospheric data was then corrected for aircraft background, cosmic radiation and Compton scatter effects resulting from possible thorium shine-around, scattering into the atmospheric uranium window. Additionally, correction was made for terrestrial uranium shine-around which was considered to vary exponentially with altitude.

The actual calculations are defined by the following expression:

$$Bi\ AIR = (AUC - TUC \times Sh)/ (R - Sh)$$

where:

AUC = Atmospheric uranium count corrected for cosmic radiation, aircraft background and Compton scattering of thorium into the uranium window.

TUC = Terrestrial uranium count corrected for cosmic radiation, aircraft background, Compton scattering of thorium into the uranium window and corrected for atmospheric bismuth.

SH = Exponential shine-around equation

$$Sh = .037 \times EXP\ (-uH)$$

and u is the empirically derived exponential coefficient.

R = Response ratio equating the atmospheric and terrestrial counts.

$$R = 1./(5.0495 + .00196*H)$$

Statistical Adequacy Test

The reduced single record count rates, (K, U, T) derived as described in the preceding sections, were tested to determine the significance of the net count rate values.

In this case significance is measured in terms of whether the net count exceeds some specified multiple of the computed standard deviation of the net count. From the paper presented by Currie (Analystical Chemistry 1968), the standard deviation of the net count may be expressed as:

$$\text{NET} = 1.41\ (B)^{\frac{1}{2}}$$

where B is the total background which in the context of this discussion is considered to be the sum of the corrections applied to the observed count.

The confidence level, suggested by Currie and commonly adopted as a standard statistical measure, is .95 or 95%. The standard normal variable (multiple of standard deviation) corresponding to the 95% to evaluate the single record data is therefore:

$$2.33\ (\text{obs. count} - \text{net count})^{\frac{1}{2}}$$

In summation, if the net count is less than 2.33 times the square root of the total applied correction (background) the sample is considered statistically inadequate and is flagged. The net counts are normalized to 100 feet and the ratios, U/K, U/T and T/K, are computed for all single record samples. The single record data are presented in the form of microfiche copies of the computer listings.

4.4.5 Altitude Normalization

The intensity of gamma radiation is considered to decrease exponentially with increasing distance from the source. This decrease in intensity may be defined as follows:

$$(1)\quad C_h = S \exp\ (-u_h\ h)$$

where:

C_h = the reduced count rate measured at height h above the source.

S = Source concentration expressed in counts/second.

u_h = The total attenuation coefficient compensated for air density as derived from the observed temperature and pressure.

The count rate observed at 100 feet above the source, at standard temperature of 0°C and standard pressure of 1013 milibars, is also expressed exponentially.

$$(2) \quad C_{100} = S \exp^{(-u_o\, 100)}$$

where:

u_o = the total attenuation coefficient at standard temperature and pressure.

Equating equations 1 and 2.

$$(3) \quad C_{100} = C_h \exp^{(-u_o\, 100)} / \exp^{(-u_h\, h)}$$

and since $\exp^{(-u_o\, 100)}$ is a constant = K

$$(4) \quad C_{100} = K\, C_h / \exp^{(-u_h\, h)}$$

Record Averaging

The single record data was averaged over successive groups of five samples each. The averaging interval is determined by the following criteria.

(1) The interval over which the data is averaged must be less than 1200 feet.

(2) Ninety percent of the averaged uranium data must pass the statistical adequacy test.

$$2.33\ (\text{average correction}/N)^{\frac{1}{2}}$$

The average correction is determined from the reduced count prior to normalization to 100 feet. Single records failing the statistical adequacy test are included when calculating the averaged record sample; the only restriction imposed is that the single record data be within the altitude limits of 50 to 1000 feet.

The averaged data values failing the test are flagged and excluded from all further analysis.

STATISTICAL ANALYSIS

The purpose of this phase of the data processing sequence is to identify potentially anomalous averaged record data. This is accomplished by the statistical evaluation of the averaged record data which is predicated on the assumption that the averaged count is normally distributed about the mean count of the geologic unit to which the record belongs.

This assumption is valid for all large samples consisting of 30 or more records. Statistics relating to samples consisting of fewer than 30 records are at best suspect.

All averaged data records corresponding to the same geologic unit are grouped and processed as a single statistical sample.

The pertinent statistics defining a given sample are the mean and standard deviation. These statistics are computed for each data parameter (K, U, T, U/T, T/K, T/K) utilizing only those data values determined to be statistically adequate.

Each averaged record data parameter was evaluated, relative to its sample mean and standard deviation, by computing the standard normal variable Z.

$$Z_k = (X_k - M_k)/Sigma_k$$

where K = subscript identifying data parameter

X_k = Averaged record value

M_k = Mean value of parameter K

Sigma K = Standard deviation of parameter K

Z_k = Standard normal variable of averaged record parameter K

The standard normal variable is considered to have a normal distribution with a mean of zero and standard deviation of ±1. Values of the standard normal variable greater than ±1 are considered potentially anomalous.

Although the departure of the averaged record count from the mean of its corresponding geologic unit may be classified as potentially anomalous, it remains for the geologic interpreter to evaluate each anomaly so as to eliminate those which are obviously caused by climatic or topographic conditions. (Histograms of each geologic unit and a summary of the pertinent statistics are presented in Appendix 9).

MAGNETIC DATA PROCESSING

The recorded magnetic total field is edited simultaneously with the gamma-ray data. The edit listing generated by the digital edit program together with the identified film intersections are the basic information required to adjust the magnetics network.

Initially a tie-line is selected as a datum to which all intersecting traverses are adjusted. All other tie-line and traverse line intersection values are evaluated in terms of the magnitude and linearity of the level corrections required to adjust each traverse line to agree with the corresponding tie-line value.

Excessively large non-linear corrections generally indicate erroneous positional information. In practice slight positional adjustments are usually applied so as to insure the required level corrections approach linearity.

The last step in the adjustment processes was the calculation and removal of the earth's regional magnetic field component. This was computed using the 1975 IGRF Model updated to 1979.

DATA PROCESSING FLOW CHART

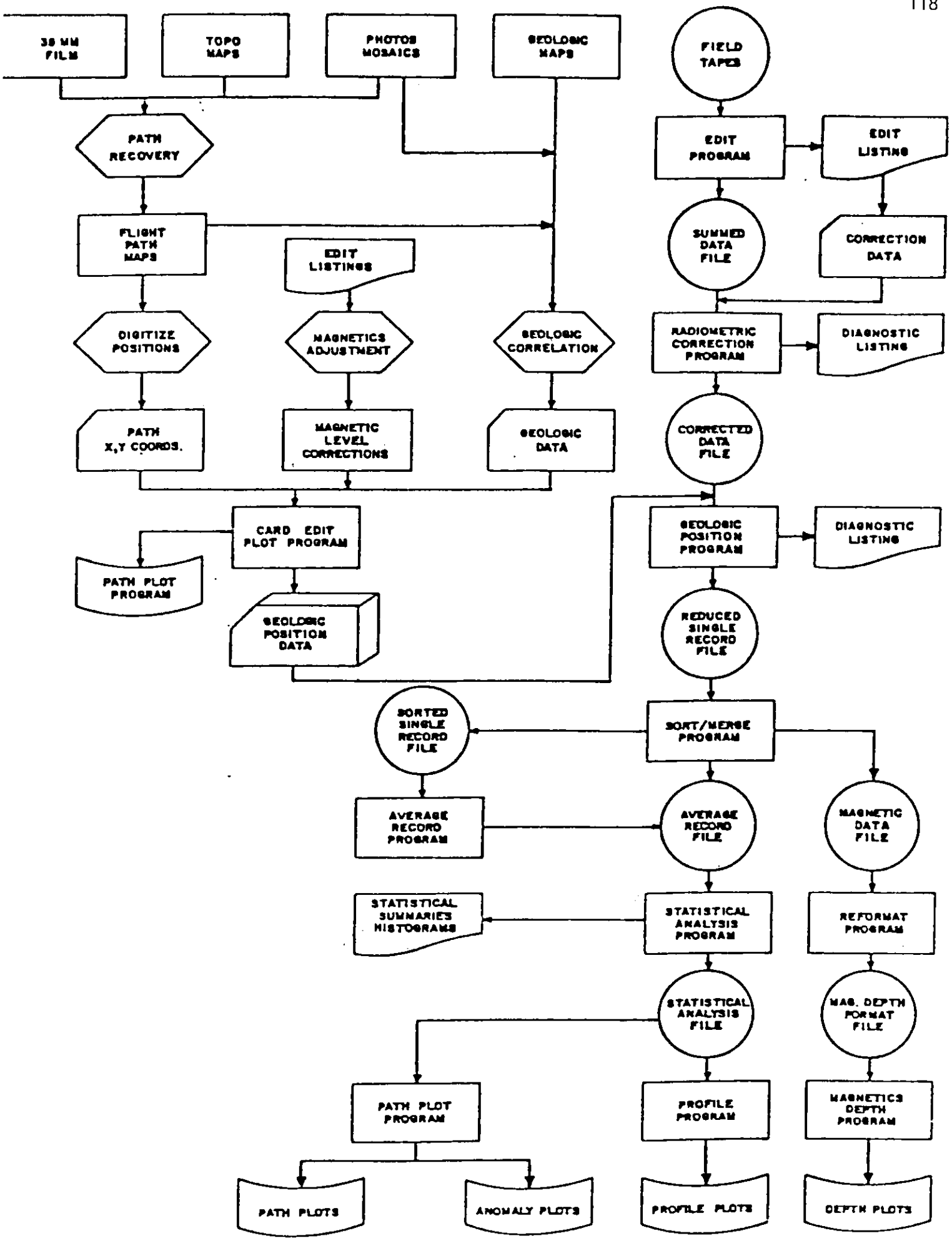

FIGURE - 5

GRAPHIC DATA PRESENTATION

The graphic data, produced at a scale of 1:6000, consists of the following specific items:

(1) Radiometric Multiple-Parameter Stacked Profiles

(2) Magnetic Multiple Parameter Stacked Profiles

(3) Magnetic, Radiometric Contour Maps

(4) Count Rate Histograms

(5) Single Record Data Listings

(6) Averaged Record Data Listings

RADIOMETRIC MULTIPLE-PARAMETER STACKED PROFILES

The profiles of the averaged record data contain the following information:

Flight Line Number
Appropriate Title Information
Fiducial Numbers
Residual Magnetic Profile
Radar Altimeter
Corrected Total Count in CPS
Atmospheric Bismuth (Bi Air) Correction in CPS
Corrected U in CPS
Corrected T in CPS
Corrected K in CPS
Ratio U/K
Ratio U/T
Ratio T/K
Geologic Strip Map with Flight Path

Flags appearing under the K, U, and T traces indicate that the computed average record value for the corresponding element has failed the calculated statistical adequacy test. Flags appearing under the altitude trace indicate the averaged record has exceeded the altitude limits.

MAGNETIC MULTIPLE-PARAMETER STACKED PROFILES

The magnetic data profiles were generated from the single record data file and contain the following information:

Flight Line Number
Appropriate Title Information
Fiducial Numbers
Barometric Altitude in Feet
Temperature in Degrees Centigrade
Radar Altimeter in Feet
Ground Station Magnetic Data
Residual Magnetic Profile in Gammas
Geologic Map Strip with Flight Path

Samples obtained at terrain clearance less than exceeding the altitude limits are identified by a plotted symbol appearing at the bottom of the radar altimeter trace.

HISTOGRAMS

The histograms of the count rate distribution of Uranium, Uranium/Thorium, Uranium/Potassium, Thorium, Potassium and Thorium/Potassium for each lithologic unit were computed and printer plots generated. Additional information presented are the mean, standard deviation and number of records contained in each distribution plot. (see section 10.8.3)

DATA LISTINGS

The data listings of the reduced data are produced on microfiche and included in this report. Each printer page is identified by a header label specifying survey company, survey area, year survey was flown and line number.

Single Record Reduced Data Listings

The following elements are listed for each record:

HEADING	DESCRIPTION
REC	Fiducial Number (time in seconds past midnight)
AF	Altitude Flag
KF	Potassium Flag (Failed statistical adequacy test)
UF	Uranium Flag (Failed statistical adequacy test)
TF	Thorium Flag (Failed statistical adequacy test)
UNIT	Geologic Unit Code
LAT	Latitude in decimal degrees
LONG	Longitude in decimal degrees
TEMP	Temperature in Degrees Centigrade
BARM	Barometric Pressure Height in Feet
RADR	Radar Terrain Clearance in Feet
MAG	Total Magnetic Field in Gammas

HEADING	DESCRIPTION
GROSS	Total Count (.4 to 3.0 MeV) in Counts/Second
K	Potassium Counts/Second
U	Uranium Counts/Second
T	Thorium Counts/Second
U/K	Ratio Uranium/Potassium
U/T	Ratio Uranium/Thorium
T/K	Ratio Thorium/Potassium
COS	Cosmic Count (3 to 6 MeV) in Counts/Second
Bi	Atmospheric Bismuth Correction in Counts/Second

Averaged Record Data Listings

The following elements are listed for each averaged record:

HEADING	DESCRIPTION
REC	Fiducial Number of Central Records (time in seconds past midnight)
AF	Altitude Flag
KF	Potassium Flag (Failed statistical adequacy test)
UF	Uranium Flag (Failed statistical adequacy test)
TF	Thorium Flag (Failed statistical adequacy test)
UNIT	Geologic Unit Code
LAT	Latitude in decimal degrees
LONG	Longitude in decimal degrees
RADR	Radar Terrain Clearance in feet
MAG	Total Magnetic Field in Gammas
TC	Total Count (.4 to 3.0 MeV) in Counts/Second
K	Potassium Counts/Second
U	Uranium Counts/Second
T	Thorium Counts/Second
U/K	Ratio Uranium/Potassium
U/T	Ratio Uranium/Thorium
T/K	Ratio Thorium/Potassium
COS	Cosmic Counts/Second (3.0 to 6.0 MeV)
Bi	Atmospheric Bismuth Correction in Counts/Second
K	Potassium Standard Deviation units from the mean
U	Uranium Standard Deviation units from the mean
T	Thorium Standard Deviation units from the mean
U/K	Ratio Standard Deviation units from the mean
U/T	Ratio Standard Deviation units from the mean
T/K	Ratio Standard Deviation units from the mean

10.8.2.1 DATA INTERPRETATION

DATA INTERPRETATION

For the three radio-elements (K,U,T) there is a fairly good correlation between concentrations and count rates.

The potassium radiometric map exhibits a linear high running close to due north along the centre of the test range. The geochemical iso-concentration map shows a similar feature broken only by a minor cross-cutting low. This slight discrepancy, however, appears to be due to the interpolation of geochemical data across a region with no samples.

The correlations for uranium and thorium are less readily apparent. Only the larger highs and lesser lows exhibit reasonable correlations. For both cases this appears to be due to the lack of a strong pattern to the radio-element distribution, combined with significant variability in radio-element concentrations between sample sites.

CONCLUSION

The radiometric measurements "average" the concentrations over a significant area (99% of the contribution to the count rates at the detector at an altitude of 100' are calculated as coming from a ground circle of 600' radius.)

Hence, significant variation in radio-element concentration over short distances with no larger scale regional patterns (as apposed to the potassium data which does exhibit well developed local trends) results in a rather bland radiometric map. Geochemical sampling, however, being concerned with very small areas/sample, can result in a highly active map. This fact demonstrates the problems inherent in a contoured presentation of a variable which may be discontinuous, or at best, which may exhibit frequencies of variability greatly in excess of the sampling frequencies.

10.8.3 COUNT RATE HISTOGRAMS

DYNAMIC TEST RANGE
UNIT WATER

POTASSIUM
RECORDS 51

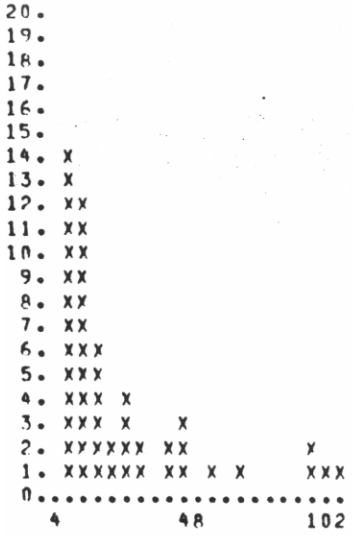

MEAN 25. SIGMA 25.0

URANIUM
RECORDS 46

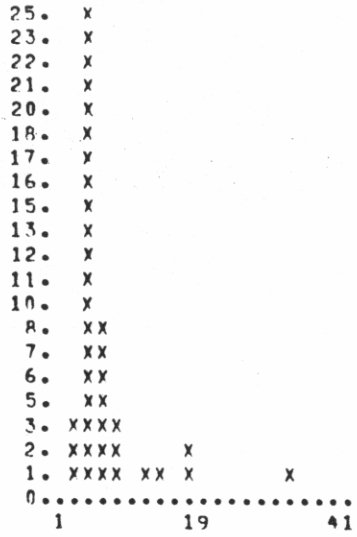

MEAN 8. SIGMA 7.5

THORIUM
RECORDS 34

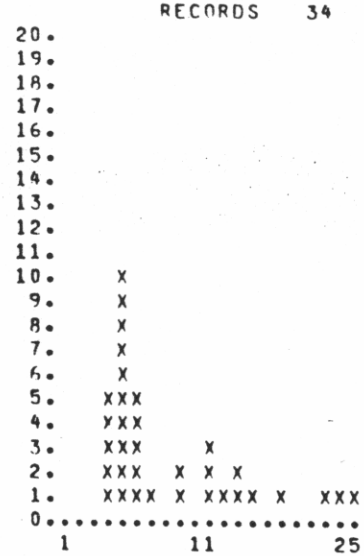

MEAN 10. SIGMA 6.3

U/K RATIO*10
RECORDS 18

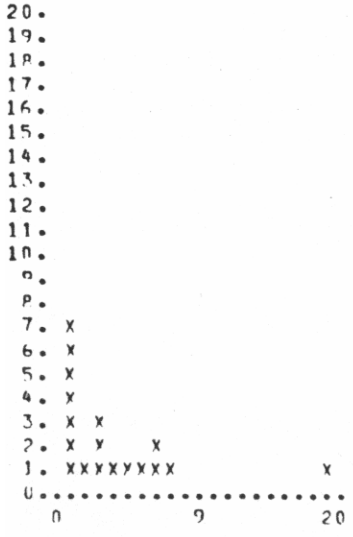

MEAN 4. SIGMA 4.4

U/T RATIO*10
RECORDS 13

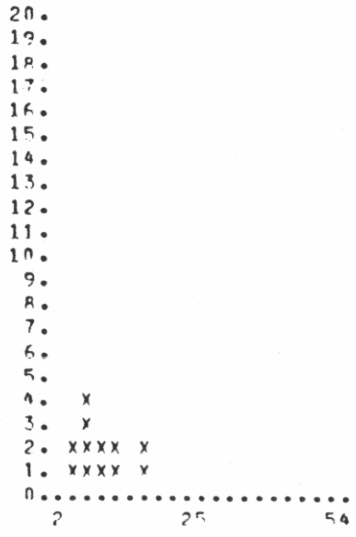

MEAN 12. SIGMA 13.8

T/K RATIO*10
RECORDS 23

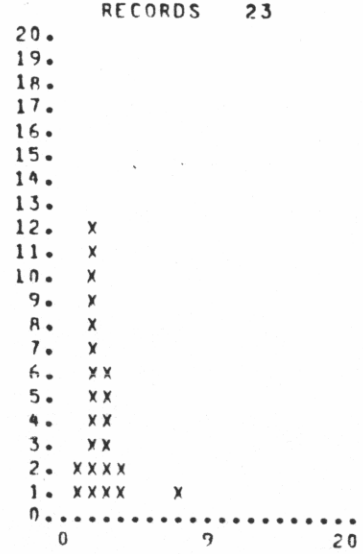

MEAN 3. SIGMA 1.4

DYNAMIC TEST RANGE
UNIT GAL

POTASSIUM
RECORDS 71

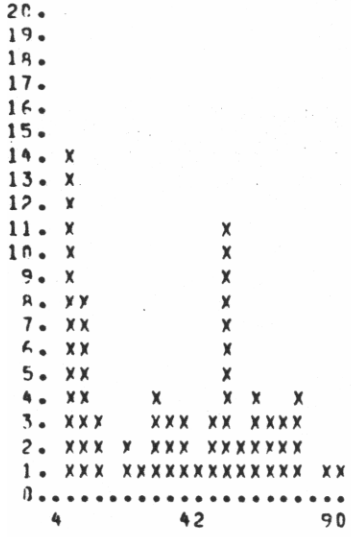

MEAN 39. SIGMA 25.6

URANIUM
RECORDS 110

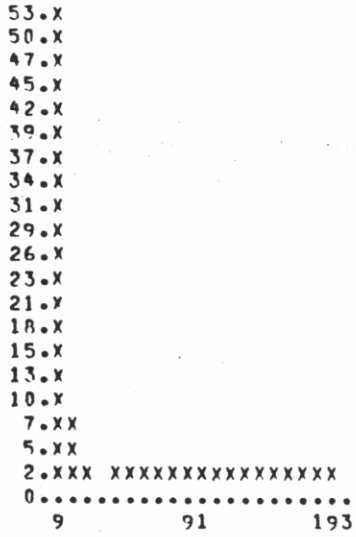

MEAN 55. SIGMA 61.7

THORIUM
RECORDS 55

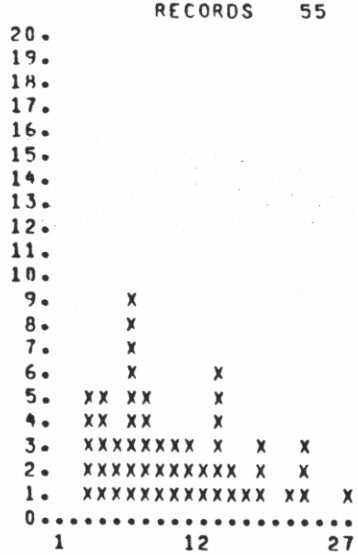

MEAN 11. SIGMA 6.0

U/K RATIO*10
RECORDS 51

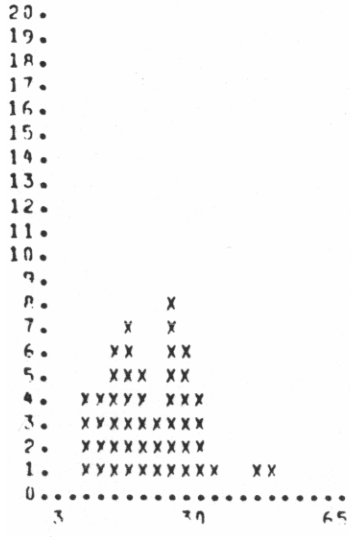

MEAN 23. SIGMA 11.4

U/T RATIO*10
RECORDS 46

MEAN102. SIGMA 63.0

T/K RATIO*10
RECORDS 46

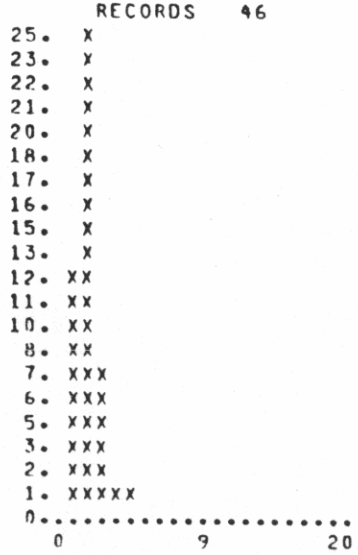

MEAN 2. SIGMA .8

DYNAMIC TEST RANGE
UNIT QADWC

POTASSIUM
RECORDS 176

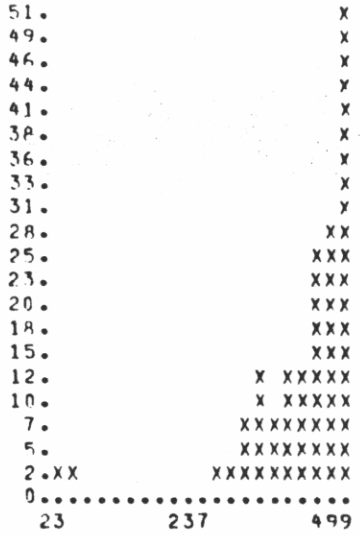

MEAN414. SIGMA100.8

URANIUM
RECORDS 173

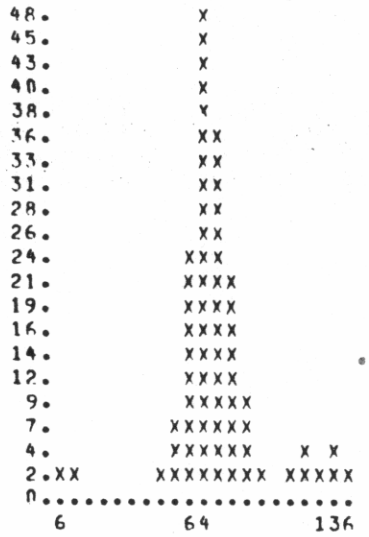

MEAN 74. SIGMA 19.6

THORIUM
RECORDS 176

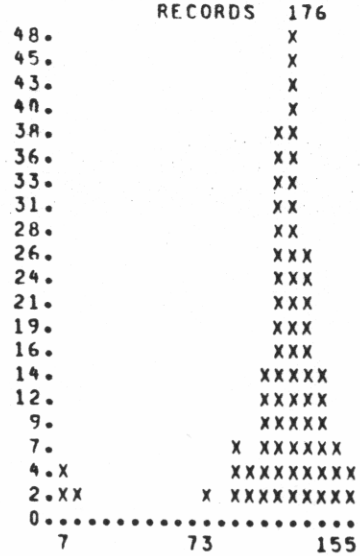

MEAN116. SIGMA 26.9

U/K RATIO*10
RECORDS 171

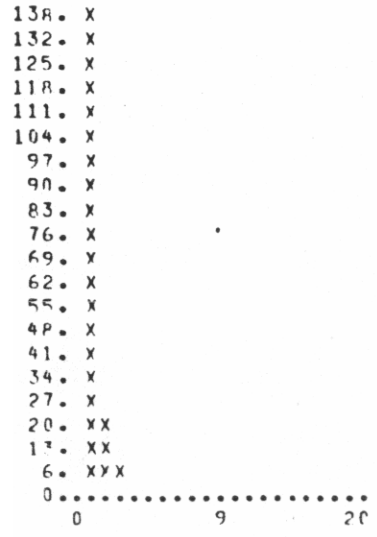

MEAN 1. SIGMA .6

U/T RATIO*10
RECORDS 173

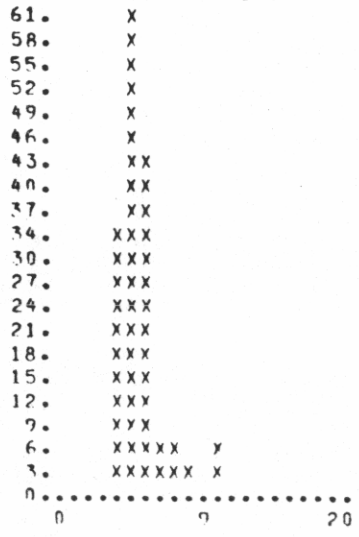

MEAN 6. SIGMA 2.2

T/K RATIO*10
RECORDS 175

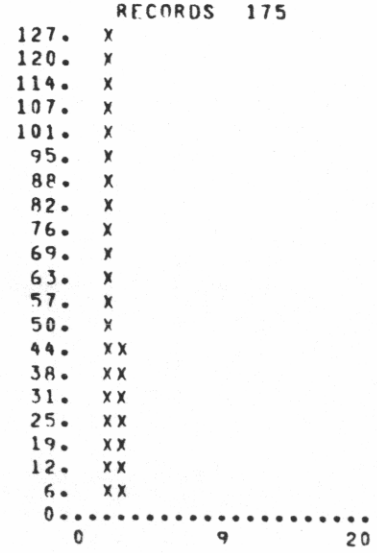

MEAN 2. SIGMA .5

DYNAMIC TEST RANGE
UNIT QADWO

POTASSIUM
RECORDS 1074

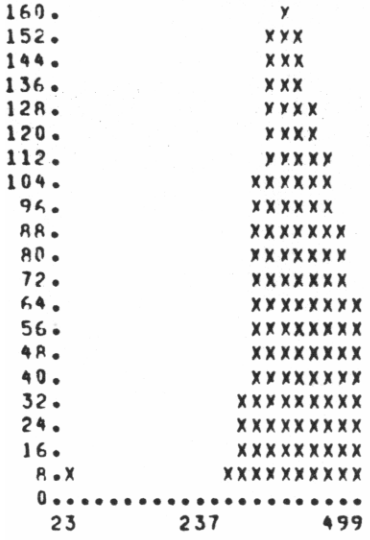

MEAN379. SIGMA 77.1

URANIUM
RECORDS 1069

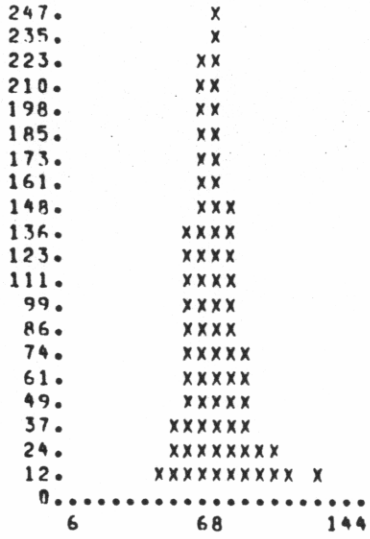

MEAN 73. SIGMA 18.1

THORIUM
RECORDS 1071

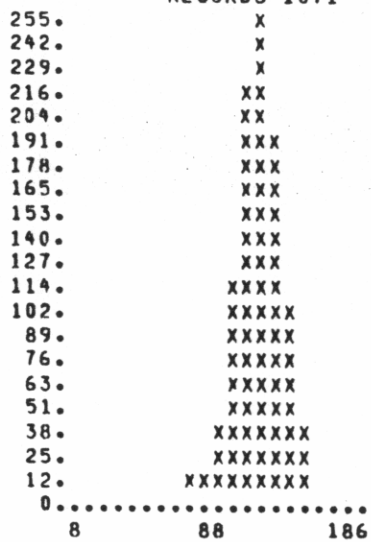

MEAN116. SIGMA 22.4

U/K RATIO*10
RECORDS 1062

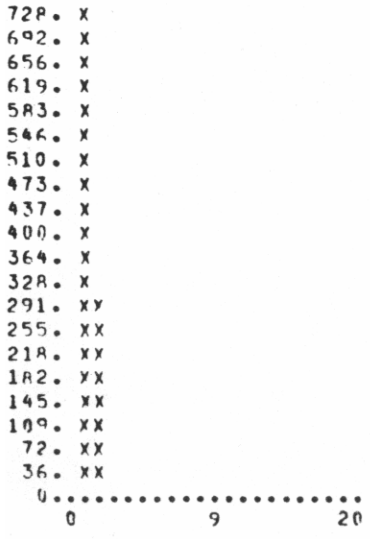

MEAN 1. SIGMA .6

U/T RATIO*10
RECORDS 1065

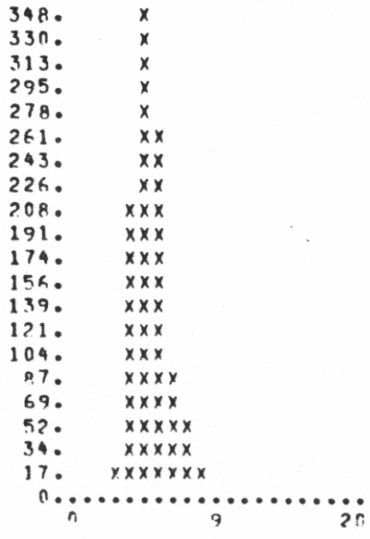

MEAN 6. SIGMA 1.7

T/K RATIO*10
RECORDS 1070

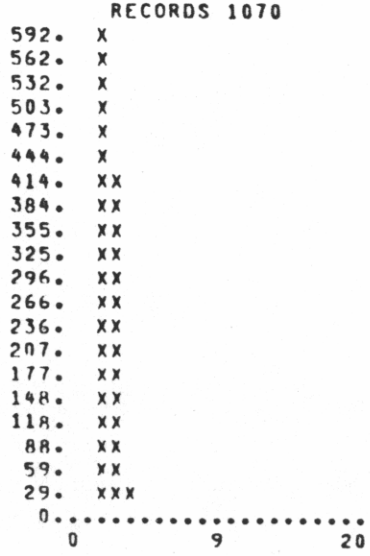

MEAN 2. SIGMA .7

DYNAMIC TEST RANGE
UNIT QATH

POTASSIUM
RECORDS 6

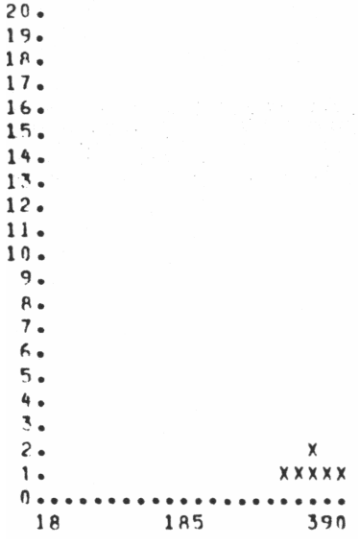

MEAN348. SIGMA 29.4

URANIUM
RECORDS 6

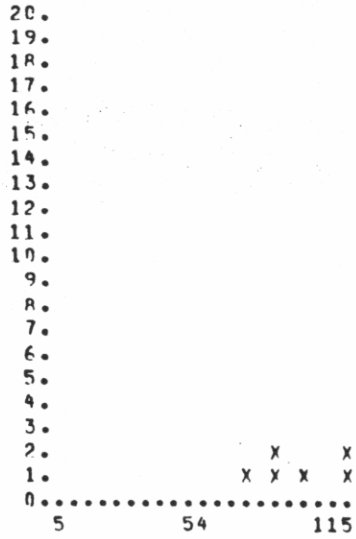

MEAN 95. SIGMA 16.3

THORIUM
RECORDS 6

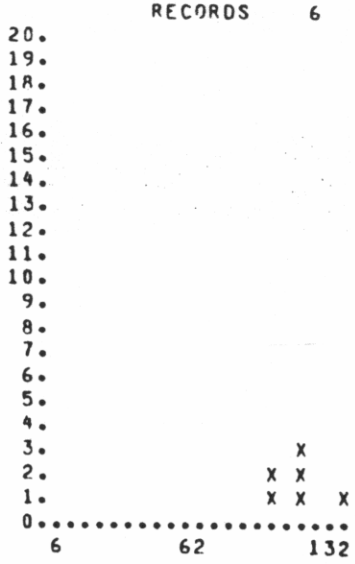

MEAN110. SIGMA 13.5

U/K RATIO*10
RECORDS 6

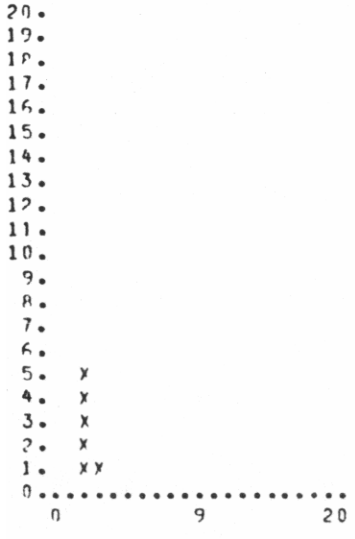

MEAN 2. SIGMA .4

U/T RATIO*10
RECORDS 6

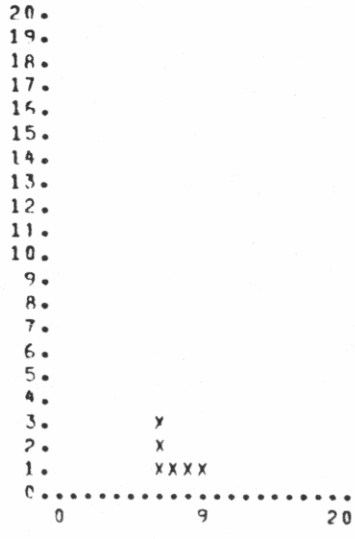

MEAN 8. SIGMA 1.3

T/K RATIO*10
RECORDS 6

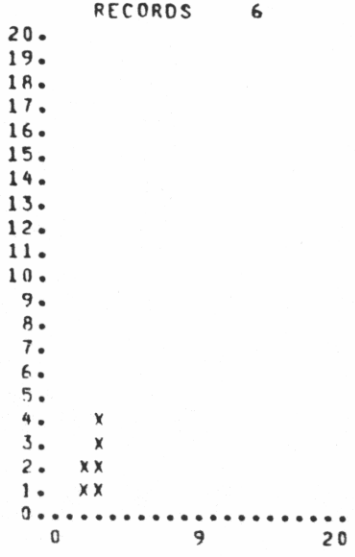

MEAN 3. SIGMA .5

DYNAMIC TEST RANGE
UNIT QSW

POTASSIUM
RECORDS 309

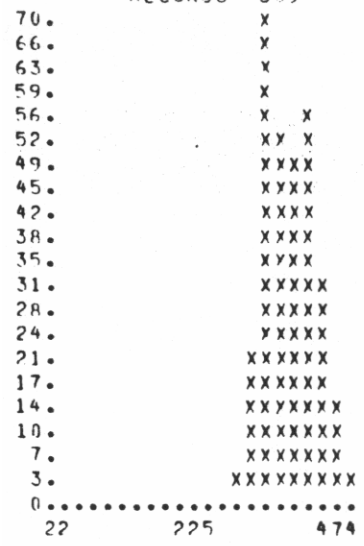

MEAN368. SIGMA 42.3

URANIUM
RECORDS 309

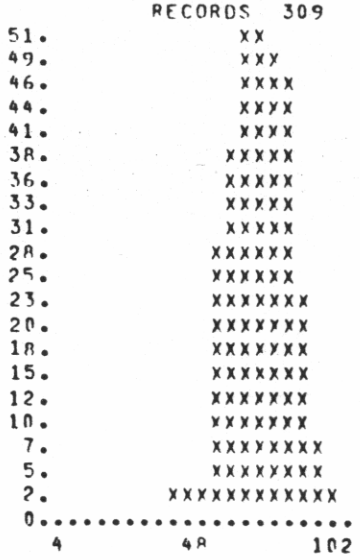

MEAN 71. SIGMA 10.6

THORIUM
RECORDS 309

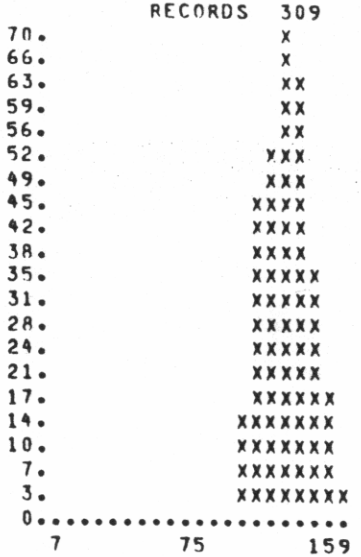

MEAN126. SIGMA 13.1

U/K RATIO*10
RECORDS 309

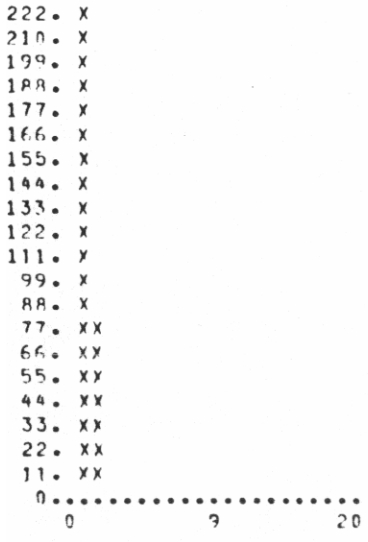

MEAN 1. SIGMA .5

U/T RATIO*10
RECORDS 309

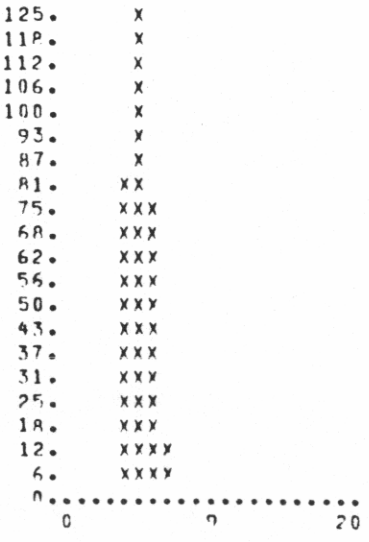

MEAN 5. SIGMA .9

T/K RATIO*10
RECORDS 309

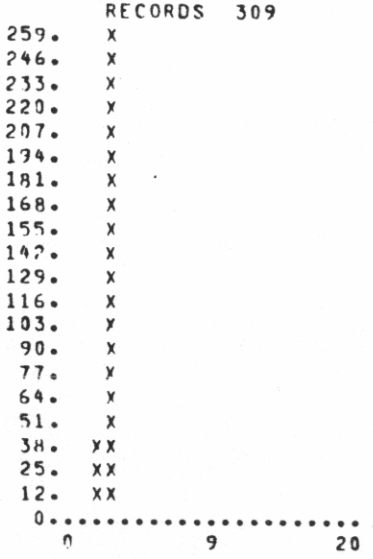

MEAN 3. SIGMA .4

DYNAMIC TEST RANGE
UNIT QG

POTASSIUM
RECORDS 21

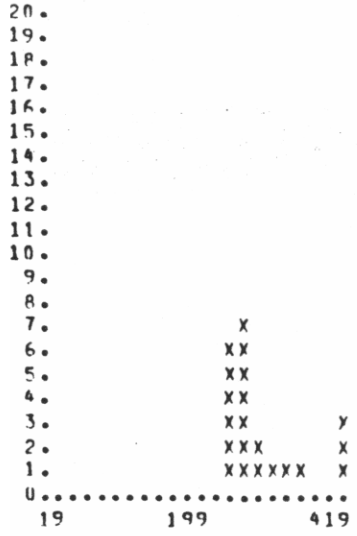

MEAN299. SIGMA 55.8

URANIUM
RECORDS 21

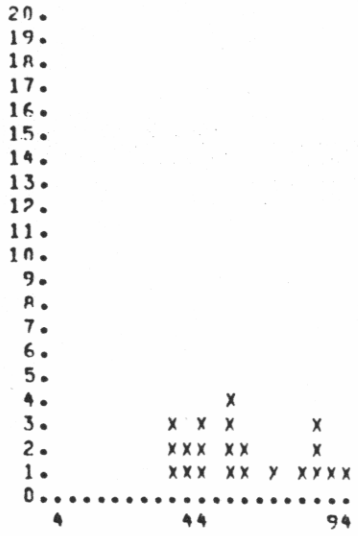

MEAN 61. SIGMA 18.6

THORIUM
RECORDS 21

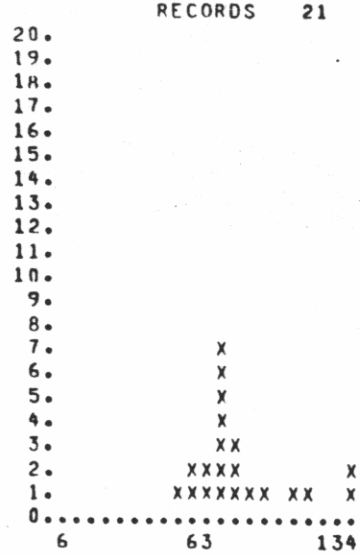

MEAN 83. SIGMA 22.0

U/K RATIO*10
RECORDS 21

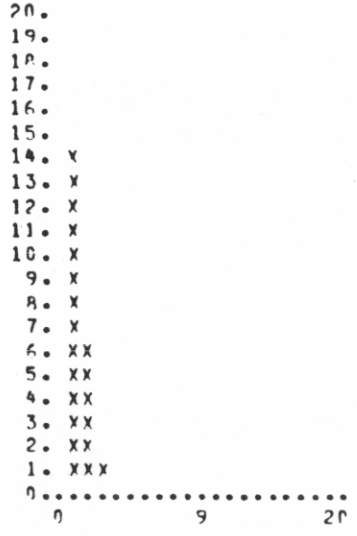

MEAN 1. SIGMA .6

U/T RATIO*10
RECORDS 21

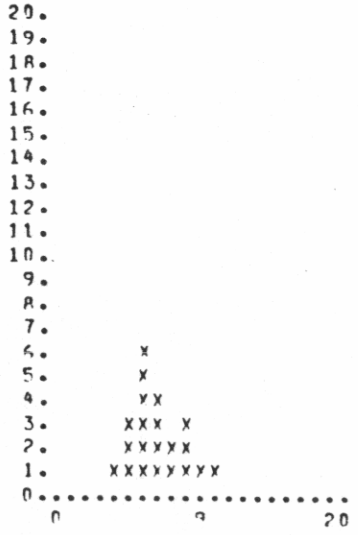

MEAN 7. SIGMA 1.8

T/K RATIO*10
RECORDS 21

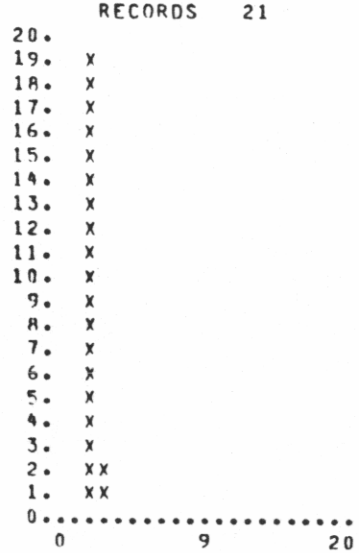

MEAN 2. SIGMA .3

DYNAMIC TEST RANGE
UNIT QC

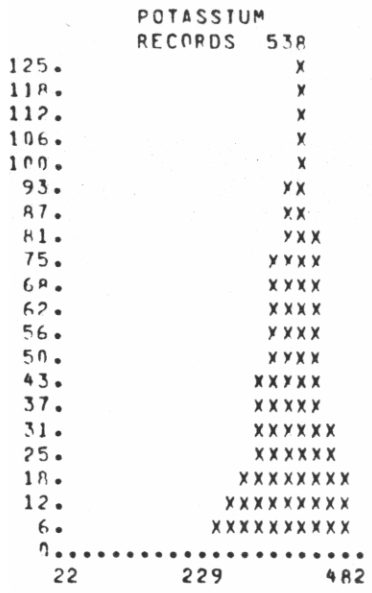

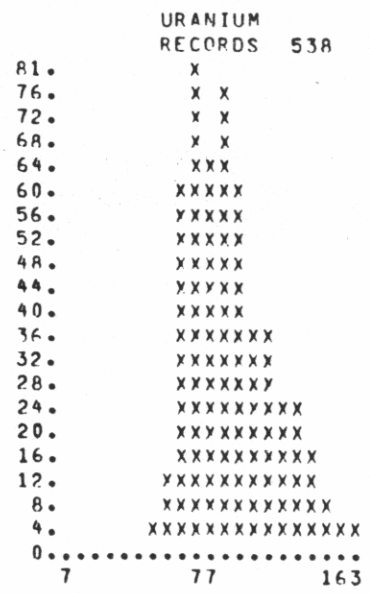

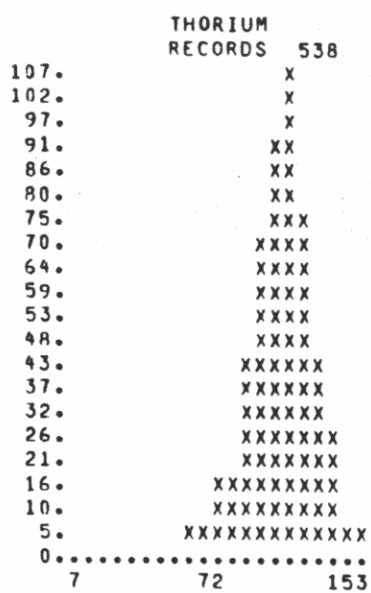

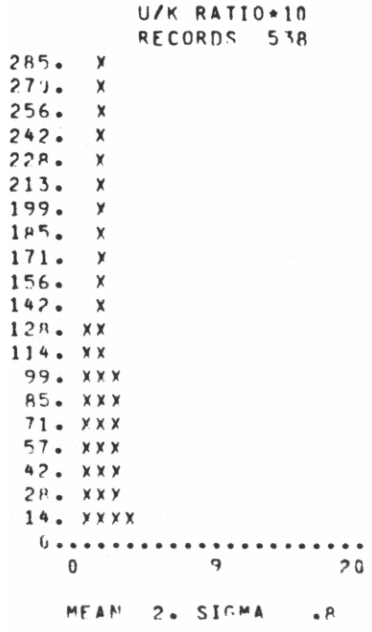

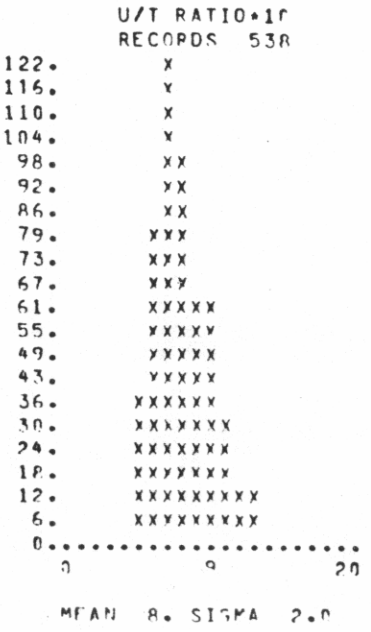

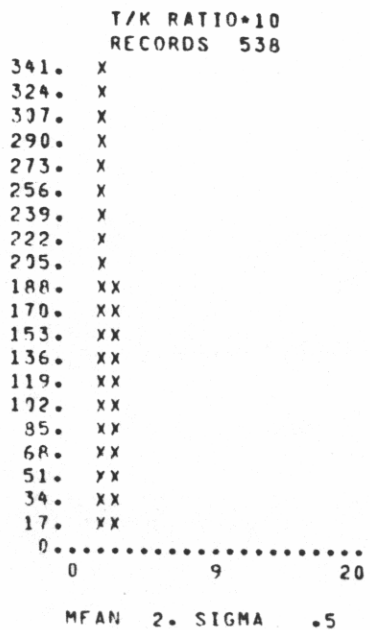

DYNAMIC TEST RANGE
UNIT TMHL

POTASSIUM
RECORDS 8

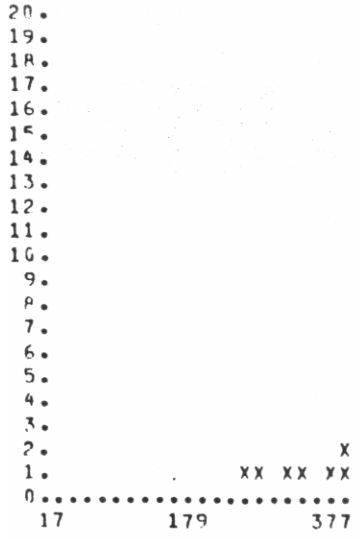

MEAN319. SIGMA 51.5

URANIUM
RECORDS 8

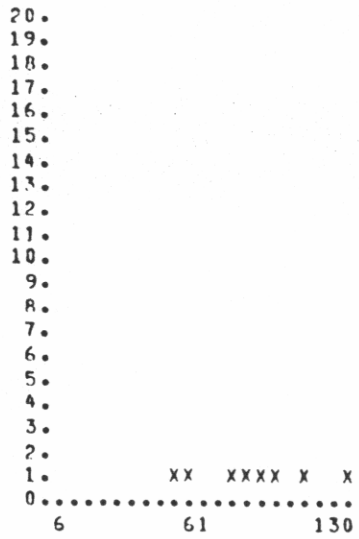

MEAN 89. SIGMA 25.5

THORIUM
RECORDS 8

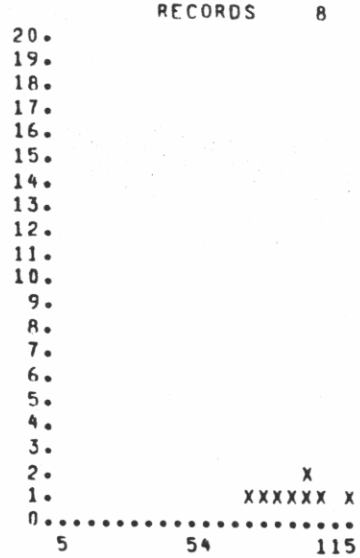

MEAN 92. SIGMA 13.1

U/K RATIO*10
RECORDS 8

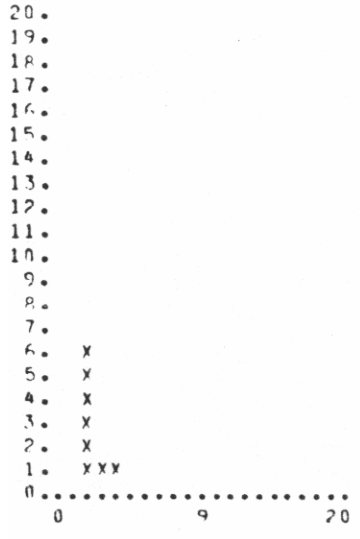

MEAN 2. SIGMA .7

U/T RATIO*10
RECORDS 8

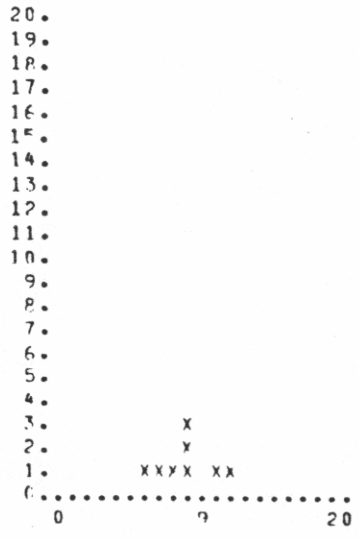

MEAN 2. SIGMA 2.0

T/K RATIO*10
RECORDS 8

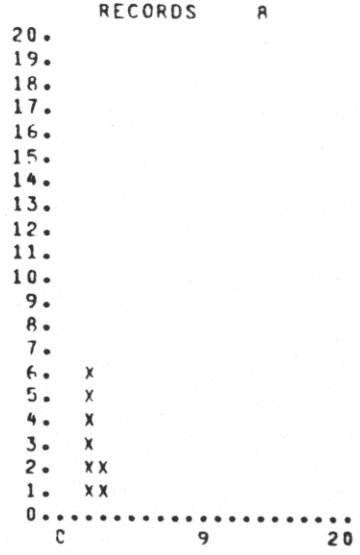

MEAN 2. SIGMA .5

DYNAMIC TEST RANGE
UNIT TM

POTASSIUM
RECORDS 91

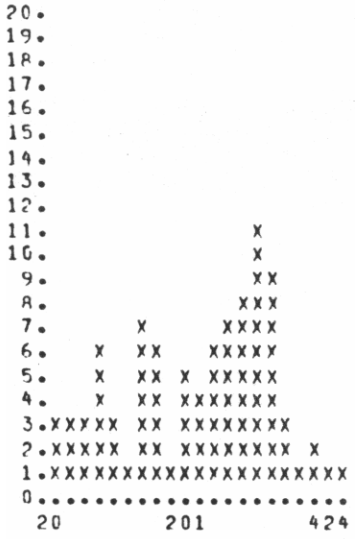

MEAN211. SIGMA102.1

URANIUM
RECORDS 89

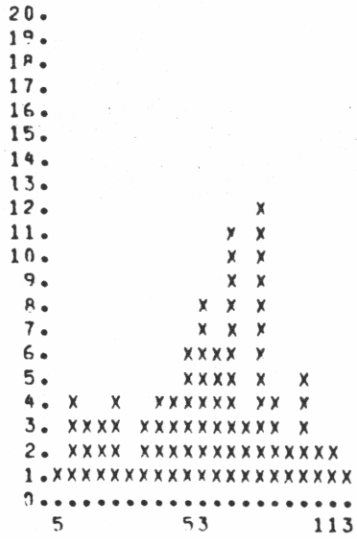

MEAN 60. SIGMA 26.9

THORIUM
RECORDS 90

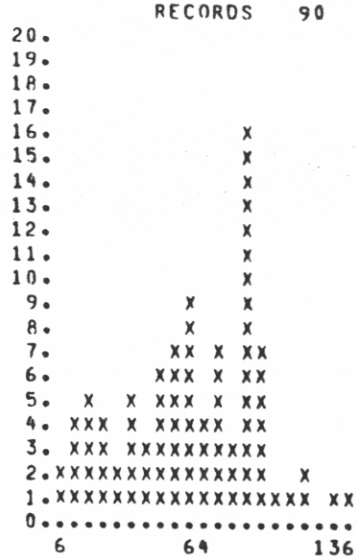

MEAN 63. SIGMA 30.3

U/K RATIO*10
RECORDS 88

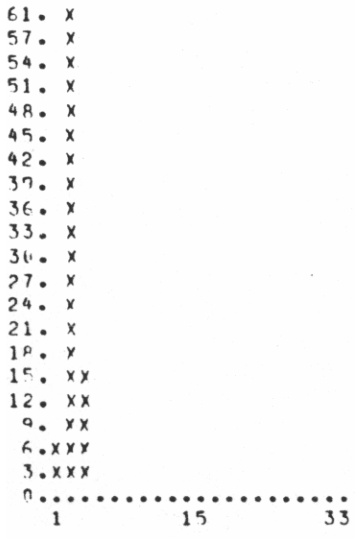

MEAN 3. SIGMA 3.8

U/T RATIO*10
RECORDS 89

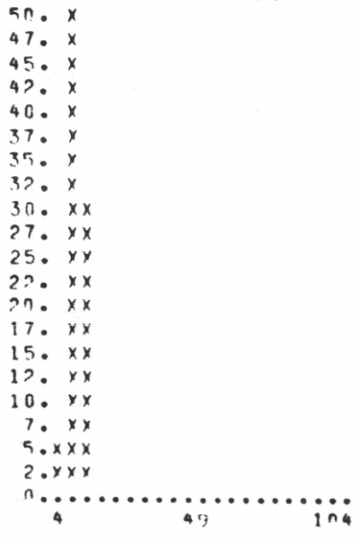

MEAN 11. SIGMA 14.0

T/K RATIO*10
RECORDS 90

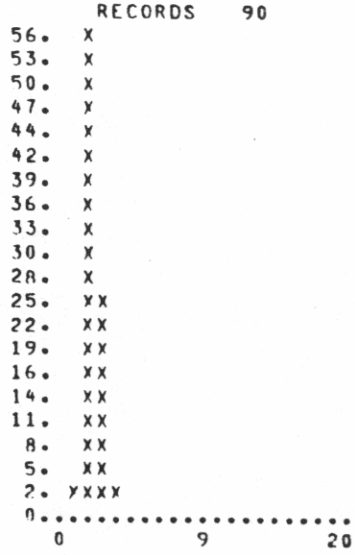

MEAN 2. SIGMA .7

10.8.4 STATISTICAL SUMMARIES

DYNAMIC TEST RANGE

STATISTICAL SUMMARY

CODE	UNIT	RECS	* * * K * * *		* * * U * * *		* * * T * * *		* * U/K*10 * *		* * U/T*10 * *		* * T/K*10 * *	
			MEAN	ST.DEV.	MEAN	ST.DEV.	MEAN	ST.DEV.	MEAN	ST.DEV.	MEAN	ST.DEV.	MEAN	ST.DEV.
1.	WATER	46.0	25.3	25.0	8.3	7.5	9.6	6.3	4.1	4.4	12.3	13.8	2.6	1.4
3.	QAL	110.0	38.8	25.6	55.5	61.7	11.4	6.0	22.9	11.4	102.1	63.0	2.0	.8
4.	QADWC	173.0	414.5	100.8	74.1	19.6	116.4	26.9	1.3	.6	5.9	2.2	2.3	.5
5.	QADWO	1069.0	379.2	77.1	72.9	18.1	115.7	22.4	1.4	.6	5.8	1.7	2.5	.7
6.	QATH	6.0	347.8	29.4	95.3	16.3	109.7	13.5	2.2	.4	8.0	1.3	2.7	.5
7.	QSW	309.0	367.5	42.3	70.9	10.6	125.7	13.1	1.3	.5	5.1	.9	2.9	.4
8.	QG	21.0	298.8	55.8	61.1	18.6	82.8	22.0	1.4	.6	7.0	1.8	2.1	.3
9.	QC	538.0	361.5	51.9	92.7	24.0	108.6	18.6	2.0	.8	8.0	2.0	2.4	.5
10.	TMHL	8.0	319.4	51.5	89.1	25.5	92.1	13.1	2.4	.7	8.9	2.0	2.2	.5
11.	TM	89.0	211.0	102.1	59.8	26.9	62.9	30.3	2.7	3.8	10.8	14.0	2.3	.7

DYNAMIC TEST RANGE

STATISTICAL SUMMARY BY LINE

LINE	RECS	K		U		T		U/K*10		U/T*10		T/K*10	
		MEAN	ST.DEV.	MEAN	ST.DEV.	MEAN	ST.DEV.	MEAN	ST.DEV.	MEAN	ST.DEV.	MEAN	ST.DEV.
10.	75.	341.5	178.2	59.8	23.6	102.3	38.3	1.2	.5	5.8	1.9	2.1	.5
130.	114.	278.2	143.5	74.1	22.6	99.8	50.6	4.6	6.9	19.6	33.7	2.7	.7
131.	128.	303.8	114.6	73.6	28.8	112.1	37.8	4.3	9.0	16.2	41.1	3.0	.6
132.	127.	317.5	124.3	74.5	31.5	110.0	42.2	5.0	10.2	19.9	45.1	2.8	.5
133.	88.	347.9	88.0	65.6	21.7	120.2	24.2	1.3	.5	5.3	1.3	2.8	.5
134.	92.	346.3	63.3	63.7	20.1	118.9	29.7	1.3	.5	5.0	1.2	3.0	.7
135.	99.	347.1	79.4	67.3	18.5	118.0	26.7	1.3	.5	5.2	.9	2.9	.4
136.	97.	375.1	71.2	67.1	18.2	123.1	17.1	1.2	.5	5.3	1.0	2.7	.5
137.	80.	375.3	109.9	63.4	13.5	116.0	22.5	1.0	.2	4.9	.9	2.3	.5
138.	84.	357.9	100.7	63.8	16.5	110.8	32.8	1.2	.6	5.4	2.2	2.6	.6
139.	89.	376.3	137.2	58.5	19.8	110.5	30.0	1.1	.3	5.2	1.5	2.2	.4
141.	85.	361.4	169.3	60.5	27.2	98.5	43.0	1.3	.8	6.0	2.4	2.2	.4
142.	89.	387.9	129.4	62.0	22.6	106.9	34.1	1.3	.8	5.7	1.6	2.3	1.3
143.	101.	394.6	104.9	73.6	26.5	106.1	27.5	1.4	.6	7.1	2.1	2.1	.2
144.	98.	387.3	101.5	82.4	21.6	108.0	28.1	1.6	.6	7.1	1.8	2.2	.4
145.	100.	371.5	92.4	83.8	27.0	109.8	23.8	1.9	1.2	7.6	2.6	2.4	.5
146.	127.	354.9	85.5	90.2	28.0	105.9	25.7	2.0	.8	8.0	2.3	2.4	.5
147.	128.	351.2	73.7	86.1	26.8	105.7	21.1	1.8	.7	7.7	2.0	2.3	.5
148.	164.	335.3	64.1	83.3	30.8	106.4	25.0	2.1	.9	7.9	2.1	2.5	.6
149.	141.	350.3	74.8	83.2	28.3	104.4	26.4	1.9	.8	7.5	2.2	2.4	.5
150.	147.	334.2	88.1	91.1	29.1	101.9	23.6	2.1	.8	8.5	2.0	2.3	.5
5001.	12.	274.2	69.1	63.1	16.1	69.2	29.0	1.7	.5	8.2	1.4	2.0	.4
5002.	30.	379.4	51.6	82.5	22.0	113.2	14.7	1.5	.9	6.9	2.8	2.3	.5
5003.	21.	383.0	43.4	79.1	25.5	114.5	9.1	1.5	.5	6.4	2.8	2.4	.5
5004.	30.	409.5	34.4	76.4	7.9	119.7	13.5	1.2	.4	5.8	1.1	2.4	.6
5005.	23.	392.2	39.3	73.3	18.6	119.4	12.3	1.3	.5	5.7	1.3	2.4	.5

10.8.5 REDUCTION PARAMETERS

REDUCTION PARAMETERS

N870W SYSTEM

Window	4 Pi Sensor Background 'B'	4 Pi Sensor Cosmic Ratio 'R'	2 Pi Sensor Background 'B'	2 Pi Sensor Cosmic Ratio 'R'
TC	189.4	3.3450		
K	24.5	.1816		
U	7.1	.1596	1.0	.1985
T	4.9	.2052	0.9	.2245

Stripping Ratios

ALPHA (α_0), (α_1)	.3015 + .00008*H
Beta (B_0)	.4486
Gamma (γ)	.8395
b	.066

Attenuation Coefficients

K (U_h)	.06526 Cm_2^2/gm x Density g/Cm_3^3 x Cm/FT = .00257/Ft.
U (U_h)	.06130 Cm_2^2/gm x Density g/Cm_3^3 x Cm/FT = .00241/Ft.
T (U_h)	.05019 Cm^2/gm x Density g/Cm^3 x Cm/FT = .00198/Ft.

Density at $0^{\circ}C$, 1013.mlb = .0012923 g/Cm^3

Sensitivities at 400 Feet

K	80.2 cps/%
U	12.2 cps/ppm
T	5.5 cps/ppm

Shine Around Correction Coefficients

Sh = .037*exp(.0004*H) * TUC

TUC = Corrected 4 Pi Uranium Count

H = Altitude in Feet

Radon 4 Pi/2 Pi Sensor Ratio

R=1/(5.0495 + .00196 *H)

10.8.6 PRODUCTION SUMMARY

PRODUCTION SUMMARY

The aerial survey of the Test Range was performed in conjunction with the system calibration. The survey was initiated on the 25th of February and was concluded on the 28th.

A test line of 5 minutes duration was flown prior to and following the completion of each day's flying. A summary of the gross count in CPS follows:

Date	Start Summed CPS	Mean CPS	End Summed CPS	Mean CPS	% Change
2/25/79	1037466	3458	1021437	3405	- 1.54
2/26/79	1001289	3338	988208	3294	- 1.31
2/27/79	988395	3295	1004655	3349	+ 1.62
2/28/79	1043347	3478	1036151	3454	- 0.69

DYNAMIC TEST RANGE

AIRSPEED HISTOGRAM

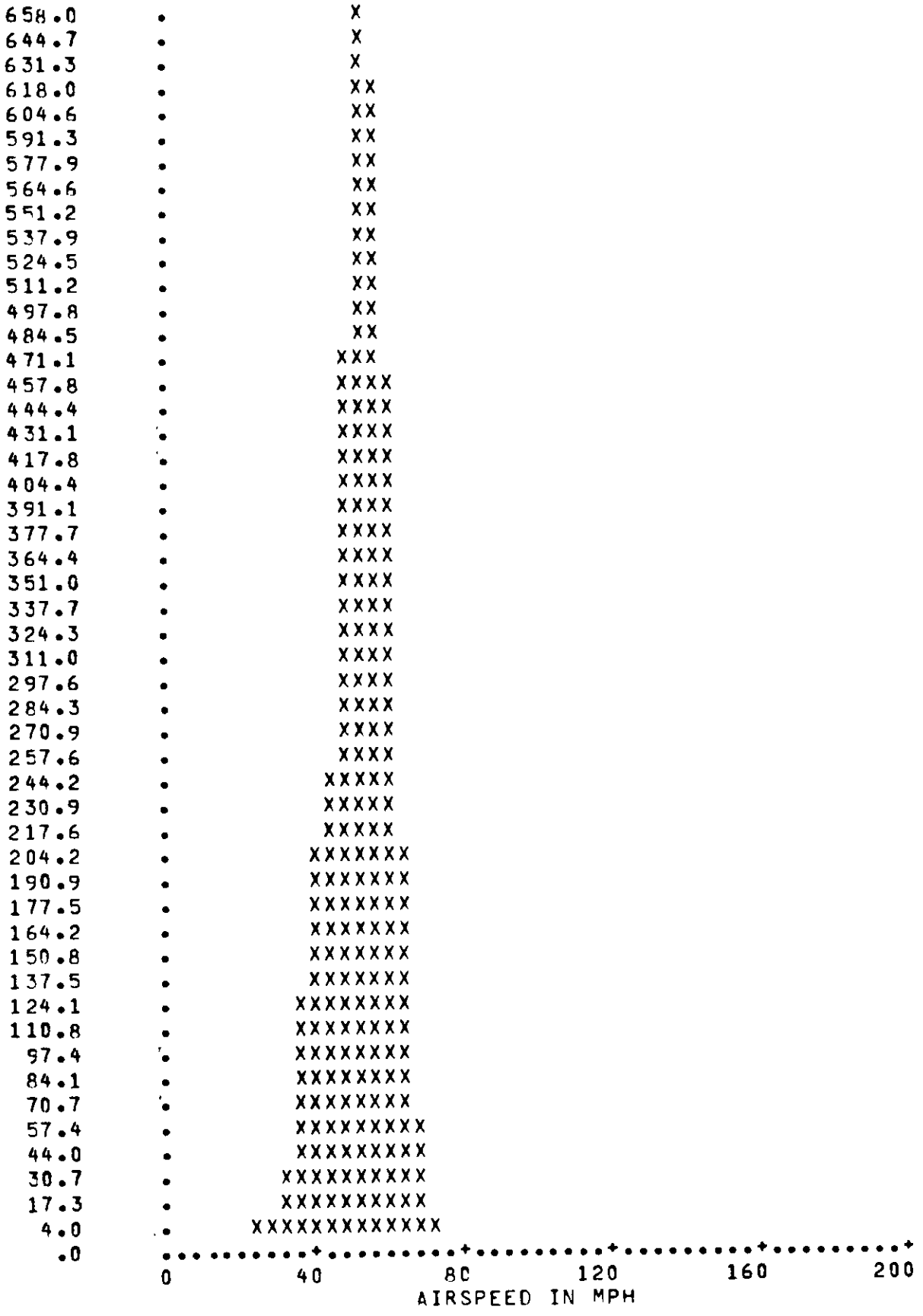

DYNAMIC TEST RANGE
RADAR ALTITUDE HISTOGRAM

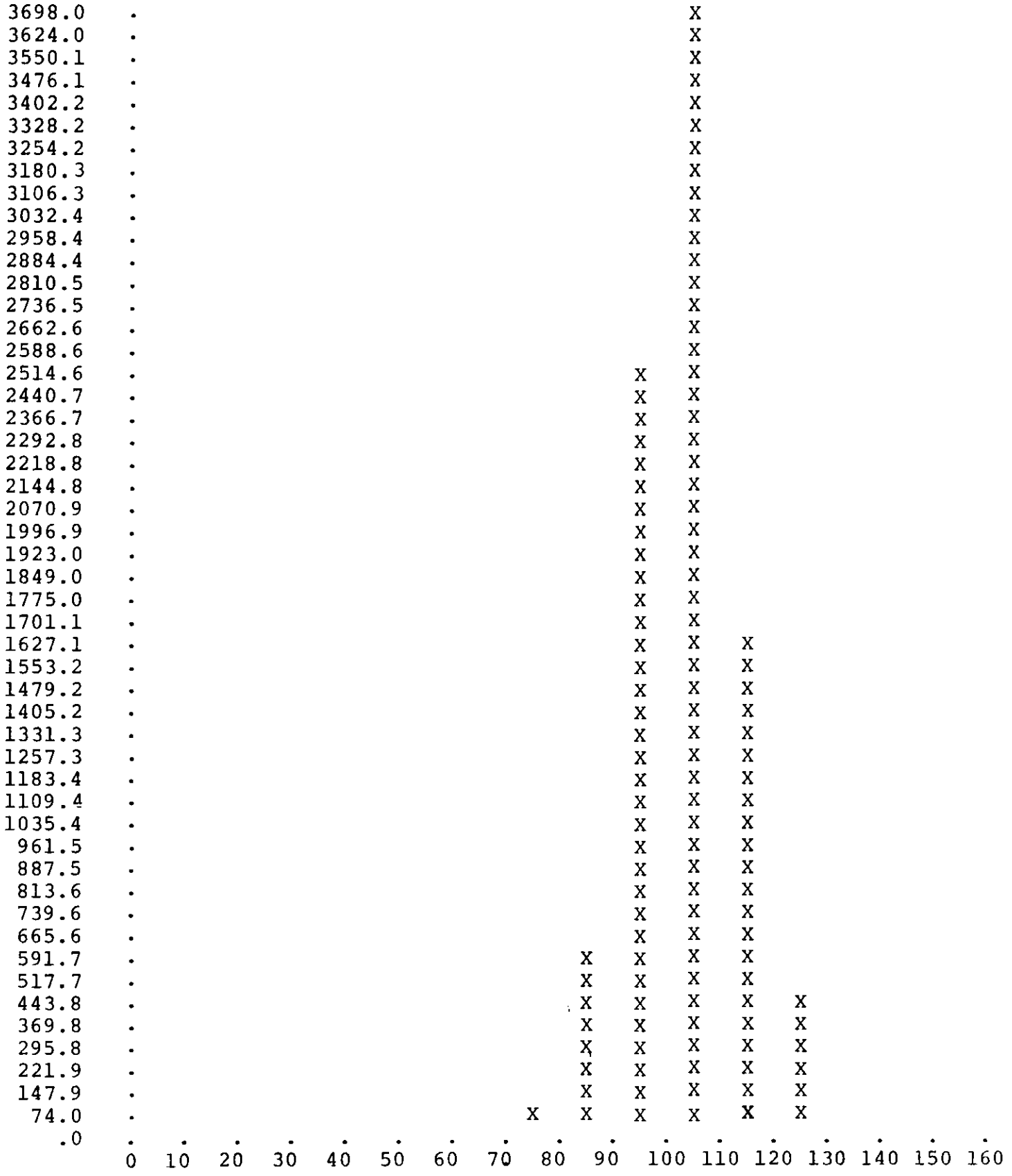

10.8.7 TAPE FORMATS

TAPE FORMATS

All tape files are 9 track EBCDIC written at a density of 800 BPI and have a fixed word length of 9 characters.

TAPE HEADER

The first record of each tape file is a tape label of 972 characters containing the following standard information:

(1)	Project Identification	Characters 1-45
(2)	LKB Resources, Inc.	Characters 46-63
(3)	Date of Survey	Characters 64-72
(4)	Sequence of lines in this file	Characters 73-972

LINE HEADER

A standard 10 word line header preceeds and identifies each line contained in the file.

Word	Definition
1	Line Number
2	Start Fiducial Number
3	End Fiducial Number
4	4π Sampling Interval (millisecs)
5	2π Sampling Interval (millisecs)
6	Date (YYDDD)
7	Number of Samples
8-10	Not used

RAW SPECTRAL DATA FILE

The raw data sub-set will immediately follow the line header and will contain 416 words per logical record.

Word	Definition
1	Record Number
2	Latitude (.0001 degrees)
3	Longitude (.0001 degrees)
4	Time (seconds past midnight)
5	Magnetic Field (.1 gamma)
6	Terrain Clearance (feet)
7	Barometric Pressure (feet)
8	Temperature (.1 degree C)
9	* Altitude Flag
10	* K Flag
11	* U Flag
12	* T Flag
13-212	Terrestrial Detector 0 to 3 MeV
213	Terrestrial Detector LIVE time (millisecs)

Word		Definition
214-413		Atmos. Detector 0 to MeV
414		Atmos. Detector LIVE time (millisecs.)
415	**	Terrestrial Detector Cosmic Sum
416	**	Atmos. Detector Cosmic Sum (.1 Count)

SINGLE RECORD DATA FILE

The single record data will be blocked 10 logical records per block. Each logical record will contain 19 words defined as follows:

Word		Definition
1		Record Number
2		Latitude (.0001 degrees)
3		Longitude (.0001 degrees)
4		Magnetic Field (.1 Gamma)
5		Terrain Clearance
6		Geologic Unit Code
7	*	Altitude Flag
8	*	K Flag
9	*	U Flag
10	*	T Flag
11		Terrestrial Cosmic Sum
12		Atmos. Bi^{214} Correction (.1 Count)
13		Terrestrial Gross Count
14		Terrestrial Thorium Count
15		Terrestrial Uranium Count
16		Terrestrial Potassium Count
17		Ratio U/K (.1 Count)
18		Ratio U/T (.1 Count)
19		Ratio T/K (.1 Count)

STATISTICAL ANALYSIS TAPE

The statistical data file contains an additional tape header record which identifies the statistical parameters relative to each geologic map unit.

The data associated with a single geologic map unit is considered as one logical record and contains 14 words.

The logical records are blocked 200 thus the physical record is 2800 words.

The statistical header is defined as follows:

Word	Definition
1	Map Unit Code
2	Number of Records

Word	Definition
3	K Mean Value
4	K Standard Deviate
5	U Mean Value
6	U Standard Deviate
7	T Mean Value
8	T Standard Deviate
9	U/K Mean Ratio (.1 Count)
10	U/K Standard Deviate (.1 Count)
11	U/T Mean Ratio (.1 Count)
12	U/T Standard Deviate (.1 Count)
13	T/K Mean Ratio (.1 Count)
14	T/K Standard Deviate (.1 Count)

STATISTICAL DATA RECORD

The statistical data record contains the averaged reduced data records. Each averaged record is considered a logical record having 22 words. The logical records are blocked 10 per physical record.

Word		Definition
1		Record Number
2		Latitude (.0001 Degrees)
3		Longitude (.0001 Degrees)
4		Magnetic Total Field (.1 Gamma)
5		Geologic Map Unit Code
6	*	Altitude Flag
7	*	K Flag
8	*	U Flag
9	*	T Flag
10		Gross Count
11		Thorium Count
12		Thorium Standard Deviate (.1 Count)
13		Uranium Count
14		Uranium Standard Deviate (.1 Count)
15		Potassium Count
16		Potassium Standard Deviate (.1 Count)
17		U/T Ratio (.1 Counts)
18		U/T Standard Deviate (.1 Count)
19		U/K Ratio (.1 Counts)
20		U/K Standard Deviate (.1 Count)
21		T/K Ratio (.1 Count)
22		T/K Standard Deviate (.1 Count)

MAGNETIC DATA TAPES

The magnetic data record contains 10 words per logical record and is blocked 50 logical records per physical record.

Word	Definition
1	Record Number
2	Latitude (.0001 degrees)
3	Longitude (.0001 degrees)
4	Time (seconds past midnight)
5	Terrain Clearance (feet)
6	Barometric Pressure (feet)

Word	Definition
7	Geologic Code
8	Observed Magnetic Field (.1 Gamma)
9	Corrected Magnetic Field (.1 Gamma)
10	Filler word or Diurnal (if required)

* Quality Flag Code: 1 = Record exceeds altitude specifications or failed statistical significance test.

0 = Data is acceptable

** Cosmic sums have been corrected for live time.

10.8.8 MICROFICHE LISTINGS